Heidelberger Institut für Theoretische Studien,
Zentrum für Astronomie der Ruprecht-Karls-Universität Heidelberg

Interfacing High-Energy Astrophysics and Cosmological Structure Formation

vorgelegt von Christoph Pfrommer aus Ulm/Donau

Heidelberg, 7. Oktober, 2013

Habilitationsschrift
zur Erlangung der Venia Legendi
für das Fach Physik der
Ruprecht-Karls-Universität Heidelberg

Christoph Pfrommer:
Interfacing High-Energy Astrophysics and Cosmological Structure Formation
Habilitationsschrift zur Erlangung der Venia Legendi für das Fach Physik der
Ruprecht-Karls-Universität Heidelberg

Contents

Abstract

In this Habilitation thesis I am studying a broad range of research topics bridging cosmological structure formation, high-energy astrophysics, and plasma and astro-particle physics. I explore connections between these ostensibly separated areas with the goal to find completely novel viewpoints onto long-standing problems, which enables substantial progress: something that would not have been possible within these research topics only.

(1) *Cosmic rays.* I construct a comprehensive model of cosmic rays in galaxy clusters that is based on cosmological hydrodynamical simulations. The model quantifies the effects of cosmic rays on the thermal plasma and predicts non-thermal cluster emission throughout the entire electro-magnetic spectrum from radio to gamma-ray wavelengths. Thorough data comparison projects with various observational collaborations have now established first constraints on cosmic ray acceleration physics.

(2) *Magnetic fields.* I study how moving cluster cores, bubbles, and galaxies interact with the ambient magnetized plasma. Magneto-hydrodynamical simulations and analytical calculations suggest physical solutions to the puzzling observations of cluster "cold fronts", the hydrodynamical stability of buoyantly rising radio lobes, and the polarized synchrotron ridges at spiral galaxies in the Virgo cluster. This immediately presents a novel technique for probing local orientations of cluster magnetic fields, with important implications for cluster formation scenarios.

(3) *Cosmological shocks.* I propose to use radio galaxies for probing otherwise invisible properties of formation shocks, which play a key role during the hierarchical assembly of cosmological structure. Structure formation shocks are also traced by giant radio relics. Modeling those in our cosmological simulations allows both statistically inferring properties about cluster magnetic fields and improving our understanding of the detailed shock acceleration mechanism of electrons.

(4) *Galaxy and cluster formation.* Our hydrodynamical galaxy formation simulations show that cosmic ray streaming is responsible for driving galactic winds and for suppressing subsequent star formation. I further show that cosmic rays injected by the active galactic nucleus in the Virgo cluster heat the fast cooling central cluster gas at a rate that balances that of radiative cooling at each radius. Cosmic ray heating imposes a temperature floor that is in accordance with X-ray observations, thereby suggesting a solution to the famous "cooling flow problem".

(5) *Indirect dark matter searches.* Galaxy clusters are among the best extragalactic targets to indirectly detect dark matter owing to the large substructure enhancement. Non-detections of gamma-rays from clusters enable us to severely challenge a popular class of leptophilic cold dark matter models with Sommerfeld-enhanced cross sections and to constrain representative benchmark models of supersymmetric dark matter in the near future.

(6) *The cosmological impact of blazars.* Blazar heating substantially alters the thermal history of the Universe. Powerful plasma instabilities are able to dissipate most of the bolometric energy output from blazars, thereby heating the intergalactic medium. This has far-reaching consequences for the Lyman-α forest, and the formation of dwarf galaxies and galaxy clusters. Additionally, this transforms our understanding of the evolution of blazars, their contribution to the extra-galactic gamma-ray background, and how their individual spectra can be used to constrain intergalactic magnetic fields.

Part I.

Introduction

Scientific Context

Understanding the formation and evolution of galaxies and galaxy clusters is one of the most fascinating problems in modern cosmology. While there exists a basic paradigm—the theory of hierarchical formation of galaxies and clusters within the ΛCDM cosmology (i.e., cold dark matter with a cosmological constant Λ)—many aspects of it are not well understood and appear to be in conflict with the data. Most prominently, the observed galaxy luminosity and H I-mass functions show much shallower faint-end slopes than predicted by ΛCDM models; one incarnation of this is known as the 'missing satellites problem' of the Milky Way, which should contain many more dwarf-sized subhalos than observed (Kravtsov 2010). At the same time, simulations predict an inner dark matter (DM) cusp for the density structure of galaxies, seemingly at odds with the cored profiles found in observed low surface brightness galaxies and dwarf satellites. While these problems may point to an incomplete understanding of the underlying theory of DM (e.g., van den Aarssen et al. 2012), they certainly have put our still inadequate understanding of galaxy formation into focus. This is exemplified by comparing the simulated DM halo mass function with the accurately determined stellar mass function of the SDSS survey. Assuming that stellar mass monotonically increases with halo mass, an abundance matching analysis demonstrates that baryonic mass is most efficiently converted into stellar mass for halo masses around $10^{12}\,M_\odot$, similar to our Galaxy, and sharply declines towards lower and higher masses (Moster et al. 2010, Guo et al. 2010). In low-mass halos, atomic cooling is even more efficient in comparison to our Galaxy, however a much smaller fraction of baryons is turned into stars. For more massive halos at the scales of galaxy groups and clusters, simple estimates of the cooling efficiencies would also predict larger galaxies than observed and too much cold gas at the centers of groups and clusters of galaxies.

Galaxy clusters are the rarest and largest gravitationally-collapsed objects in the Universe and form at sites of constructive interference of long waves in the primordial density fluctuations. Clusters exhibit a well-defined number count that steeply falls as mass and redshift increase, which makes them very sensitive tracers of the growth of structure (Voit 2005). In particular, the number density of high-mass clusters is very sensitive to changes in cosmological parameters. This has already provided excellent constraints on our cosmological standard model, including the dynamical characteristics of dark energy and the matter content in the Universe (Vikhlinin et al. 2009). Hence, future large surveys of clusters (in the optical, X-ray, and microwave regimes) with substantially increased statistics and resolution can potentially provide a gold mine for fundamental physics and cosmology. However, each derived observable from these windows into clusters is fraught with complications. Numerical simulations are required to understand these. In clusters, most of the baryons are in a hot diffuse plasma that emits X-rays. Observations of this cluster plasma were not only critical in establishing our current picture of DM as "collisionless" particles but also reveal the detailed astrophysical processes at work. Those govern the dynamics of the intracluster medium (ICM) and shape the thermal histories of clusters. Cluster cores that show a central temperature dip should have long since cooled and collapsed, which has been dubbed the "cooling flow problem" (McNamara & Nulsen 2007, 2012). Others instead have central cooling times that are longer than the age of the Universe (Cavagnolo et al. 2009, Hudson et al. 2010). Understanding what physics produces this cluster bimodality is arguably one of the most fundamental problems in theories of cluster formation and imperative if clusters are to be used as precision probes for cosmological parameters in the future.

In fact, the formation of galaxies and clusters is intimately connected: on one hand, galaxies form through gravitational collapse of the high-redshift intergalactic medium (IGM) and galaxy clusters form successively by mergers of smaller galactic halos and the collapse of the intervening IGM. On the other hand, various baryonic feedback processes recycle mass and energy to the IGM and enrich it with metals and magnetic fields, which are flux-frozen into the plasma. Common ideas for these feedback processes that suppress and regulate the formation of gas-rich spiral galaxies include galaxy-scale winds driven by evolving stars or supernovae shocks (Veilleux et al. 2005). On larger scales of elliptical galaxies and galaxy clusters, popular ideas for feedback involve quasar activity or jets from accreting supermassive black holes, so-called active galactic nuclei (AGN, McNamara & Nulsen 2012). Primary physical processes underlying those scenarios include energy and momentum deposition through radiation, shocks, turbulence, or high-energy processes associated with magnetic fields and relativistic particle populations (cosmic rays, CRs) that modify the gas dynamics, the (angular) momentum transport, and the energy release time scales.

To date, it is very uncertain where and how efficiently this energy is dissipated and what the consequences are. The non-linear and dynamical interplay of these processes can be viewed as a great cycling of energy and mass in between the diffuse phase of the IGM and the collapsed phase in form of the ICM and the interstellar medium. Details of this cycle remain enigmatic and also point to the importance of understanding the thermodynamic history of the IGM for understanding the formation and evolution of galaxies and clusters.

Energetic processes in galaxies such as powerful shock waves and turbulence driven by exploding stars and stellar winds have accelerated electrons and protons to relativistic energies. Dynamo processes have amplified seed magnetic fields in the interstellar medium. These non-thermal components play a decisive role within our Galaxy since each of their pressures is at least comparable to that of the thermal gas and their cumulative pressure force balances gravity. CRs may drive powerful galactic winds, trace past energetic events such as supernovae, and reveal the underlying structure of the baryonic matter distribution through their interactions in the radio and gamma-ray regime. Despite their dynamical impact and their importance as high-energy multi-messengers, so far they have been largely unexplored in galaxy formation models except for a few notable exceptions (Jubelgas et al. 2008, Wadepuhl & Springel 2011). This Habilitation thesis presents first steps toward understanding the physics of the wind driving mechanism (Chapter 4, Uhlig et al. 2012). This work triggered a number of very recent papers that all confirm our initial findings (Dorfi & Breitschwerdt 2012, Salem & Bryan 2013, Booth et al. 2013), possibly opening an avenue to a new rich field of research.

The gravitational energy associated with cluster mergers—the most energetic events of the Universe—is dissipated in enormous shock waves. A fraction of this energy is used for accelerating CRs and amplifying magnetic fields that permeate entire galaxy clusters, as inferred from observations of cluster-sized diffuse structures of radio synchrotron emission in form of "radio halos" and "radio relics". The last years have seen an increasing number (∼ 80) of those radio phenomena that seem to be ubiquitous in merging clusters. However, these relativistic electrons have relatively short cooling times which makes them quickly invisible in the radio band. Hence they have to be accelerated close to the sites where they are observed, challenging theoretical models to find a cluster-wide efficient acceleration process that can explain all "radio-halo" data. In this Habilitation thesis, I will present advances in our modeling of radio halos and the expected gamma-ray emission that provides a critical test for certain model classes (Chapter 1, Pfrommer et al. 2008, Enßlin et al. 2011, Brunetti & Lazarian 2011).

On the other side, giant "radio relics" in clusters appear to be associated with individual merger shocks. These are mostly weak shocks, i.e., the shock speed exceeds the sound speed by only a factor of a few, since these shocks propagate in a hot plasma of keV energies. However, observations of weak interplanetary shocks in the solar system render those to be extremely inefficient accelerators, which also challenges our theoretical understanding of the plasma physics of particle acceleration at cluster shocks—a problem that will be solved within the context of this Habilitation thesis (Chapter 3, Pinzke et al. 2013). Moreover, observations of radio synchrotron emission in form of radio jets and lobes in cooling cluster cores put the underlying non-thermal components such as CRs and magnetic fields into the limelight for solving the cooling flow problem (Chapter 4, Guo & Oh 2008, Pfrommer 2013).

So far, this introduction was mostly written from an astronomically centered viewpoint, i.e., we asked the question how a refined modeling of high-energy astrophysical processes can help improving our understanding of the formation of galaxies and clusters. A complete exploration of "the interface of high-energy astrophysics and cosmological structure formation" necessarily also calls for adopting the opposite approach, i.e., using astrophysical objects as cosmic laboratories to improve our understanding of the underlying (fundamental) physics. In the last two chapters, I employ exactly this approach by constraining DM models and by highlighting a potentially deep connection between gamma-ray spectra of blazars and an extremely interesting regime of plasma physics (dilute relativistic beam-plasma instabilities) that so far has been overlooked. (1) Gamma-ray energies are well adapted to the weak energy scale, which coincides with DM particle masses in the most popular models. Those models predict the existence of weakly interacting massive particles that would naturally account for the observed relic density if they had thermally decoupled in the early universe. In this Habilitation thesis I put galaxy clusters into the focus of indirect DM searches (Chapter 5, Pinzke et al. 2009, 2011), which enables us to seriously challenge the theoretically interesting class of leptophilic DM models (Arkani-Hamed et al. 2009). (2) In practice, gamma-ray emission probes the most extreme physics laboratories of the cosmos. This allows us to assess questions about the mechanism of particle acceleration and magnetic field amplification, and to study plasma physical processes at conditions that are quite different from those achievable in our laboratories on Earth (e.g., collisionless plasmas, extreme Lorentz factors). In particular, the physics associated with the propagation of TeV photons appears to be richer than previously thought. TeV photons produce electron-positrons pairs upon annihilating with soft photons of the extragalactic background light, which is emitted by galaxies and quasars. The kinetic pair energy can be reprocessed to the GeV

gamma-ray band via inverse Compton interactions with the photons of the cosmic microwave background. Studying this process through gamma-ray spectra of blazars may provide us with insights into intergalactic magnetic fields (which could be of primordial origin). Alternatively, if the kinetic pair energy can be efficiently dissipated, this novel "blazar heating" mechanism may even provide the dominant energy source to the intergalactic medium at late times (for redshifts $z < 3$) and hence impact the thermal history of the intergalactic medium, the Lyman-α forest and late-time structure formation (Chapter 6, Broderick et al. 2012, Chang et al. 2012, Pfrommer et al. 2012).

To pursue these topics, in this Habilitation thesis I employ a multi-faceted approach ranging from high-resolution hydrodynamical simulations to paper-and-pencil theory of the accompanying physical processes to observational data analyses embedded within international collaborations. To this end I joined the *Fermi*, MAGIC, and VERITAS Collaborations as an external lead theory author for gamma-ray searches in galaxy cluster with the aim to detect CR populations and DM annihilation radiation. This is complemented with thorough computational work ranging from cosmological simulations of the formation and evolution of galaxy clusters to well-posed magneto-hydrodynamical (MHD) problems that even have analytical solutions in some asymptotic regimes, hence enabling to develop an analytic understanding on the scaling with dimensionless parameters of the flow.

Structure of the Habilitation thesis

This *cumulative Habilitation thesis* is composed of a total of 24 papers (listed in topical order in Supplement A), which I either wrote by myself or significantly contributed to. The entire work on all of these papers has been started after I received my PhD in 2005. For convenience, I will summarize the main findings of these papers on the following pages. This shall serve as a *compendium of the Habilitation thesis* while it is *not* meant as a replacement of the constituting papers. To keep the thesis focused on the topic "Interfacing high-energy astrophysics and cosmological structure formation", I decided not to include any body of further work on understanding the cluster physics of Sunyaev-Zel'dovich and X-ray surveys with the goal to improve cosmological parameter estimates that are associated with the growth of structure. Those papers are listed as "extra-curriculum work" in Supplement A.

In Chapter 1, I explore the role of CRs in galaxy clusters. Using a number of high-resolution hydrodynamical simulations in a cosmological setting and taking different injection scenarios into account (structure formation shocks and galactic supernovae), I assess the impact of CRs on the thermodynamic structure of clusters. I put forward a unified model of the non-thermal emission from cluster from the radio to the gamma-ray band. Testing this model prediction against observational data enables to constrain CR physics.

In Chapter 2, I study the magnetic draping effect in high-resolution MHD simulations. As a galaxy or merging subcluster moves through the weakly magnetized ICM, a comparably thin sheath of strong magnetic field is draped around it. This has important astrophysical consequences ranging from the suppression of particle transport processes across the interface to observable radio emission, enabling a new window onto cluster magnetic fields.

In Chapter 3, I investigate different radio probes of cosmological formation shocks. A radio galaxy that is interacting with the cluster accretion shock enables us to infer otherwise invisible properties of the shock and the infalling gas. Modeling giant "radio relics" in our cosmological simulations allows both to statistically infer properties about cluster magnetic fields and to improve our understanding of diffusive shock acceleration of electrons.

In Chapter 4, I study how CRs impact on galaxy and cluster formation. CRs transport energy and momentum comparably loss-less from the dense star-forming regions to the dilute interstellar medium. This launches and drives powerful and sustained winds in galaxies. Non-thermal observations of the central AGN of the Virgo cluster, M87, suggest that CRs are mixed with the ambient cluster plasma. These CRs heat the thermal cluster plasma at a rate that exactly balances the energy lost to radiative cooling, thus suggesting a solution to the "cooling flow problem".

Chapter 5 summarizes a simulation-based model for the different gamma-ray emission components from galaxy clusters including DM annihilation from the smooth halo and substructures as well as the dominant astrophysical component, i.e., pion decay emission induced by hadronic CR interactions with the ambient gas. This enables us to constrain various DM models through the non-observations of gamma-rays from galaxy clusters.

Chapter 6 introduces the plasma physics of "blazar heating" and its implications for gamma-ray astronomy. I also present the possible consequences of this novel heating mechanism for the thermal history of the intergalactic medium, the Lyman-α forest, and late-time structure formation.

I conclude and provide an outlook of this research area in Part III. The list of publications that cumulatively constitute this Habilitation thesis is presented in Supplement A while the complete list is given in Supplement B.

Part II.

Main part

1. Cosmic rays in galaxy clusters

Abstract

We construct a comprehensive model of cosmic rays (CRs) in galaxy clusters with the aid of cosmological hydrodynamical simulations and theoretical considerations. This enables us (1) to study the effect of cosmic rays on the thermal plasma and characterize the CR modifications of the X-ray emission and the Sunyaev-Zel'dovich effect, (2) to understand the physics underlying the non-thermal emission of radio halos and relics and to identify necessary physics extensions to make the models agree with the data, and (3) to characterize the gamma-ray emission of clusters and explore the different properties of the leptonic and hadronic emission components. We find that CRs obey a universal momentum spectrum and follow a similar spatial distribution within clusters, which allows us to construct a semi-analytical model for CRs in galaxy clusters. Such a baseline model is not only critical for reliably constraining the CR pressure with gamma-ray observations but also enables us to understand plasma physical properties associated with CR propagation and the shock acceleration efficiency.

1.1. Introduction

In the standard cosmological model, large scale structures grow hierarchically through merging and accretion of smaller systems into larger ones, and clusters are the latest and most massive objects to form. During the course of cluster assembly, energies of order of the final gas binding energy $E_b \sim 3 \times (10^{61} - 10^{63})$ erg should be dissipated through merger and accretion shocks (collectively called "structure formation shocks") as well as turbulence. The energy is expected to be dissipated on a dynamical timescale of $\tau_{\mathrm{dyn}} \sim 1$ Gyr. Hence the corresponding rates of energy release are $L \sim (10^{45} - 10^{47})$ erg s^{-1}, so even a small fraction of this energy channeled into non-thermal particles can be of major observable consequence. Shocks and turbulence are also likely to accelerate non-thermal electrons and protons to high energies.

Moreover, clusters are home to different types of energetic outflows, and the ICM can function as an efficient energy reservoir for CR protons, which have cooling times that are longer than the Hubble time (Völk et al. 1996). Most clusters are seen to harbor radio galaxies around their central regions, whose large, powerful jets of relativistic plasma are interacting vigorously with the ICM. An approximate estimate of the total energy output by a single powerful radio galaxy is $E_{\mathrm{RG}} \sim (10^{60} - 10^{62})$ erg, taking reasonable values for the kinetic luminosity $L_{\mathrm{RG}} \sim (10^{45} - 10^{46})$ erg s^{-1} and effective duration of activity $\tau_{\mathrm{RG}} \sim (10^7 - 10^8)$ yr (McNamara & Nulsen 2007). The integrated output from the whole cluster radio galaxy population should be even greater (Enßlin et al. 1998b). Although rarely seen in present-day clusters, another source which should have been active in the past are galactic winds, i.e. outflows driven by the joint action of numerous supernovae (Völk et al. 1996). Taking the observed mass of Fe in the ICM to be $M_{\mathrm{Fe,ICM}} \sim 3 \times (10^9 - 10^{10})$ M$_\odot$, the energy and Fe mass ejected by each supernovae to be respectively $E_{\mathrm{SN}} \sim 10^{51}$ erg and $M_{\mathrm{Fe,SN}} \sim 0.1M_\odot$, and an outflow efficiency $\xi_{\mathrm{GW}} \sim 0.1$ (Veilleux et al. 2005), we estimate the total galactic wind energy output to be $E_{\mathrm{GW}} \sim \xi_{\mathrm{GW}} M_{\mathrm{Fe,ICM}} E_{\mathrm{SN}} / M_{\mathrm{Fe,SN}} \sim 3 \times (10^{60} - 10^{61})$ erg. In any case, along with releasing energy, these sources can inject substantial quantities of non-thermal particles into the ICM, or could have done so in the past.

These arguments suggest that CRs may substantially contribute to the pressure support of the ICM. We already know that this non-thermal component plays an important role within our Galaxy since the CR pressure is comparable or larger to that of the thermal gas. If this were also the case for clusters, then their use for estimating cosmological parameters would be seriously jeopardized. This is because a substantial CR pressure substantially biases cluster mass estimates that are based on the assumption of hydrostatic equilibrium as well as the observed Sunyaev-Zel'dovich signal of clusters. On the other side, a large CR abundance would make clusters significant gamma-ray emitters because hadronic interactions of CR protons with the ambient dense gas produce gamma rays following the decay of the produced neutral pions. The additionally injected secondary electrons (from the decay of charged pions) would give rise to ubiquitous radio-halo emission that should be observable in every galaxy cluster—in conflict with the data. Hence previous to this Habilitation thesis time was ripe to develop a detailed theory of

the effect of CRs in clusters.[1] Given the complexity and non-linearity of the problem, this must be pursued with a necessarily heavy computational component that self-consistently follows CR physics on top of the hydrodynamics in a cosmological setting.

To this end, I use the formulation of CR physics that I have developed in collaboration with colleagues during my PhD thesis (Pfrommer et al. 2006, Enßlin et al. 2007, Jubelgas et al. 2008). The CR model follows the most important injection and loss processes self-consistently while accounting for the CR pressure in the equations of motion. In our methodology, the non-thermal CR population of each gaseous fluid element is modeled by one or several power law spectra in particle momentum (with different spectral indices). Taking different moments of this distribution function gives the CR density, pressure, and internal energy, which in concert with the thermodynamic quantities of the gas feed back onto the hydrodynamic flow properties. Adiabatic CR transport processes such as compression and rarefaction, and a number of physical source and sink terms, which modify the CR pressure of each particle, are also modelled. The most important sources considered are injection by supernovae and diffusive shock acceleration at cosmological structure formation shocks, which we detect and characterize during the run time of the simulation (Pfrommer et al. 2006). Primary sinks are thermalization by Coulomb interactions, and catastrophic losses by hadronic interactions. This allows us to answer the following important and profound puzzles in this chapter:

- How do CRs modify thermodynamic properties of galaxy clusters?

- Which physical process makes clusters glow as radio halos and relics?

- What is the dominant gamma-ray emission process in clusters?

- How do the different gamma-ray emission components look like spectrally and spatially?

- How large is the CR bias of hydrostatic equilibrium masses and of the Sunyaev-Zel'dovich effect in clusters?

1.2. How cosmic rays effect the thermal plasma

We performed high-resolution simulations of a sample of 14 galaxy clusters that span a mass range of almost two orders of magnitude to study the effects of CRs on thermal cluster properties and observables such as X-ray emission and the Sunyaev-Zel'dovich effect. Our simulations were carried out with an updated and extended version of the distributed-memory parallel smoothed particle hydrodynamics code GADGET-2 (Springel 2005). We visualize the cosmic web surrounding a massive galaxy cluster in such a zoom cosmological simulation in Fig. 1.1 and show gas density, temperature, and cosmological shock strengths. Following the CR physics on top of the hydrodynamics enables us to characterize the resulting CR pressure distribution, which is shown in Fig. 1.2. Assuming optimistic values for the maximum CR acceleration efficiency, we find that the volume average of the CR-to-thermal pressure ratio within the virial radius is about $X_{CR} = \langle P_{CR} \rangle / \langle P_{th} \rangle \simeq 0.02$ (Pfrommer et al. 2007, Pinzke & Pfrommer 2010), and correspondingly lower for smaller acceleration efficiencies. The relative CR pressure rises toward the outer regions to assume $X_{CR} \simeq 0.03$ at the virial radius (and increases steadily for larger radii) due to a combination of the following effects: CR acceleration is more efficient at peripheral strong accretion shocks compared to weak central flow shocks, adiabatic compression of a composite of CRs and thermal gas disfavours the CR pressure relative to the thermal pressure due to the softer equation of state of CRs, and CR loss processes are more important at the dense centres. In the radiative simulations (that include radiative cooling, star formation, and supernova feedback) the relative CR pressure reaches high values of the order of equipartition with the thermal gas in each cluster galaxy due to the fast thermal cooling of gas which diminishes the thermal pressure support relative to that in CRs. This also leads to a lower effective adiabatic index of the composite gas toward the cluster center that increases the compressibility of the intra-cluster medium. This effect slightly increases the central density, thermal pressure and the gas fraction. While the X-ray luminosity in low mass cool core clusters is boosted by up to 40 per cent, the integrated Sunyaev-Zel'dovich effect appears to be remarkably robust and the total flux decrement only slightly reduced by 2 per cent (as expected from the volume averaged CR pressure fraction). The resolved Sunyaev-Zel'dovich maps, however, show a larger variation with an increased central flux decrement.

---

[1] The earlier published body of work (Miniati et al. 2000, 2001) lacked the resolution sufficient to predict CR properties within clusters and their distribution of shock strengths, which is critical for accurately simulating CR acceleration, disagrees with any other published distribution (Vazza et al. 2011).

Gas density:

Gas temperature:

Shock Mach numbers weighted by $\dot{E}_{\mathrm{diss}}$:

Shock Mach numbers weighted by $\dot{E}_{\mathrm{CR,inj}}$:
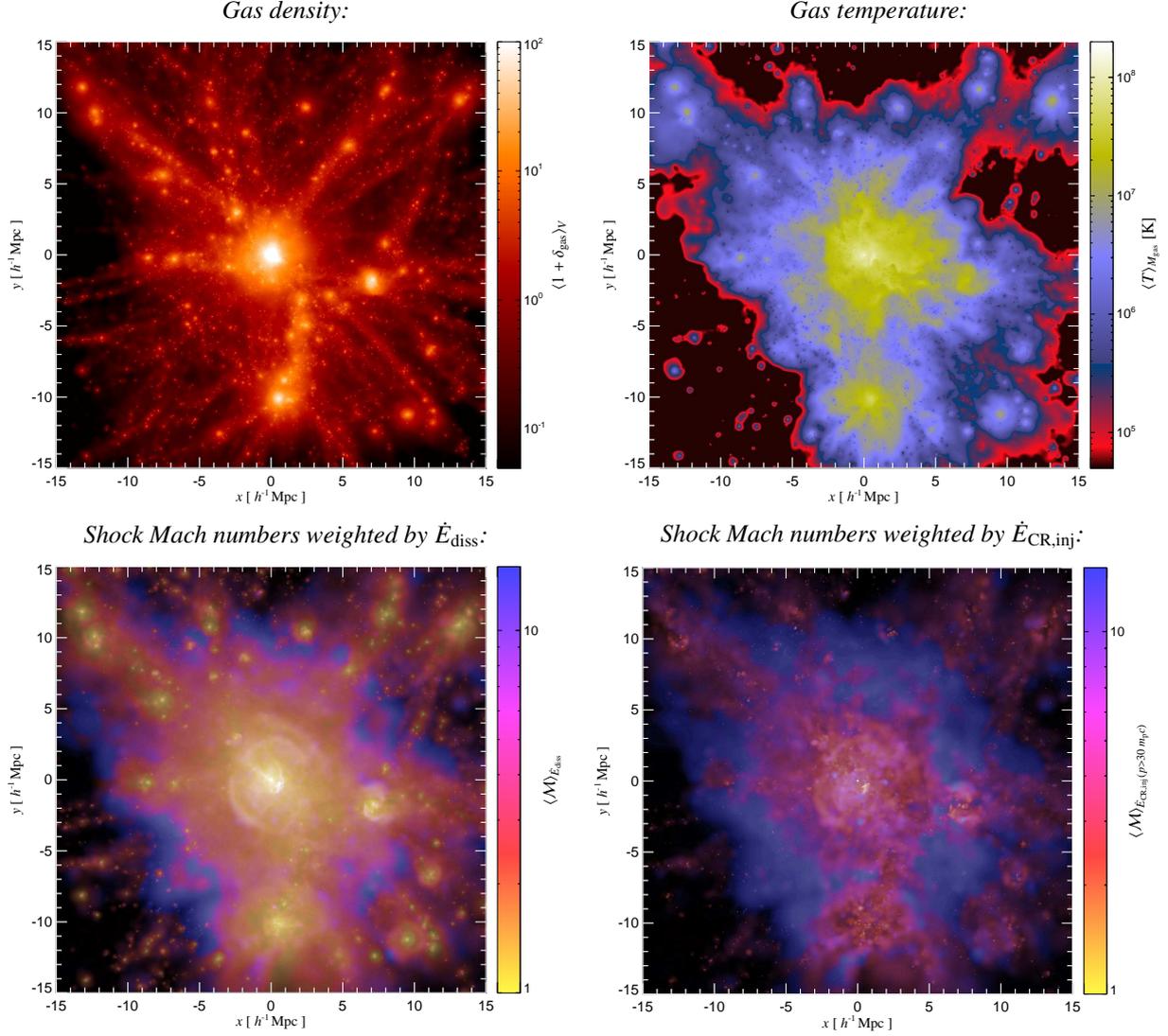
Figure 1.1.: The cosmological environment of a large post-merging galaxy cluster ($M \simeq 10^{15}\,\mathrm{M}_\odot$). Our simulation follows radiative gas physics and star formation and accounts for CR acceleration at structure formation shocks. Shown are the line-of-sight averaged density (top left), the mass weighted temperature (top right), the Mach number $\mathcal{M} = \upsilon/c_{\mathrm{s}}$, i.e., the shock speed in units of the pre-shock sound speed, weighted by the energy dissipation rate in colour (while the brightness displays the logarithm of the dissipation rate, bottom left), and the Mach number of shocks weighted by the energy injection rate of CR protons in colour (while the brightness displays the logarithm of the CR proton energy injection rate, bottom right). For better comparison, we used the same colour and brightness scale in the bottom plots. Only CR protons with a momentum $p > 30\,m_{\mathrm{p}}c$ have been considered for calculating the CR pressure since lower energetic CR protons are not detectable at radio frequencies $\nu > 120$ MHz by means of hadronically produced secondary electrons (from Pfrommer et al. 2008).
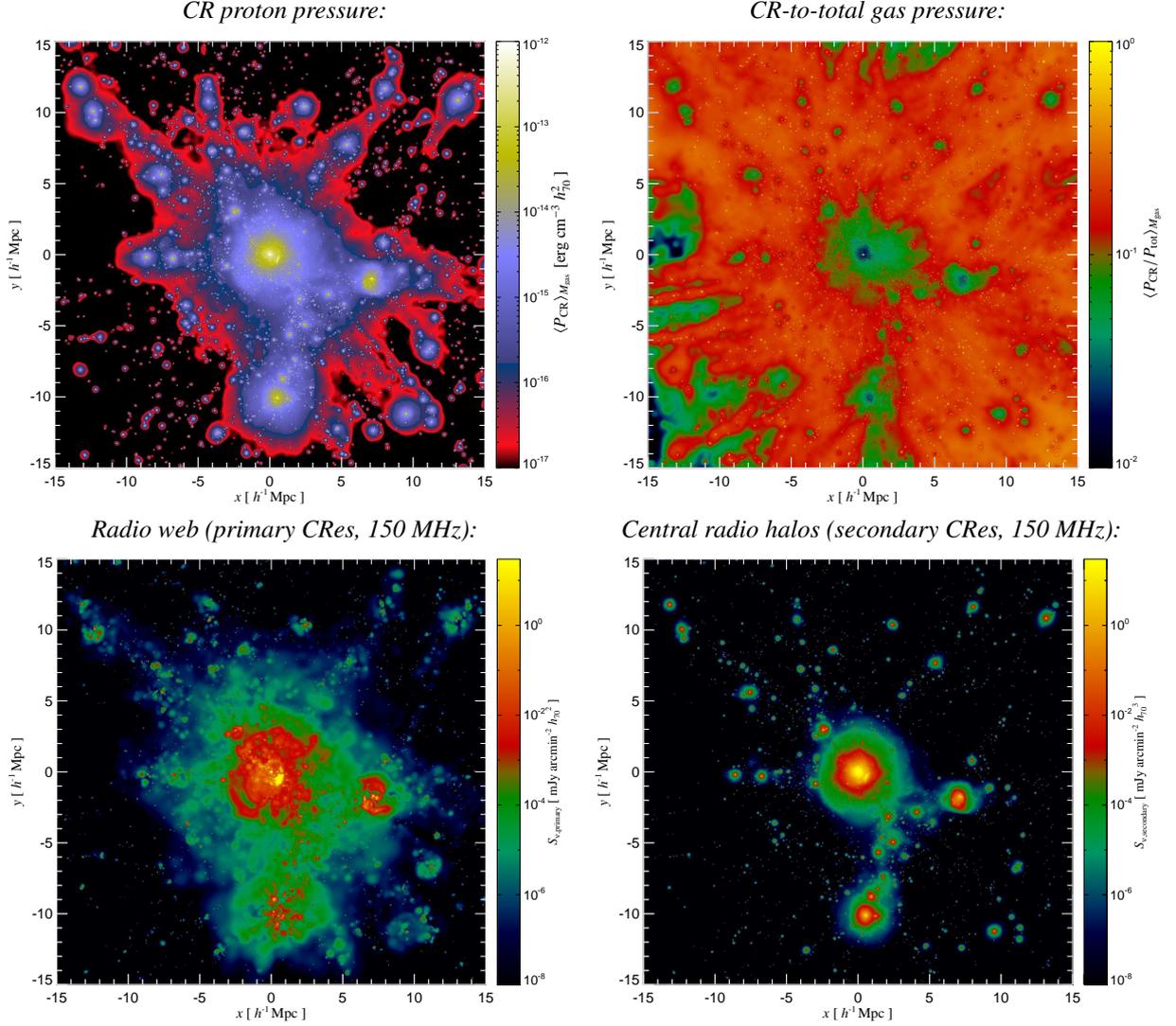
Figure 1.2.: CR proton pressure and synchrotron emission maps in the simulated super-cluster environment of Fig. 1.1. The mass weighted CR pressure (top left) is contrasted with the mass weighted CR-to-total gas pressure ratio (top right). Since the CR proton pressure decreases less steeply than the gas pressure as a function of cluster radius, this results in an increasing relative CR pressure profile toward the periphery. In the bottom panels, we show the simulated radio emission of the magnetized cosmic web at 150 MHz of large-scale environment of our Coma-like cluster that experienced a recent merger. We show the synchrotron emission of *primary CR electrons* that were directly accelerated at structure formation shocks (bottom left) as well as the radio emission of *secondary CR electrons* that results from hadronic CR proton interactions with ambient gas protons (top right). The secondary radio emission is characterized by a regular morphology, which reflects that of the parent CR proton population (top left), and dominates in the centre. At larger radii, we observe a transition to the the irregularly shaped primary radio "gischt" emission with a prominent radio relic to the lower right of the cluster (from Pfrommer et al. 2008).
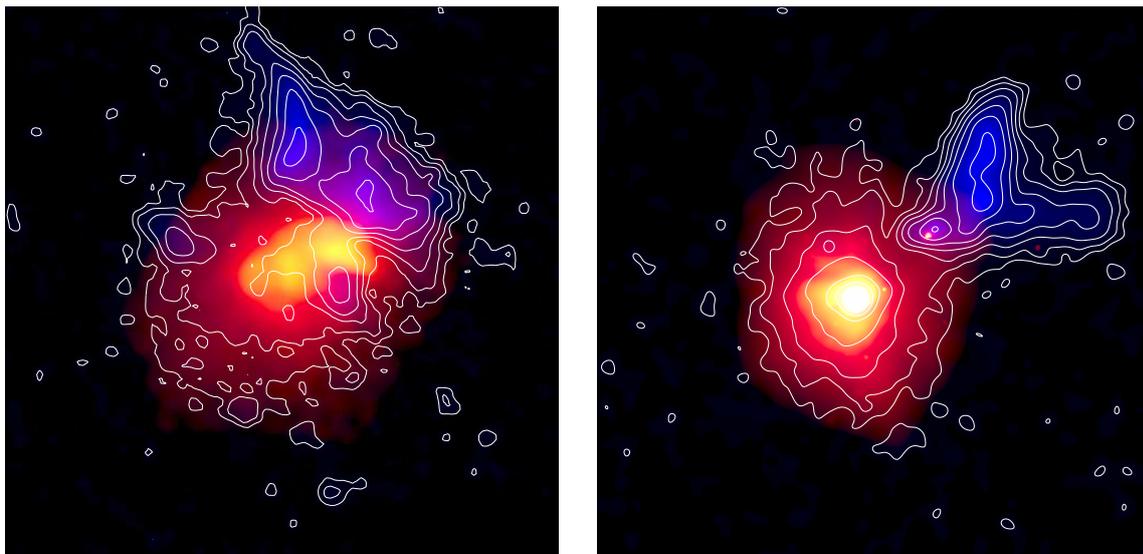
Figure 1.3.: Cluster radio emission (blue/contours) superposed on the X-ray emission (red/yellow). The overall emission morphology of A2256 (left panel, Clarke & Ensslin 2006) compares well to the radio emission of our simulated merging cluster (right panel), which we smooth to the same resolution and add Gaussian noise at a comparable level as the data (Pfrommer, in prep.). In our simulation models, the centrally located giant radio halo is due to hadronically produced secondary electrons, while the peripheral radio relic emission is generated by primary shock-accelerated CR electrons. However, the simulated cluster center is too dense and cold, resulting in too much radio and X-ray emission.

1.3. The physics of radio halos and relics

The thermal plasma of galaxy clusters lost most of its information on how structure formation proceeded as a result of dissipative processes. In contrast, non-equilibrium distributions of CRs preserve the information about their injection and transport processes and provide thus a unique window of current and past structure formation processes. This information can be unveiled by observations of non-thermal radiative processes, including radio synchrotron, hard X-ray, and gamma-ray emission. To explore this, we model relativistic electrons that are accelerated at cosmological structure formation shocks and those that are produced in hadronic interactions of CRs with ambient gas protons. We find that the CR proton pressure traces the time integrated non-equilibrium activities of clusters and is modulated by the recent dynamical activities (Pfrommer et al. 2008). In contrast, the pressure of primary shock-accelerated CR electrons resembles current accretion and merging shock waves that break at the shallow cluster potential in the virial regions. The resulting synchrotron emission is predicted to be polarised and has an inhomogeneous and aspherical spatial distribution which matches the properties of observed giant radio relics (see Fig. 1.2).

We propose a unified scheme for the generation of giant radio halos as well as radio mini-halos that naturally arises from our simulated synchrotron surface brightness maps and emission profiles (Pfrommer et al. 2008). Giant radio halos are dominated in the centre by hadronically produced, secondary synchrotron emission with a transition to the radio synchrotron radiation emitted from primary, shock-accelerated electrons in the cluster periphery. The successful model is demonstrated in Fig. 1.3. Comparison to the X-ray and radio observations argues for including self-regulated AGN feedback in the next generation of simulations to arrest the overcooling in the cluster center. Calibrating the magnetic fields of our model with Faraday rotation measurements, the synchrotron emission of our relativistic electron populations matches the radio luminosities and morphologies of observed giant radio halos and mini-halos well (Pfrommer 2008). This model is able to explain the regular structure of radio halos by the dominant contribution of hadronically produced electrons. At the same time, it is able to account for the irregular morphology of the peripheral radio emission and the larger variation of the spectral index due to the prevailing primary emission there. However, the model is unable to explain the absence of radio halo emission in the so-called "radio-quite" cluster population.

15
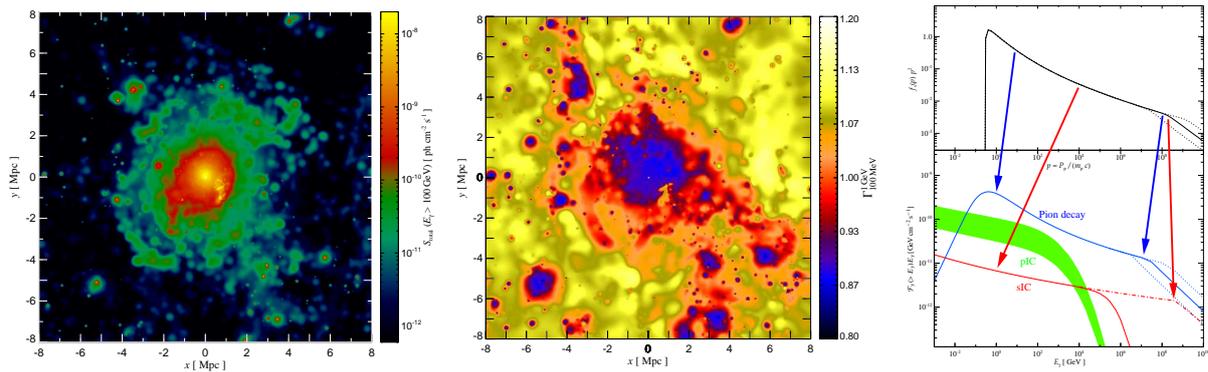
Figure 1.4.: Expected gamma-ray emission in a cosmological hydrodynamical simulation of a galaxy cluster. The surface brightness emission (left) and spectral index map, $\Gamma_{100\,\mathrm{MeV}}^{1\,\mathrm{GeV}}$, (middle) is dominated in the center by pion decay and outside the virial radius (of 2.4 Mpc) by primary inverse Compton (pIC) emission from shock-accelerated relativistic electrons. The total CR proton spectrum shows a universal shape across clusters (top right) that is inherited by the pion decay and secondary inverse Compton emission (sIC) following hadronic p-p interactions (bottom right). The primary inverse Compton emission contributes a negligible fraction to the total emission at $E > 30\,\mathrm{MeV}$ (from Pinzke & Pfrommer 2010).

To solve this problem, we need to investigate the interplay of CR propagation and advection in galaxy clusters (which will also be of great importance for the formation and evolution of galaxies, see Chapter 4). Advection of CRs by the turbulent gas motions produces centrally enhanced profiles. In contrast, CR streaming and diffusion along magnetic field lines implies a net outward flux of CRs that causes the profiles to flatten, approaching an equal CR number density everywhere (Enßlin et al. 2011). As a consequence, the CR spatial distribution will be bimodally distributed. Strongly turbulent, merging clusters should have a more centrally concentrated CR energy density profile in comparison to relaxed clusters, in which CR streaming should be the dominant CR transport process since this class of clusters is characterized by decaying subsonic turbulence. This translates into a bimodality of the expected diffuse radio and gamma-ray emission of clusters, since more centrally concentrated CR will find higher target densities for hadronic CR proton interactions, higher plasma wave energy densities for CR electron and proton re-acceleration, and stronger magnetic fields. Thus, the observed bimodality of cluster radio halos appears to be a natural consequence of the interplay of CR transport processes, independent of the model of radio halo formation, be it hadronic interactions of CR protons or re-acceleration of low-energy CR electrons. Future low-frequency radio telescopes (LOFAR, GMRT, MWA, LWA) are expected to probe the accretion shock regions of clusters and the warm-hot intergalactic medium, depending on the adopted model for the magnetic fields. The hadronic origin of radio halos can be scrutinised by the detection of pion-decay induced gamma-rays following hadronic CR interactions (Pfrommer 2008).

1.4. Simulating the gamma-ray emission

To complement these modeling efforts in the radio band, we simulate the expected gamma-ray emission from clusters. The high-energy gamma-ray emission above 100 MeV is dominated by pion decays resulting from hadronic cosmic ray interactions (Pfrommer et al. 2008). Using the complete sample of the brightest X-ray clusters observed by ROSAT in combination with our simulated scaling relation between gamma-ray luminosity and cluster mass, we predict the brightest clusters for the gamma-ray space telescope Fermi and current imaging air Cherenkov telescopes MAGIC, H.E.S.S., and VERITAS (Pfrommer 2008). However, the expected gamma-ray luminosity scales with the abundance of CRs, which itself depends on the assumed acceleration efficiency at structure formation shocks. This quantity is very uncertain as it depends on unknown plasma physical processes at structure formation shocks during the epoch of cluster formation and in principle could be very low. However, for clusters with a giant radio halo, we can construct an absolute lower flux limit for the gamma-ray emission in the hadronic model for the radio emission (Pfrommer 2008). This is because in the limit of strong magnetic fields, steady state CR electrons lose all

their energy through synchrotron radiation, which becomes virtually independent of the magnetic field strength. The strong field limit implies the lowest CR electron abundance that is still able to produce the observed radio luminosity. Since these CR electrons are by assumption injected in hadronic CR proton interactions, this also corresponds to the lowest CR proton abundance and hence lowest induced gamma-ray emission, providing thus a unique test for the possible hadronic origin of radio halos.

In a follow-up work, we refine the CR modeling and study the detailed CR proton spectra as well as the different contributions of the pion decay and inverse Compton emission to the total flux and present spectral index maps (Pinzke & Pfrommer 2010). We find a universal spectrum of the CR component in clusters with surprisingly little scatter across our cluster sample (see Fig. 1.4). When CR diffusion is neglected, the spatial CR distribution also shows approximate universality; it depends however on the cluster mass. This enables us to derive a semi-analytic model for both, the distribution of CRs as well as the pion-decay gamma-ray emission and the secondary radio emission that results from hadronic CR interactions with ambient gas protons. The model represents a non-linear map from the CR shock acceleration efficiency and CR propagation parametrization to the final distribution. Observationally constraining the latter allows to draw conclusions on the underling CR physics. Identifying the gamma-ray flux fraction contributed by cluster galaxies (some of which may be artifacts of the numerical method), we provide somewhat more conservative predictions for the gamma-ray fluxes in the energy regimes of Fermi and imaging air Cherenkov telescopes in comparison to the earlier result (Pfrommer 2008). We find that it will be challenging to detect cluster gamma-ray emission with Fermi after the second year but this mission has the potential of constraining interesting values of the shock acceleration efficiency after several years of surveying. Comparing the predicted emission from our semi-analytic model to that obtained by means of our scaling relations, we find that the gamma-ray scaling relations underpredict, by up to an order of magnitude, the flux from cool core clusters.

1.5. Observationally constraining cosmic rays

Gamma rays cannot penetrate the Earth's atmosphere to the ground. To directly detect them, we have to go to space, where the Large Area Telescope onboard *Fermi* is currently surveying the entire sky at energies ranging from around 100 MeV to 100 GeV. The upper energy limit is determined by the finite size of the detector, which uses the pair conversion technique to detect gamma rays. However, for a gamma-ray energy above 30 GeV, it is feasible to detect the flash of Cherenkov light that is emitted in the electromagnetic cascade initiated by the gamma ray penetrating the Earth's upper atmosphere. This allows to reconstruct the energy and arrival direction of the original gamma ray and opens a second window to the gamma-ray sky that is employed by the imaging air Cherenkov telescope collaborations H.E.S.S., MAGIC, and VERITAS. Those have to conduct pointed observations of interesting targets. While this allows deeper observations on single objects with better angular resolution, it complicates the characterization of the selection function for population studies.

There is an exciting quest for the first detection of gamma-ray emission from clusters of galaxies as we are entering a new era of high-energy gamma-ray experiments. I have joined various observational collaborations as lead theory author including *Fermi*, MAGIC, and VERITAS. My role in these consists of the source modeling required for providing model predictions, for finding promising targets and (in the case of the Cherenkov technique) for convincing the collaborations to invest their precious observational time, for translating non-detections into physical constraints, and for testing self-consistent models against data. We conducted the deepest to date observational campaign targeting a galaxy cluster at very high-energy gamma-rays and observed the Perseus cluster with the MAGIC Cherenkov telescopes for a total of ~ 85 h of effective observing time. This campaign resulted in the detection of the closest known TeV blazar IC 310 (Aleksić et al. 2010) and the central radio galaxy NGC 1275 at energies $E > 100$ GeV with a very steep energy spectrum (Aleksić et al. 2012b).

As a result of these endeavours, we still have not been able to detect any cluster-wide gamma-ray emission at GeV and TeV energies yet. These deep gamma-ray limits from *Fermi*, MAGIC, and VERITAS translate into tight constraints on the CR pressure contribution and limit $X_{CR} < 0.017$ in the Coma and Perseus clusters (Arlen et al. 2012, Aleksić et al. 2012a) and typically to less than a few per cent for the next to best targets (Ackermann et al. 2010, Pinzke et al. 2011). A joint likelihood analysis searching for spatially extended gamma-ray emission at the locations of 50 galaxy clusters in 4 years of *Fermi*-LAT data does not reveal any CR signal and limits the CR-to-thermal pressure ratio to be below $0.012 - 0.014$ depending on the morphological classification (Ackermann et al. 2013).

1.6. Summary and Outlook

We developed a self-consistent model for CRs in galaxy clusters. It successfully explains some properties of cluster radio emission, but also highlights shortcomings. Those are addressed by the next generation of models, which are characterized by CR physics of higher complexity such as CR propagation. Modeling these theoretical ideas in 3D magneto-hydrodynamical simulations within a cosmological setting is required to progress to the next level. In any case, the tight CR pressure constraints that have been obtained in this chapter are excellent news for the use of clusters to estimate cosmological parameters. Those guarantee that the bias due to a CR component that is fully mixed with the ICM is at most at the per cent level for hydrostatic equilibrium masses or the Sunyaev-Zel'dovich flux decrement.

2. Magnetic fields in galaxy clusters

Abstract

Using three-dimensional magneto-hydrodynamical simulations and analytic calculations, we study the draping of magnetic fields over moving cores, radio lobes, and galaxies. If such an object moves through a weakly magnetized medium, as we e.g., encounter in a cluster, a sheath of strong magnetic field drapes around the object, with important astrophysical consequences. (1) Thermal conduction and diffusion are substantially suppressed across the magnetized interface, giving rise to some of the observed "cold fronts" in merging galaxy clusters. (2) The magnetic tension of the draping sheath around a buoyantly rising radio lobe stabilizes the interface against hydrodynamic instabilities that would otherwise disrupt it. (3) Magnetic draping at spiral galaxies orbiting in the Virgo cluster can explain the presence of the observed radio synchrotron ridges offset from the galaxies' centres. This magnetic drape is then lit up with cosmic rays from the galaxies' exploding stars, generating coherent polarized emission at the galaxies' leading edges. This immediately presents a novel technique for probing local orientations and characteristic length scales of cluster magnetic fields. The first application of this technique, mapping the field of the Virgo cluster, shows that the magnetic field is preferentially oriented radially, which implies important consequences for cluster evolution.

2.1. Introduction

Despite many observational efforts to measure galactic and intergalactic magnetic fields, their properties and origin are currently not well understood. The magnetic fields influence the physics of the plasma in several important ways. They couple the collisionless charged particles to a single but complex fluid through the Lorentz force, and trace dynamical processes in the Universe. Magnetic pressure and tension mediate forces and provide the plasma with additional macroscopic degrees of freedom in terms of Alfvénic and magnetosonic waves. They cause the turbulent cascade to become anisotropic toward smaller scales and suppress transport processes such as heat conduction and CR diffusion across the mean magnetic field. They are essential for accelerating CRs by providing macroscopic scattering agents which enables diffusive shock acceleration and through magneto-hydrodynamic (MHD) turbulent interactions with CRs that energize them. They illuminate distant CR electron populations by enabling synchrotron emission and tell us indirectly about violent high-energy astrophysical processes such as formation shock waves. The magnetic fields in spiral field galaxies are highly regular, showing alignment with the spiral arms. They are believed to arise from weak seed fields amplified by dynamo processes, driven by differential rotation in galactic disks. The seed fields could have been produced by many sources, ranging from stellar winds and jets of AGN, to plasma instabilities and battery effects in shock waves, in ionization fronts, and in neutral gas-plasma interactions. More hypothetical ideas for the seed field origins invoke primordial generation in early universe processes, such as phase transitions during the epoch of inflation. In order to understand more about magneto-genesis, we need to study the least processed plasma possible that still shows some primordial memory. This points us to the magnetized plasma in intergalactic space, in particular to the plasma in galaxy clusters. There, magnetic fields show a smaller degree of ordering compared to spiral galaxies. However, their primordial properties may be masked in clusters because of processing by turbulent gas flows, driven by galaxy cluster mergers, and the orbits of the member galaxies.

High-resolution X-ray observations have revealed cavities and "cold fronts" with sharp edges in temperature and density within galaxy clusters. Their presence poses a puzzle since these features are not expected to remain sharp in the presence of diffusion and thermal conduction. In fact, the sharp temperature drop implies the suppression of heat conduction across the interface by a factor of more than two orders of magnitude of the Spitzer value (Ettori & Fabian 2000) while the density drop requires a suppression of Coulomb diffusion by a factor of several (Vikhlinin et al. 2001). In some clusters, AGN blown radio lobes remain intact to radii that are larger than the pressure scale heights. However, these lobes are not expected to remain hydrodynamically stable in the presence of Kelvin-Helmholtz and Rayleigh-Taylor instabilities that should long have disrupted these underdense lobes. Faraday
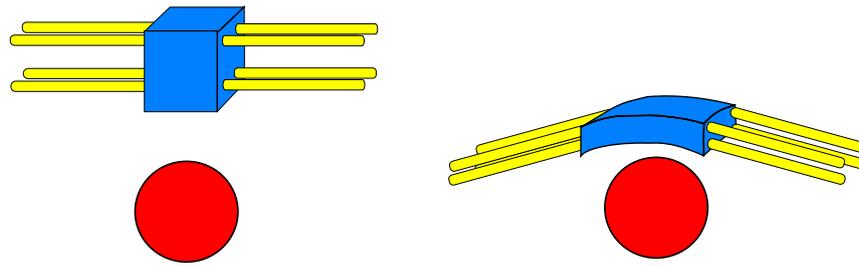
Figure 2.1.: A cartoon showing the distortion of incoming fluid elements and stretching of field lines as a red spherical projectile moves upwards through the ambient, weakly magnetized medium (from Dursi & Pfrommer 2008).

rotation measurements of extended radio sources seen in projection on a cluster have revealed that magnetic fields are dynamically not important in the bulk of the intra-cluster plasma. So naively one would expect that magnetic fields can be neglected when studying the problems presented above but as we will demonstrate below, such naive considerations are very misleading. In particular, we will answer the following questions (or parts of them) in this chapter:

- How are "cold fronts" produced in clusters?

- How are rising radio lobes stabilized against disruption?

- What is the prevailing morphology of cluster magnetic fields?

- Do dynamically weak magnetic fields always remain weak during their evolution?

2.2. Magnetic draping

We start by addressing the last, ostensibly innocent question. A super-alfvénically moving object in even a very weakly magnetized plasma necessarily sweeps up enough magnetic field to build up a dynamically important sheath; the layer's strength is set by a competition between "plowing up" and slipping around of field lines (Lyutikov 2006, Dursi & Pfrommer 2008). The plasma is *not* compressed at the contact discontinuity between the moving object and the ambient plasma. Instead the incoming fluid elements are distorted, which causes the field lines to be stretched and increases the magnetic tension force (see Fig. 2.1). In steady state, the magnetic energy density in the layer balances the ram pressure seen by the moving object and hence becomes dynamically important. For clusters, this implies an amplification of the magnetic energy density by typically a factor of 100 from its value in the bulk of cluster plasma. As the fluid enters the region of strong magnetic field, the flow is decelerated by the magnetic backreaction. We provide three-dimensional (3D) renderings of the magnetic energy density and fiducial magnetic field lines (see Fig. 2.2) as well as renderings of representative streamlines of the flow (see Fig. 2.3).

In this inherently three dimensional problem, our numerical experiments and analytic arguments show that this layer modifies the dynamics of a plunging core, greatly modifying the hydrodynamic instabilities and mixing, changing the geometry of stripped material, and slowing the core through magnetic tension (Dursi & Pfrommer 2008). This magnetic draping effect stabilizes the interface against the shear that creates it in first place (Dursi 2007), suggesting a physical solution to the puzzling stability of rising radio lobes (as successfully demonstrated in MHD simulations by Ruszkowski et al. 2007). We derive an analytic expression for the maximum magnetic field strength and thickness of the layer, as well as for the opening angle of the magnetic wake. The morphology of the magnetic draping layer implies the suppression of thermal conduction across the layer, thus conserving strong temperature gradients and suggesting a natural explanation for the existence of cold fronts across merging cluster cores. The intermittent amplification of the magnetic field as well as the injection of MHD turbulence in the wake of the core is identified to be due to vorticity generation within the magnetic draping layer. These results have important consequences for understanding the complex gasdynamical processes of the intra-cluster medium, and apply quite generally to motions through other magnetized environments, e.g., the interstellar medium.
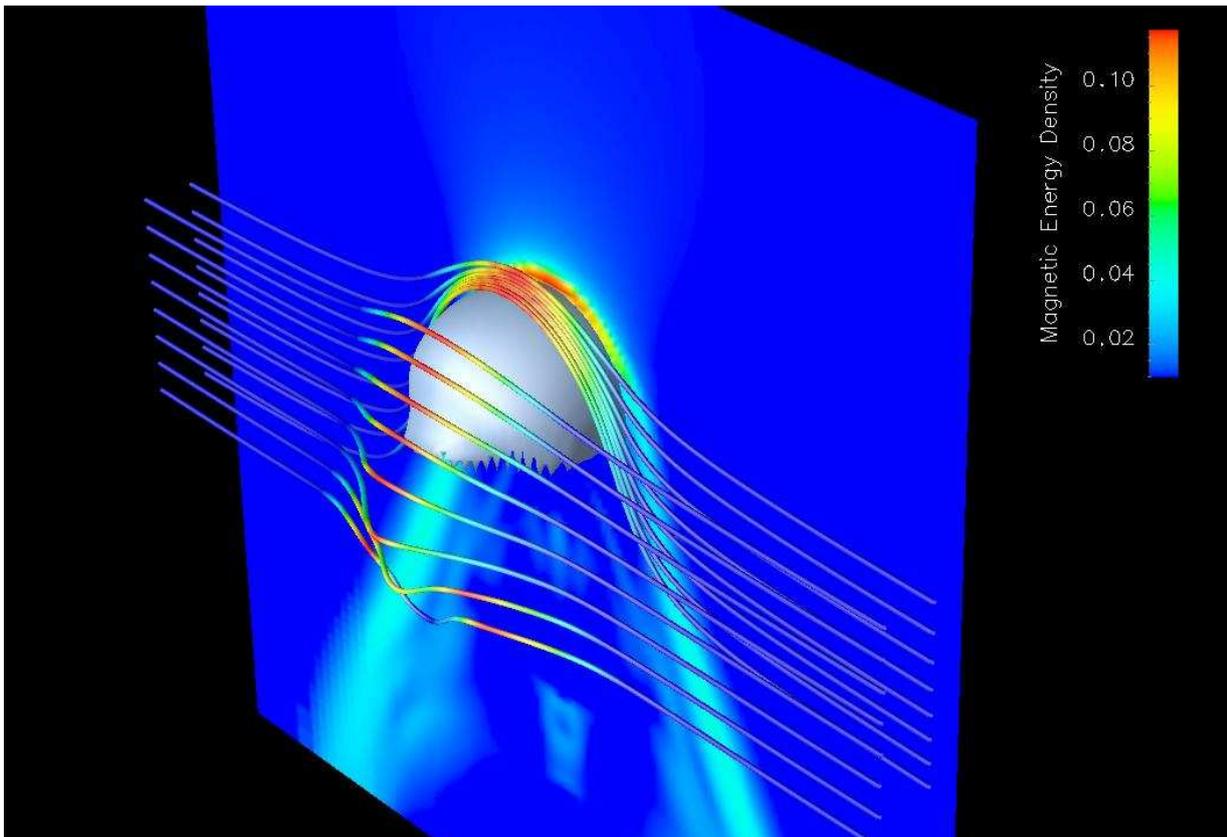
Figure 2.2.: A rendering of our 3D MHD simulation to illustrate the "magnetic draping" effect (from Dursi & Pfrommer 2008). An overdense projectile is moving through a uniformly magnetized medium, sweeping up magnetic field ahead of it. Plotted is a density isosurface, corresponding to the mean density of the bullet, and some fiducial magnetic field lines. The cut plane is coloured by magnetic energy density, as are the field lines. The magnetic field is "draped" into a thin layer forming a bow wave, leaving turbulence in a wake behind the bullet. Magnetic field lines pile up along the stagnation line of this initially axisymmetric bullet, while in the plane perpendicular to the initial field, the field lines can slip around the bullet.
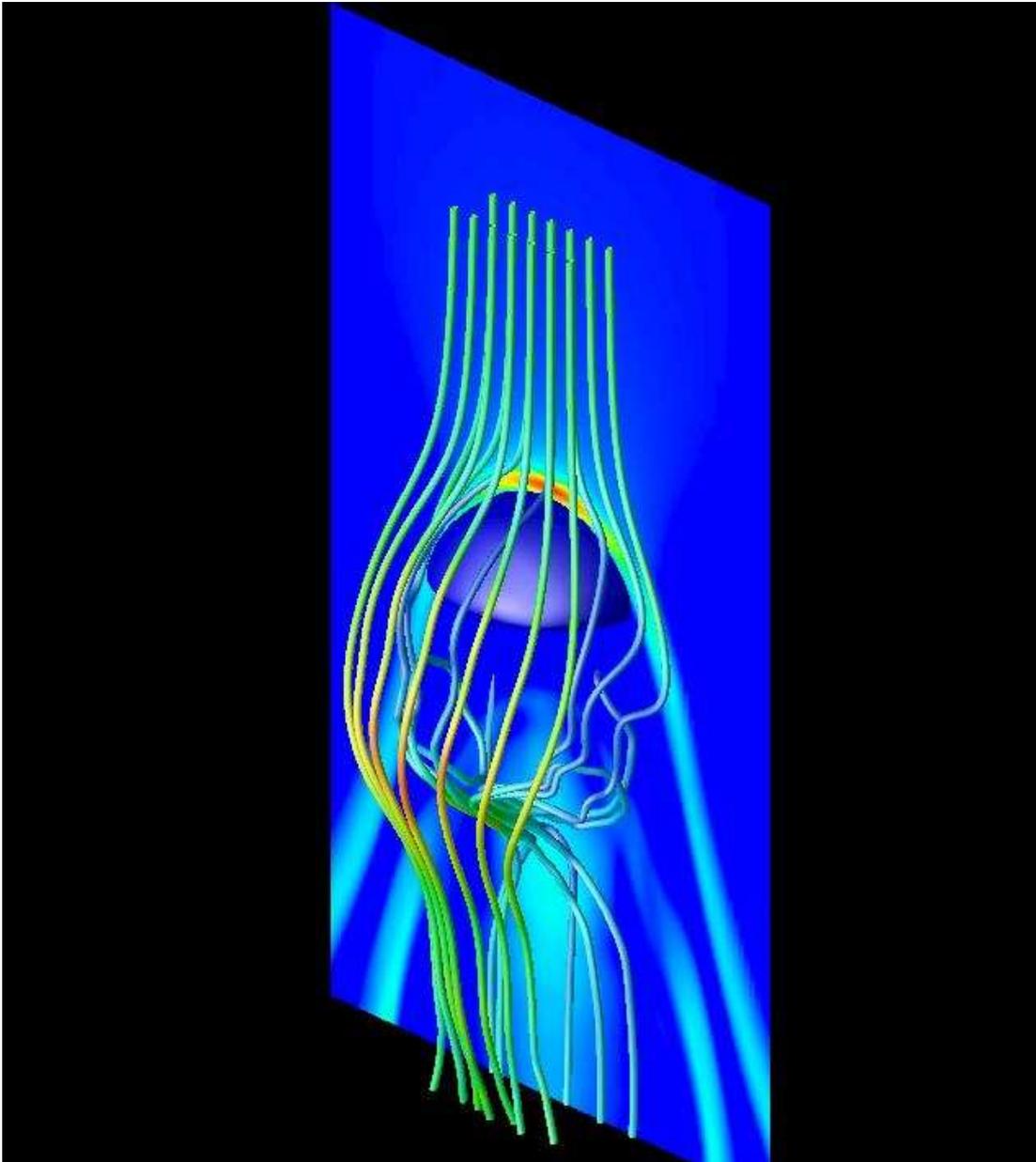
Figure 2.3.: We show streamlines over a projectile that moves through a weakly magnetized medium (from Dursi & Pfrommer 2008). Streamlines are calculated in the frame of the mean velocity of the projectile. The streamlines are coloured by the magnitude of velocity, and the cut plane is colored by magnetic energy density. Fluid that does not intersect the magnetic draping layer flows smoothly over the projectile and is accelerated as the flow volume decreases at the sides of the projectile through the Bernoulli effect. However, fluid that enters the draping layer is decelerated by the magnetic backreaction. This plot visualizes the vorticity generation within the magnetic draping layer, which injects MHD turbulence in the wake of the projectile.

Total PI = 8.2 mJy
Max PI = 220 μJy/beam

Total PI = 8.4 mJy
Max PI = 330 μJy/beam
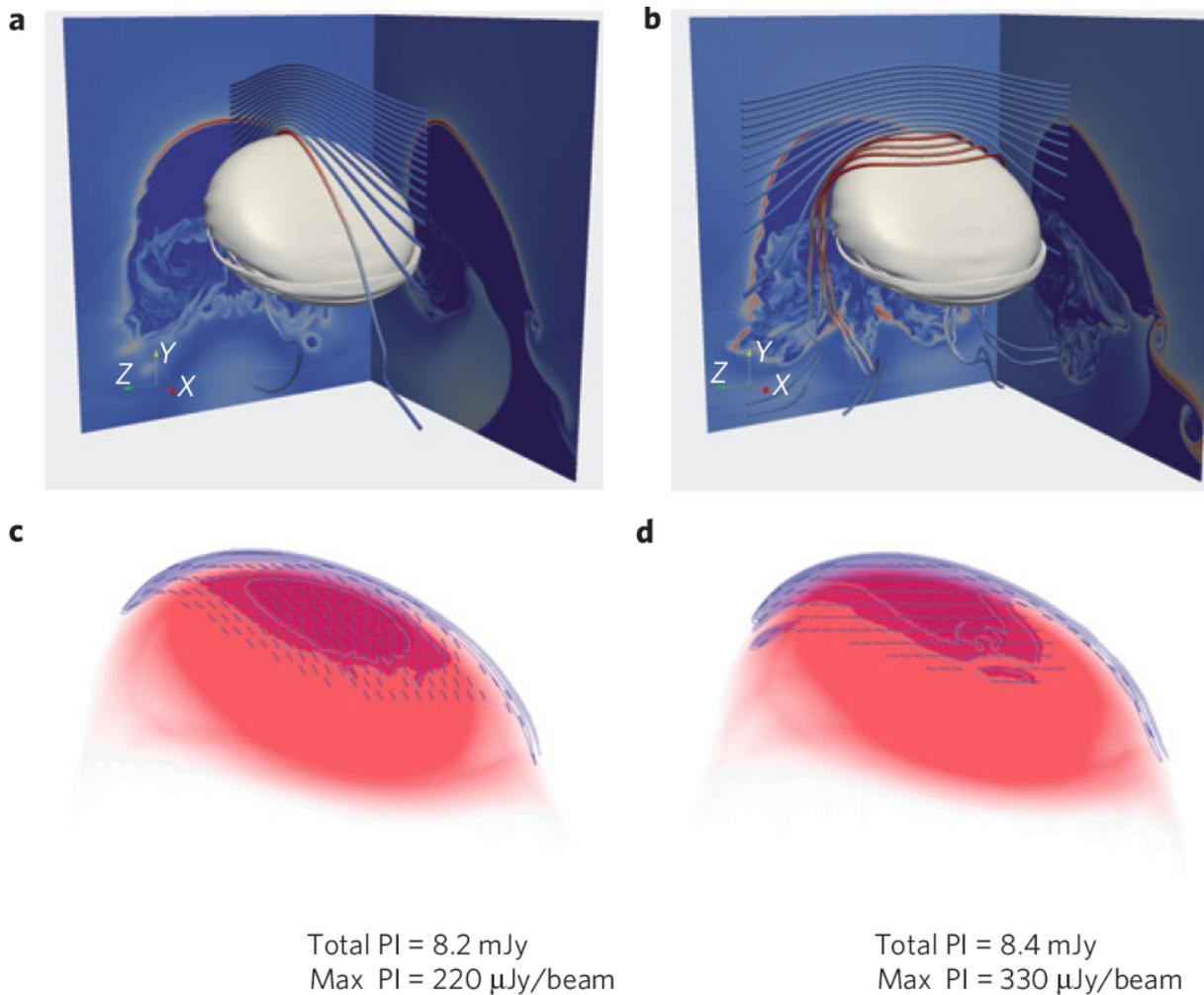
Figure 2.4.: Magnetic draping in a high-resolution MHD simulation (from Pfrommer & Dursi 2010). Top panels: as the galaxy (represented by a grey isosurface) moves upwards through a weakly magnetized medium a sheath of strong magnetic field is draped around. The left and right panels differ only by the field orientations (visualized by representative field lines and color-coded by the local magnetic field strength), causing distinct dynamics in the wake and observational signatures. This is demonstrated in the bottom panels that show projected density (red) and polarized synchrotron emission (blue contours). Lines indicate local polarization direction rotated by 90° to indicate the magnetic field orientation and nicely match the simulated field orientations.
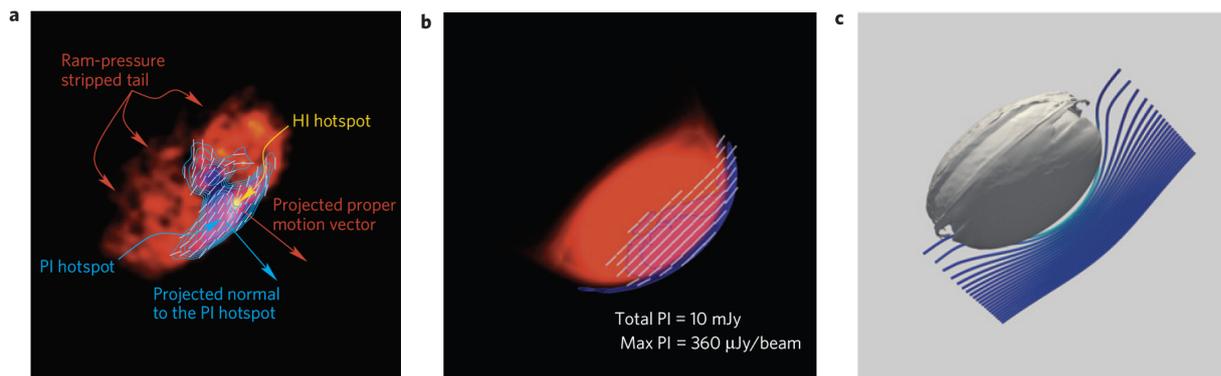
Figure 2.5.: Polarized radio emission: observation versus simulation. **a**, HI emission of the Virgo spiral NGC 4501 tracing the neutral hydrogen distribution that is severely affected by the ram pressure resulting from the galaxies' motion in the intracluster plasma (red-to-yellow). Over-plotted is the polarized intensity (PI) of the radio ridge (blue/contours) with the B-vectors indicated in white. **b**, Simulated synchrotron map of our best-matching MHD galaxy model that drapes a homogeneous cluster magnetic field around its front side. **c**, A 3D volume rendering of our MHD galaxy simulation (grey isosurfaces) and representative magnetic field lines (from Pfrommer & Dursi 2010).

2.3. Polarized radio ridges at cluster galaxies

High-resolution radio continuum observations of cluster spirals in Virgo show strongly asymmetric distributions of polarized intensity with elongated ridges located in the outer galactic disk (Vollmer et al. 2007). The polarization angle is observed to be coherent across the entire galaxy. The origin and persistence of these polarization ridges poses a puzzle as these unusual features are not found in field spiral galaxies where the polarization is generally relatively symmetric and strongest in the inter-arm regions (Beck 2001).

We propose a new model that explains this riddle self-consistently (see Fig. 2.4). A spiral galaxy orbiting through the very weakly magnetized intra-cluster plasma necessarily sweeps up enough magnetic field around its dense interstellar medium to build up a dynamically important sheath (Pfrommer & Dursi 2010). The ram pressure felt by the galaxy as it moves through the ICM displaces and strips some of the outermost layers of interstellar medium gas in the galaxy; but the stars, being small and massive, are largely unaffected. Thus the stars lead the galactic gas at the leading edge of the galaxy, crossing the boundary between interstellar medium and ICM, as is seen in observations (Vollmer et al. 2007), and so overlap with the magnetic drape. As in the bulk of the galaxy, and in our own, these stars produce energetic particles; once these stars end their life in a supernova they drive shock waves into the ambient medium that accelerates electrons to relativistic energies. These CR electrons are then constrained to gyrate around the field lines of the magnetic drape, which results in radio synchrotron emission in the draped region, tracing out the field lines there. The size and shape of this synchrotron-illuminated region is determined by the transport of the CRs. The CRs diffuse along field lines, smoothing out emission; but they are largely constrained to stay on any given line, and thus are advected by the lines as they are dragged over the galaxy by the ambient flow. These CR electrons emit synchrotron radiation until they have lost enough energy to no longer be visible.

Figure 2.4 shows this process of draping magnetic field lines at a galaxy in our simulations. During the draping process, the intra-cluster magnetic field is dynamically projected onto the contact surface between the galaxy's interstellar medium and the intra-cluster plasma that is advected around the galaxy. This great degree of regularity of the magnetic field in the upstream of the galaxy is then reflected in the resulting projection of magnetic field in the draping layer. In particular, it varies significantly and fairly straightforwardly with different ICM field orientations with respect to the directions of motion. The regularity of the draped field implies then a coherent synchrotron polarization pattern across the entire galaxy (bottom panels in Fig. 2.4). Thus in the case of known proper motion of the galaxy and with the aid of 3D MHD simulations to correctly model the geometry, it is possible to unambiguously infer the orientation of the 3D ICM magnetic field that the galaxy is moving through. We note that this method provides information complementary to the Faraday rotation measure, which gives the integral of the field component along the line-of-sight.

Figure 2.5 compares an observation of these polarization ridges to our best matching simulation that is also

shown with a 3D volume rendering. We simulated our galaxy that encountered a homogeneous field with varying inclinations, and changed the magnetic tilt with respect to the plane of symmetry as well as the viewing angle to obtain the best match with the observations. The impressive concordance of the overall magnitude as well as the morphology of the polarized intensities and B-vectors in this case (and all others, not shown here) is a strong argument in favour of our model.

2.4. Orientation of cluster magnetic fields

We now explain the method of how we can infer the orientation of cluster magnetic fields by using the observation of polarized radio ridges. We use the morphology of the H I, the total synchrotron emission, and the galaxy redshift to obtain an estimate of the galaxy's 3D velocity component. We then compare the data to our mock observations where we iteratively varied galactic inclination, magnetic tilt, and viewing angle so that they matched the H I morphology and polarized intensity. Preserving the field line mapping from our simulated polarized intensity map to the upstream orientation of the field in our simulation enables us to infer an approximate 3D orientation of the upstream magnetic field. Applying this new tool to spiral galaxies in the Virgo cluster, we are now able to infer the geometry of the magnetic field in this cluster and find it to be preferentially radially aligned outside a central region (see Fig. 2.6)—in stark disagreement with the usual expectation of turbulent fields. The alignment of the field in the plane of the sky is significantly more radial than expected from random chance.

The isotropic distribution with respect to the centre (M87) is difficult to explain with the past activity of the active galactic nucleus in M87 and the spherical geometry argues against primordial fields. In contrast, such a radial bias is consistent with the inhomogeneous radial gas flows due to substructures as demonstrated by cosmological simulations of cluster formation, which obtain a similar result regardless of the type of simulated physics (Ruszkowski et al. 2011). Alternatively, this could be suggestive that the magneto-thermal instability is operating; at these distances outside the cluster center it encounters a decreasing temperature profile which is the necessary condition for it to operate (Balbus 2000). In the low-collisionality plasma of a galaxy cluster, the heat flux is forced to follow field lines as the collisional mean free path is much larger than the electron Larmor radius. On displacing a fluid element on a horizontal field line upwards in the cluster potential, it is conductively heated from the hotter part below, gains energy, and continues to rise—displacing it downwards causes it to be conductively cooled from the cooler part on top and it continues to sink deeper in the gravitational field. As a result, the magnetic field will reorder itself until it shows residual radial field rearrangements that are expected even in the presence of turbulence (Parrish & Stone 2007, Parrish et al. 2008); provided the temperature gradient as the source of free energy is maintained by constant heating through AGN feedback or shocks driven by gravitational infall. Future work is needed to demonstrate the physical cause of the radially biased field configuration.

2.5. Summary and Outlook

In this chapter we studied a general MHD effect that may equally well be important for problems in the context of the interstellar medium or elsewhere. The physics is rich and we are only at the beginning of chartering the necessary parameter space. A number of problems are still left to explore in detail such as the dependence of draping on the ambient magnetic topology and the transition to supersonic velocities. In particular it will be important to explore the exact conditions for stabilizing the buoyantly rising radio lobe against disruption as this may turn out to be critical for understanding the "cooling flow problem" (see Chapter 4).

It is expected that magnetic draping alters the transformation of gas-rich spiral galaxies to gas-depleted passive galaxies during their accretion onto clusters. In this context, it will be essential to study draping at realistic galaxy models as obtained from cosmological MHD simulations. The strong magnetic field in the drape is expected to interact with the interstellar medium magnetic field and possibly subject to fast magnetic reconnection. This could be a source of efficient first-order particle acceleration and heating and have important observational consequences.
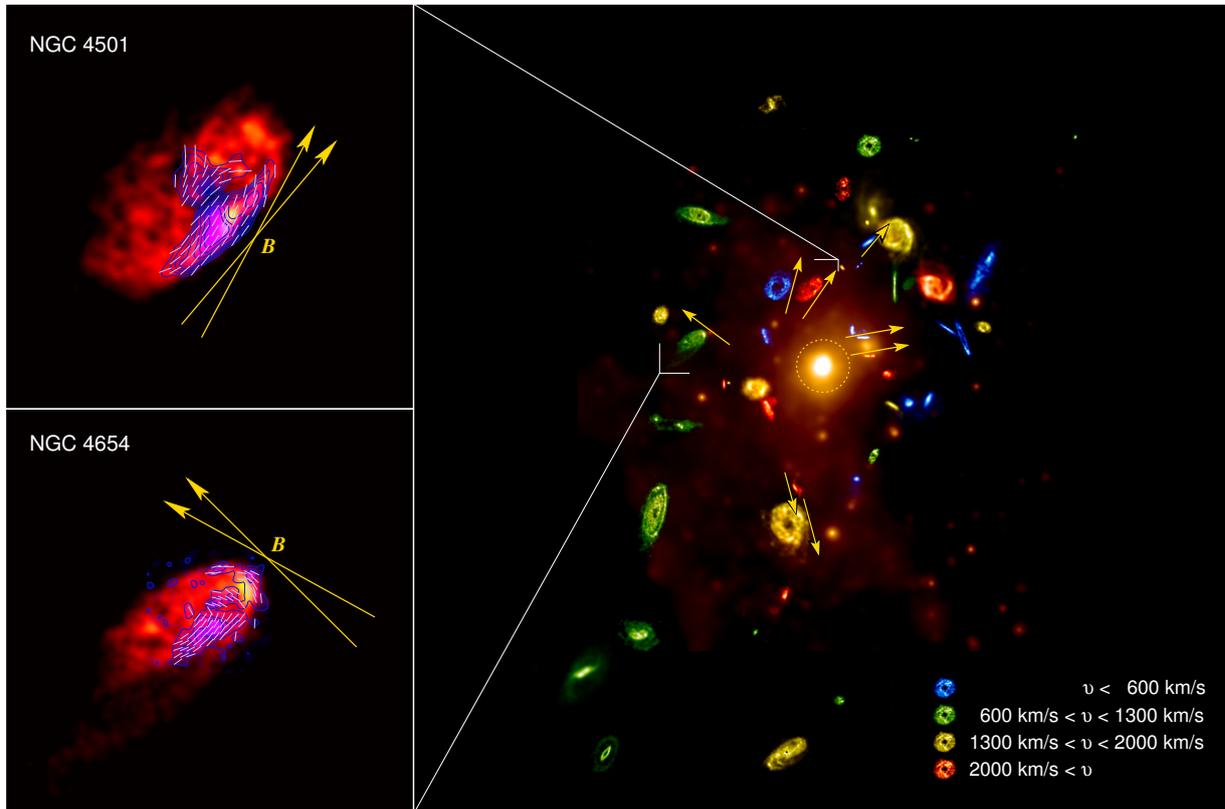
Figure 2.6.: Mapping out the magnetic field orientations in the Virgo galaxy cluster as inferred from the polarized synchrotron emission ridges of cluster spirals (from Pfrommer & Dursi 2010). Left: H I intensity data (red-to-yellow, Chung et al. 2009) overplotted with 6 cm polarized intensity contours and B-vectors (blue, Vollmer et al. 2007). The direction of the B-vectors directly measures the projected local orientation of the cluster magnetic fields **B** (yellow) with the range of plausible field orientations indicated by the double-arrow. Right: ROSAT X-ray image of the Virgo cluster (orange colour scale, Böhringer et al. 1994). Over-plotted is the H I emission of Virgo spirals in the VIVA survey (Chung et al. 2009) that is colour coded according to their velocities, and the green colour scale coincides with the cluster's mean heliocentric velocity of 1100 km sec^{-1} (after image by Chung et al. 2009). Galaxies are magnified by a factor of 10. The yellow arrows indicate the projected orientation of the magnetic field in Virgo at the position of the galaxies that have high-resolution polarized radio data. Note that the arrowheads could also point in the opposite direction because of the $n\pi$-ambiguity of inferring magnetic orientations from synchrotron polarization. We find that the magnetic field is preferentially oriented radially which either is caused by inhomogeneous radial gas flows due to substructures (Ruszkowski et al. 2011) or may suggest that the magneto-thermal instability is operating (Balbus 2000, Parrish et al. 2008) as it encounters the necessary conditions outside a spherical region with radius 200 kpc (Böhringer et al. 1994, as indicated with the yellow dotted circle).

3. Cosmological structure formation shocks

Abstract

Cosmological shocks play a key role during structure formation. They dissipate gravitational into thermal energy, they can accelerate protons and electrons to highly relativistic energies, and they have also been suggested as possible generation sites of intergalactic magnetic fields. We propose to use radio galaxies for probing otherwise invisible properties of formation shocks. Applying this idea to the radio galaxy NGC 1265, we find evidence for the existence of the accretion shock onto the Perseus cluster, measure the shock Mach number, estimate the properties of the infalling warm-hot intergalactic medium as well as the curvature in the shock surface. A curved shock causes post-shock shear flows and injects vorticity, a requirement for generating and amplifying magnetic fields in galaxy clusters. A complementary view onto cosmological shocks are giant "radio relics", which are thought to trace merger shocks. Modeling relics in our cosmological simulations allows both to statistically infer properties about cluster magnetic fields and to improve our understanding of diffusive shock acceleration of electrons, which has been in contradiction with expectations from shock acceleration theory and heliospheric observations. We solve this problem by showing that strong shocks during the epoch of cluster formation have built up a population of fossil electrons that can be efficiently reaccelerated at the much weaker merger shocks, giving rise to the spectacular "radio relic" emission.

3.1. Introduction

When gravitationally driven flows of pristine cosmic plasma break at the mildly overdense filaments and sheets and when these flows follow these filaments toward clusters of galaxies that represent the knots of the cosmic web (Bond et al. 1996), they will inevitably collide with the previously accreted plasma and form large-scale shock waves. Cosmological simulations predict that these formation shock waves form abundantly in the course of the hierarchically assembly of cosmic structure and exhibit a characteristic distribution of shock strengths (Ryu et al. 2003, Pfrommer et al. 2006, Vazza et al. 2011). Once excited, they propagate through the cosmic tenuous plasma, which is compressed at the transition layer of the shock while a part of the kinetic energy of the incoming plasma is dissipated into internal energy of the post-shock plasma. Because of the large collisional mean free path, the energy transfer at these "collisionless shocks" proceeds through collective electromagnetic viscosity which is provided by ubiquitous magnetic irregularities.

Cosmologically, shocks are important in several respects. (1) Of great interest is the subclass of (strong) accretion shocks that are thought to heat the baryons of the warm-hot IGM when they are accreted onto a galaxy cluster, thus supplying the intra-halo medium with entropy and thermal pressure support. (2) Weaker supersonic flows form as a result of the hierarchical merging of already virialized objects. (3) Besides thermalization, collisionless shocks are also able to accelerate ions of the high-energy tail of the thermal Maxwellian through diffusive shock acceleration (for a review see Blandford & Eichler 1987). These energetic ions are reflected at magnetic irregularities through magnetic resonances between the gyro-motion and waves in the magnetised plasma and are able to gain energy in moving back and forth through the shock front, producing a population of CRs. (4) Formation shocks have also been proposed as possible generation sites of intergalactic magnetic fields (Kulsrud et al. 1997, Ryu et al. 1998, 2008).

Prior to the work presented in this Habilitation thesis, only discrete merger shock waves have been detected in the X-rays (e.g., Markevitch et al. 2002) and there was no characterization possible of the detailed flow properties in the post-shock regime as to test whether shear flows—the necessary condition for generating magnetic fields—are present. Given the importance of structure formation shocks described above, it is certainly worthwhile to explore complementary wavebands to the X-ray band to deepen our understanding on the properties of cosmological shocks. In fact, it has been suggested that the diffuse, polarized emission from giant radio relics traces structure formation shock waves (Enßlin et al. 1998a). However, there are many open problems associated with this interpretation, namely the detailed physics of electron acceleration at these primarily weak shocks and the high magnetic field values at the relics' position. (1) While CR protons have sufficient momentum not to resonate with the electromagnetic
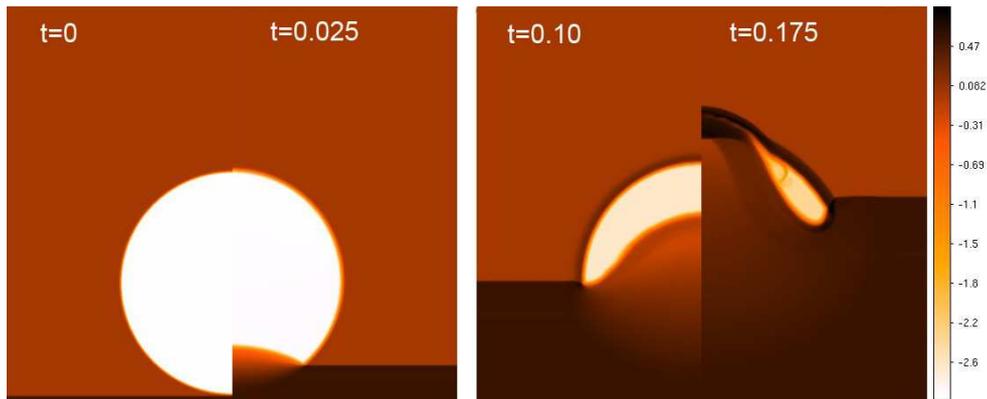
Figure 3.1.: We show images from a 2D axisymmetric simulation that follows the evolution of a spherical bubble overrun by a Mach 5 shock that transforms into a torus (each half-panel shows a selected snap shot). Base 10 log of gas density is shown. The initial bubble/ICM density contrast $\delta = 10^{-3}$, the bubble diameter is unit length, the pre-shock ICM density is unity, as is the pre-shock sound speed. Times correspond to initial shock impact on the bubble ($t = 0$), just before the internal bubble shock has crossed the bubble (not visible with this color scale, $t = 0.025$), the ICM shock has crossed a bubble radius (externally, $t = 0.1$) and just after the bubble contact discontinuity has crossed the bubble ($t = 0.175$). During this bubble-torus transition, the relativistic plasma within the bubble experiences an adiabatic compression that energizes the fossil CR electrons of the bubble, thus illuminating the previously unobservable radio plasma (from Pfrommer & Jones 2011).

turbulence in the shock transition layer itself (i.e., they experience the shock as a discontinuity over which they are adiabatically compressed), the injection problem for thermal electrons is already known to be severe at high Mach numbers, due to the substantially smaller gyroradius of thermal electrons in comparison to the shock width. (2) Electron cooling arguments and simultaneous synchrotron and X-ray observations consistently infer high magnetic field values of several μG at the relics' position. This implies a plasma beta parameter of $\beta = P_{\mathrm{th}}/P_B \simeq 5$ (i.e., an almost comparable ratio of thermal-to-magnetic pressure, Pinzke et al. 2013). Apparently, the magnetic field at the shock is substantially more enhanced in comparison to the bulk of the intra cluster plasma, which is only weakly magnetized with $\beta \gtrsim 50$ as inferred from Faraday rotation measure studies (e.g., Bonafede et al. 2010). In this chapter we will shed light on the following open issues:

- Do cluster accretion shocks exist in the Universe and how can we infer their properties?

- How are synchrotron-emitting electrons in radio relics accelerated?

- How can we use giant radio relics to illuminate the magnetized cosmic web?

3.2. Radio galaxies probing accretion shocks

Previously, the morphology of a giant radio galaxy has already been used to indirectly detect a large scale shock at an intersecting filament of galaxies (Enßlin et al. 2001) by using the radio galaxy as a giant cluster weather station (Burns 1998). We present a consistent three-dimensional model for the head-tail radio galaxy NGC 1265 that explains the complex radio morphology and spectrum by a past passage of the galaxy and radio bubble through a shock wave (Pfrommer & Jones 2011). Using analytical solutions to the full Riemann problem and hydrodynamical simulations, we study how this passage transformed the plasma bubble into a toroidal vortex ring (see Fig. 3.1). Adiabatic compression of the aged electron population causes it to be energized and to emit low surface brightness and steep-spectrum radio emission (Enßlin & Gopal-Krishna 2001, Enßlin & Brüggen 2002). The large infall velocity of NGC 1265—which is barely gravitationally bound to the Perseus cluster at its current position—and the low Faraday rotation measure values and variance of the jet strongly argue that this transformation was due to the accretion shock onto Perseus situated roughly at the virial radius. Estimating the volume change of the radio bubble enables inferring a shock Mach number of $\mathcal{M} \simeq 4.2^{+0.8}_{-1.2}$, a density jump of $3.4^{+0.2}_{-0.4}$, a temperature jump of $6.3^{+2.5}_{-2.7}$,
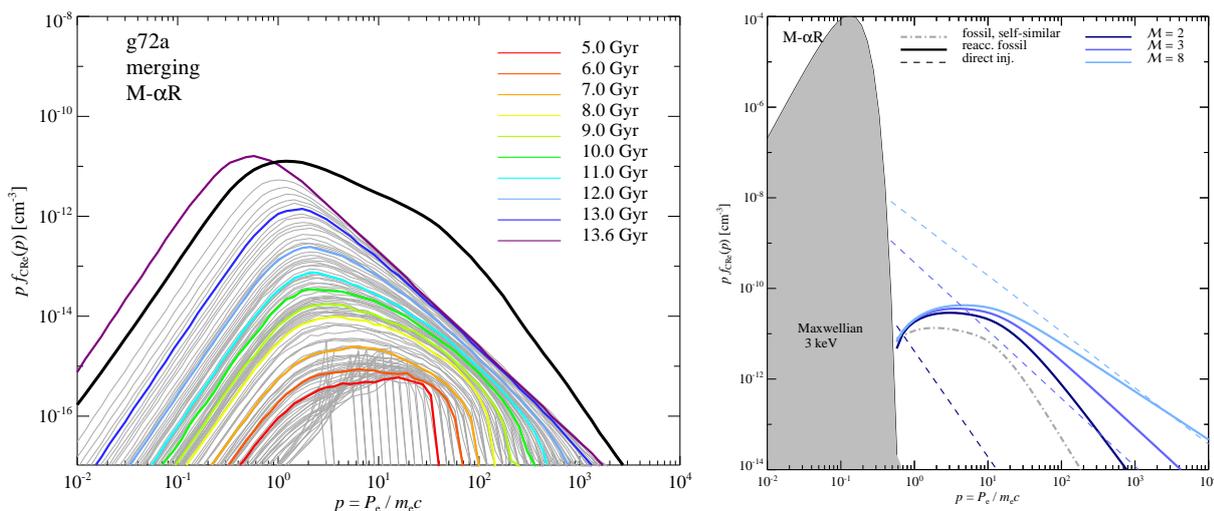
Figure 3.2.: What generates giant radio relics in clusters? The left panel shows the differential spectral build up of the fossil electron distribution function f_{CRe} as a function of cosmic time, for a post-merging cluster in the virial region. The black solid line shows the final f_{CRe}. The thin grey lines show the individual differential contributions to f_{CRe} from different times, where we highlight the contributions spaced by Gyr intervals with different colors. The spectral features are shaped by different cooling processes: non-relativistic Coulomb cooling for $p < 1$, a broad feature indicating the transition from relativistic Coulomb cooling to the adiabatic regime for $1 < p \lesssim 10^2$, and inverse Compton cooling at higher momenta. The right panel compares the shock acceleration efficiency of direct acceleration from the thermal Maxwellian and reacceleration from the fossil distribution function. We show the resulting CR electron distribution function for direct acceleration (dashed line) and for reacceleration (solid line), for different Mach numbers (color coded); also shown is the fossil distribution function (dot-dashed). The distribution function falls much more drastically at low Mach number for direct injection (dashed) than for reacceleration (solid), in particular for momenta $p > 10^3$, which radiate observable synchrotron emission in form of giant radio relics (from Pinzke et al. 2013).

and a pressure jump of 21.5 ± 10.5 while allowing for uncertainties in the equation of state of the radio plasma and volume of the torus. Extrapolating X-ray profiles, we obtain upper limits on the gas temperature and density in the infalling warm-hot intergalactic medium of $kT \lesssim 0.4$ keV and $n \lesssim 5 \times 10^{-5}$ cm^{-3}. The orientation of the ellipsoidally shaped radio torus in combination with the direction of the galaxy's head and tail in the plane of the sky is impossible to reconcile with projection effects. Instead, this argues for post-shock shear flows that have been caused by curvature in the shock surface with a characteristic radius of 850 kpc. The energy density of the shear flow corresponds to a turbulent-to-thermal energy density of 14%—consistent with cosmological simulations (Lau et al. 2009, Battaglia et al. 2012). The shock-injected vorticity might be important in generating and amplifying magnetic fields in galaxy clusters. We suggest that future polarized radio observations by, e.g., LOFAR of head-tail galaxies can be complementary probes of accretion shocks onto galaxy clusters and are unique in determining their detailed flow properties.

3.3. A model for generating radio relics

Many bright radio relics in the outskirts of galaxy clusters have low inferred Mach numbers, defying expectations from shock acceleration theory and heliospheric observations that the injection efficiency of relativistic particles plummets at low Mach numbers. With a suite of cosmological simulations, we follow the diffusive shock acceleration as well as radiative and Coulomb cooling of CR electrons during the assembly of a cluster and find a substantial population of fossil electrons (Pinzke et al. 2013). When reaccelerated at a shock (through diffusive shock acceleration), they are competitive with direct injection at strong shocks and overwhelmingly dominate by many orders of magnitude at weak shocks, $\mathcal{M} \lesssim 3$, which are the vast majority at the cluster periphery (see Fig. 3.2). Their relative importance depends on cooling physics and is robust to the shock acceleration model used. While the abundance

Mach numbers: *Radio gischt at shocks:*
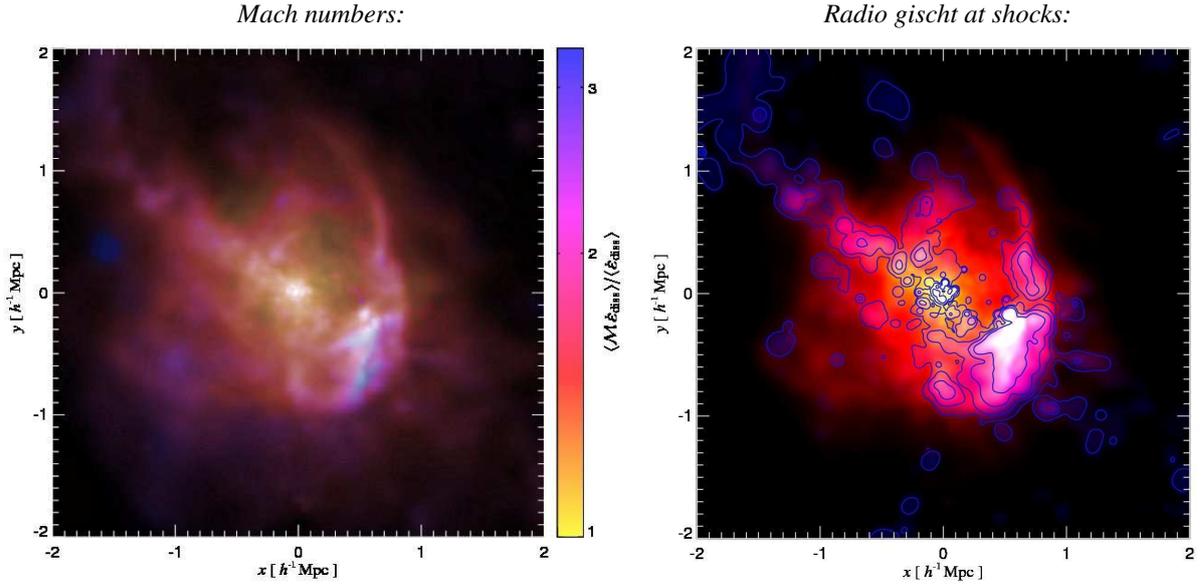
Figure 3.3.: Structure formation shocks triggered by a recent merger of a large galaxy cluster ($M \simeq 10^{15}\,\mathrm{M}_\odot$) dissipate the associated gravitational energy. Left: the Mach number of shocks weighted by the energy dissipation rate is shown by the colour (while the brightness displays the logarithm of the dissipation rate). Right: three-color image of energy dissipation rate at shocks (shown with a color scale ranging from black over red to yellow) and radio synchrotron emission at 150 MHz from shock-accelerated relativistic electrons (blue and contours with levels starting at 7×10^{-4} mJy arcmin^{-2} and increasing with a factor of 15, respectively). This "radio gischt" emission traces structure formation shock waves, highlights the intermittent nature of mass accretion in galaxy clusters, and illuminates magnetic fields that are amplified by turbulence that can be excited by these shock waves (from Battaglia et al. 2009).

of fossils can vary by a factor of ~ 10, the typical reaccelerated fossil population has radio brightness in excellent agreement with observations. Fossil electrons with $1 \lesssim \gamma \lesssim 100$ ($10 \lesssim \gamma \lesssim 10^4$) provide the main seeds for reacceleration at strong (weak) shocks; we show that these are well-resolved by our simulation. We construct a simple self-similar analytic model which assumes steady recent injection and cooling. It agrees well with our simulations, allowing rapid estimates and physical insight into the shape of the distribution function. We predict that LOFAR should find many more bright steep-spectrum radio relics, which are inconsistent with direct injection. A failure to take fossil CR electrons into account will lead to erroneous conclusions about the nature of particle acceleration at weak shocks; they arise from well-understood physical processes and cannot be ignored.

3.4. Illuminating the magnetized cosmic web

Recent improvements in the capabilities of low frequency radio telescopes provide a unique opportunity to study thermal and non-thermal properties of the cosmic web. We argue that the diffuse, polarized emission from giant radio relics traces structure formation shock waves (Enßlin et al. 1998a) and illuminates the large-scale magnetic field. To show this, we model the population of shock-accelerated relativistic electrons in high-resolution cosmological simulations of galaxy clusters and calculate the resulting radio synchrotron emission (Battaglia et al. 2009). We find that individual shock waves correspond to localized peaks in the radio surface brightness map (see Fig. 3.3), which enables us to measure Mach numbers for these shocks. We show that the luminosities and number counts of the relics strongly depend on the magnetic field properties, the cluster mass and dynamical state. By suitably combining different cluster data, including Faraday rotation measures, we are able to constrain some macroscopic parameters of the plasma at the structure formation shocks, such as models of turbulence. We also predict upper limits for the properties of the warm-hot intergalactic medium, such as its temperature and density. We predict that the current generation of radio telescopes (LOFAR, GMRT, MWA, LWA) have the potential to discover a substantially larger

sample of radio relics, with multiple relics expected for each violently merging cluster. Future experiments (SKA) should enable us to further probe the macroscopic parameters of plasma physics in clusters.

3.5. Summary and Outlook

The radio band opens an observational window onto structure formation shocks and the cluster magnetic field. We demonstrated that radio galaxies are unique in situ probes of cluster accretion shocks. Our work shows the potential of these kind of serendipitous events as ways to explore the outer fringes of clusters and dynamical features of accretion shocks that are complementary to X-ray observations. In particular, we find indirect evidence for the existence of the warm-hot IGM. Clearly, future observations of different systems similar to NGC 1265 would be beneficial to get a statistical measurement of properties of the accretions shocks and its pre-shock conditions.

We have further motivated that giant radio relics still hold a number of fundamental problems to be deciphered such as the comparable large magnetic field values at the shock position and the question how exactly the synchrotron-emitting electrons got accelerated. Based on our study, we strongly advocate that fossil electrons be considered a key ingredient in interpreting radio relic observations, rather than an exotic afterthought. Failure to account for the fossil electrons will lead to erroneous conclusions about the nature of particle acceleration at weak shocks.

4. The impact of cosmic rays on galaxy and cluster formation

Abstract

Streaming CRs along magnetic fields transfer energy and momentum to the thermal plasma. Using numerical models of isolated galaxy formation, we show that this process is responsible for driving powerful and sustained winds in (small) galaxies, which expel a large fraction of the gas from the halo and suppress subsequent star formation by a large factor. Similarly, streaming CRs that are energized by the central AGN in the Virgo cluster heat the fast cooling cluster gas in the core region at a rate that balances that of radiative cooling *on average* at each radius. However, the resulting global thermal equilibrium is locally unstable and allows for the formation of the observed cooling multi-phase medium through thermal instability. CR heating may be able to impose a central temperature floor of around 1 keV to the unstable cooling gas—in accordance with X-ray observations, thereby suggesting a solution to the famous "cooling flow problem". This indicates that CR physics may be responsible for shaping the faint and bright end of the galaxy luminosity function in a way that is consistent with the data.

4.1. Introduction

Despite heroic efforts over the last decades, our understanding of galaxy formation is still far from complete and there are a number of unsolved problems. Abundance matching of rank-ordered galaxy luminosities to the dark matter halos (e.g., Guo et al. 2010) reveals an overall low efficiency of converting gas to stars for Milky Way-type galaxies. Even more surprisingly, this efficiency declines rapidly towards the scales of dwarf galaxies as well as towards more massive systems. Understanding why these small and big galaxies are extremely baryon deficient while more regular galaxies such as the Milky Way can hold on to more baryons is certainly the most fundamental puzzle in hierarchical theories of galaxy formation. This makes a strong case for dwelling deeper into baryonic physics and motivated us to look closer at energetic processes in galaxies. Among those are exploding stars, which drive powerful shocks that are observed to be very efficient in amplifying magnetic fields and accelerating CRs (Uchiyama et al. 2007, Helder et al. 2009). The pressure of these CRs and magnetic fields is observed to dominate the pressure in our Galaxy (Schlickeiser 2002, Kulsrud 2005). Hence, these non-thermal components determine the dynamics of the interstellar medium and are undoubtedly playing a key role in galaxy formation.

Similarly, understanding the mysterious thermal histories of large ellipticals and clusters is of great importance. Approximately half of all cluster cores have radiative cooling times of less than 1 Gyr and establish a population of cool core (CC) clusters while the others have central cooling times that are longer than the age of the Universe (Cavagnolo et al. 2009, Hudson et al. 2010). In the absence of any heating process, these hot gaseous atmospheres are expected to cool and to form stars at rates up to several hundred $M_\odot$ yr^{-1} (see Peterson & Fabian 2006, for a review). Instead, the observed gas cooling and star formation rates are reduced to levels substantially below those expected from unimpeded cooling flows. High-resolution *Chandra* and *XMM-Newton* observations show that while the gas temperature is smoothly declining toward the center, there is a lack of emission lines from gas at a temperature below about 1 keV (Hudson et al. 2010). Apparently, radiative cooling is offset by a yet to be identified heating process that is associated with the AGN jet-inflated radio lobes that are co-localized with the cavities seen in the X-ray maps. The interplay of cooling gas, subsequent star formation and nuclear activity appears to be tightly coupled to a self-regulated feedback loop (for reviews, see McNamara & Nulsen 2007, 2012). Feedback is considered to be a crucial if not unavoidable process of the evolution of galaxies and supermassive black holes (Croton et al. 2006, Puchwein & Springel 2013). Progress in understanding the underlying physics is of vital importance for using future cluster observations to estimate cosmological parameters and to improve our understanding of dark matter. Hence in this chapter, we seek to answer the following questions (and present important first steps toward a possible solution):
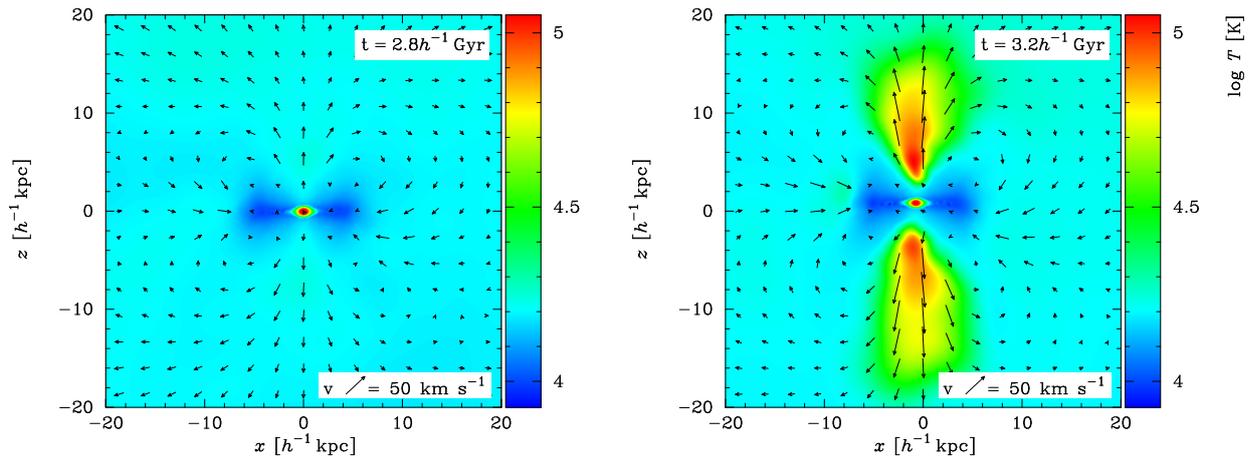
Figure 4.1.: The energy and momentum transfer of streaming CRs is responsible for launching powerful disk winds in a hydrodynamical simulation of a galaxy with a total mass $10^{10}\,\mathrm{M_\odot}$. Shown are the gas temperature and velocity in edge-on slices through the galactic disk just before and after the launch of the wind. The maximum velocities encountered in these run are 26 km s^{-1} (left) and 70 km s^{-1} (right). As a result of the damping of Alfvén waves excited by streaming CRs, collimated cavities of hot gas form below and above the disk and propagate further up in the course of time, driving a powerful disk wind (from Uhlig et al. 2012).

- How do CRs and magnetic fields regulate galaxy formation and evolution?
- What observational signatures have CR-driven winds—at early and late times?
- Can CR-driven winds enrich the intergalactic medium with metals and magnetic fields?
- The "cooling flow problem": how can these cool cluster cores manage to escape run-away cooling?

4.2. Galactic winds

Galactic winds are observed in many spiral galaxies with sizes from dwarfs up to the Milky Way, and they sometimes carry a mass in excess of that of newly formed stars by up to a factor of ten. Multiple driving processes of such winds have been proposed, including thermal pressure due to supernova-heating, UV radiation pressure on dust grains, or CR pressure. We here study wind formation due to CR physics using a numerical model that accounts for CR acceleration by supernovae, CR thermalization by Coulomb and hadronic interactions, and advective CR transport. In addition, we introduce a novel implementation of CR streaming relative to the rest frame of the gas (Uhlig et al. 2012). Streaming CRs excite Alfvén waves on which they resonantly scatter (Kulsrud & Pearce 1969), thereby limiting the CR's effective bulk velocity. Damping of these waves transfers CR energy and momentum to the thermal gas.

Using a simple model of disk galaxy formation in isolated dark matter haloes, we find that CR streaming drives powerful and sustained winds in galaxies with virial masses $M_{200} \lesssim 10^{11}\,\mathrm{M_\odot}$ (see Fig. 4.1). The forming winds in dwarf galaxies ($M_{200} \sim 10^9\,\mathrm{M_\odot}$) expel gas mass at a rate that exceeds that of star formation by a factor of ~ 5. Moreover, the winds in those galaxies expel $\sim 60\%$ of the initial baryonic mass contained inside the halo's virial radius and suppress the star formation rate by a factor of ~ 5 (see Fig. 4.2), with a progressively smaller impact for larger-mass halos (at least in our simplified models). How can we understand this? If we only account for advective CR transport, then CRs are tied to the interstellar medium and cannot escape from it. Instead, their substantial pressure support will first hinder the gas from collapsing to densities much larger than the threshold of star formation. As soon as CRs are removed by cooling processes (which are, however, much more inefficient in comparison to cooling of the thermal gas), collapse can start again and the star formation rate (SFR) increases.
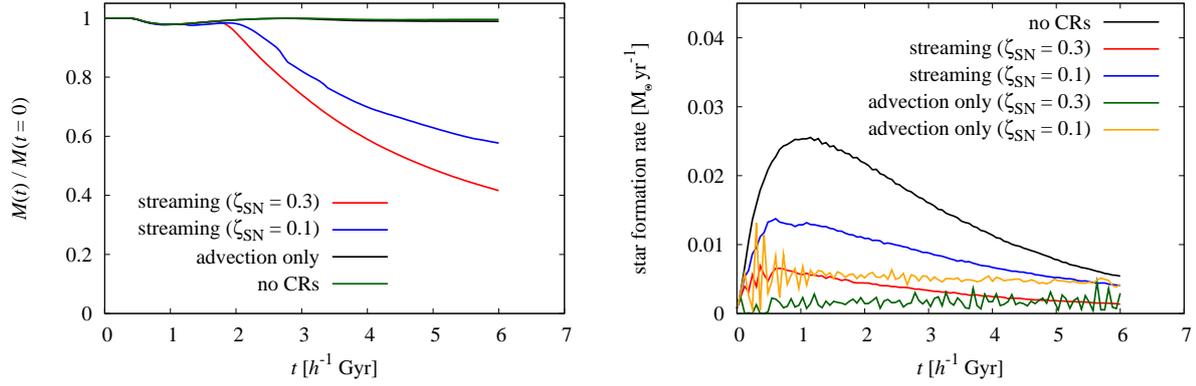
Figure 4.2.: Impact of CR-driven winds on the gas mass evolution, $M(t)$, and star formation rate (SFR) of hydrodynamic simulations of an isolated dwarf galaxy of $10^9 \, M_\odot$. In the left panel we compare $M(t)$ for four different scenarios. There is no mass loss in our simulations without CRs (green) as well as in those which only account for advective CR transport (black). In contrast, our runs with CR streaming show substantial mass loss from the halo after an initial phase, where the ram pressure from inflowing gas wins out over the wind. Depending on the CR acceleration efficiency at supernova remnants (blue line: $\zeta_{SN} = 0.1$, red line: $\zeta_{SN} = 0.3$), we observe that the galaxy loses $40\% - 60\%$ of its initial gas mass to the wind. Right: SFR as a function of time. CR feedback can substantially suppress the SFR in comparison to the reference simulation without CRs (black). Our CR streaming simulations reduce the SFRs while keeping their functional form. In simulations that only account for advective CR transport (orange line: $\zeta_{SN} = 0.1$, green line: $\zeta_{SN} = 0.3$), the SFR is even more suppressed and shows an oscillatory behaviour (from Uhlig et al. 2012).
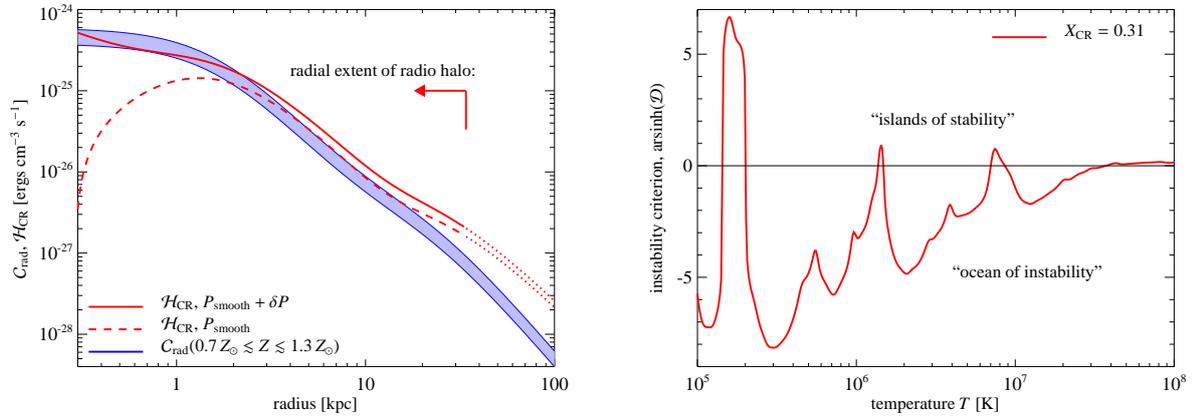
Figure 4.3.: CR heating versus radiative cooling at the center of the Virgo cluster "cooling flow". Left: the cooling rates (blue) account for a fluctuating metal distribution in the range $(0.7 - 1.3) \, Z_\odot$ and are globally balanced at each radius by CR Alfvén wave heating. We show the CR heating rate $\mathcal{H}_{CR}$ due to the azimuthally averaged pressure profile that "smoothes" out the CR pressure gradient (dashed red) and the $\mathcal{H}_{CR}$ profile, where we additionally account for pressure fluctuations due to weak shocks of typical Mach number $\mathcal{M} = 1.1$ (solid red). The CR heating rates become very uncertain outside the boundary of the radio halo of Virgo A (indicated with a dotted red). Right: local stability analysis of a fluid for which CR heating globally balances radiative cooling by bremsstrahlung and line emission. We show the instability criterion for isobaric perturbations as a function of temperature for parameters appropriate for the central AGN, M87 (red). Once the gas temperature drops below 3×10^7 K, it becomes thermally unstable. Assuming that the gas cools while maintaining approximate thermal equilibrium, its collapse is halted at around 10^7 K by the first "island of stability", which is consistent with the temperature floor seen in X-ray observations. However, the high-density tail of density fluctuations should able to cross this island and become again subject to thermal instability, likely sourcing some of the observable multi-phase gas (from Pfrommer 2013).

The overall effect is a dramatic suppression of star formation as well as an oscillatory behaviour (see Fig. 4.2). Additionally accounting for CR streaming modulates the CR pressure in the interstellar medium since CRs can now transport energy and momentum comparably loss-less from the dense star-forming regions to the dilute interstellar medium. This overpressurizes these regions and launches galactic super winds, which expel gas from the halo and hence, decreases the gas mass in the galaxy that is available for star formation. As a result, the net SFR is reduced in comparison to a case without CRs, but inherits its functional form.

In dwarfs, the winds are spherically symmetric while in larger galaxies the outflows transition to bi-conical morphologies that are aligned with the disk's angular momentum axis (see Fig. 4.1). We show that damping of Alfvén waves excited by streaming CRs provides a means of heating the outflows to temperatures that scale with the square of the escape speed, $kT \propto v_{\mathrm{esc}}^2$. In larger haloes ($M_{200} \gtrsim 10^{11}\,\mathrm{M_\odot}$), CR streaming is able to drive fountain flows that excite turbulence, providing another means of heating the halo gas. For halo masses $M_{200} \gtrsim 10^{10}\,\mathrm{M_\odot}$, we predict an observable level of Hα and X-ray emission from the heated halo gas. We conclude that CR-driven winds should be crucial in suppressing and regulating the first epoch of galaxy formation, expelling a large fraction of baryons, and—by extension—aid in shaping the faint end of the galaxy luminosity function. They should then also be responsible for much of the metal enrichment of the intergalactic medium.

4.3. Feedback by active galactic nuclei

Several physical processes have been proposed to be responsible for balancing radiative cooling of the low-entropy gas at the centers of galaxy clusters and in mitigating the star formation of elliptical galaxies. Those include an inward transport of heat from the hot outer cluster regions (Narayan & Medvedev 2001), turbulent mixing (Kim & Narayan 2003), redistribution of heat by buoyancy-induced turbulent convection (Chandran & Rasera 2007, Sharma et al. 2009), and dissipation of mechanical heating by outflows, lobes, or sound waves from the central AGN (e.g., Churazov et al. 2001, Brüggen & Kaiser 2002, Ruszkowski & Begelman 2002, Gaspari et al. 2012). In particular feedback by AGN has come into the focus of recent research (McNamara & Nulsen 2007, 2012) owing to the self-regulated nature of the proposed feedback and observational correlations between radio activity and central entropy (which is a proxy for a small cooling time).

The total energy required to inflate a cavity of volume V in an atmosphere of thermal pressure P_{th} is equal to its enthalpy $E_{\mathrm{cav}} = \gamma/(\gamma - 1)\,P_{\mathrm{th}}V = 4\,P_{\mathrm{th}}V$, assuming a relativistic equation of state with $\gamma = 4/3$ within the lobes. Initially, the partitioning to mechanical energy resulting from the volume work done on the surroundings only makes use of one quarter of the total available enthalpy. Only a fraction thereof is dissipated in the central regions, which have the smallest cooling time (since most of the temperature increase caused by weak shocks is provided adiabatically). There are two possibilities how to dissipate the remaining part of $3\,P_{\mathrm{th}}V$ that is stored in the internal energy of the (presumably) relativistic particle population. (1) If these lobes rise buoyantly and unimpeded over several pressure scale heights, the relativistic lobe filling does PdV work on the surroundings, which expands the lobe and transfers the internal lobe energy adiabatically to mechanical energy of the ambient ICM. (2) However, *if* those CRs were mixed into the ambient gas early-on during their buoyant rise, there would be a promising process to transfer CR into thermal energy. Fast streaming CRs along the magnetic field excite Alfvén waves through the "streaming instability" (Kulsrud & Pearce 1969). Damping of these waves transfers CR energy and momentum to the thermal gas at a rate that scales with the CR pressure gradient. Hence, this could provide an efficient means of suppressing the cooling catastrophe of CCs (Loewenstein et al. 1991, Guo & Oh 2008, Enßlin et al. 2011), but only *if* the CR pressure gradient is sufficiently large.

Here, we study the consequences of this CR-heating model with the aim of putting forward an observationally well-founded and comprehensive model. In particular, we intend to eliminate two of the most uncertain assumptions of this process, the mixing of CRs with the ambient plasma and the CR abundance in the central cluster regions. To this end, we focus on the closest active galaxy, M87, that is interacting with the cooling cluster gas in the center of the Virgo cluster that provides us with the most detailed view on AGN feedback possible. Low-frequency radio observations by LOFAR revealed the absence of *fossil* CR electrons in the radio halo surrounding M87. This puzzle can be resolved by accounting for the CR release from the radio lobes and the subsequent mixing of CRs with the dense ambient intracluster gas, which thermalizes the electrons by means of Coulomb interactions on a timescale similar to the radio halo age of 40 Myrs (Pfrommer 2013). Hadronic interactions of similarly injected CR protons with the ambient gas should produce an observable gamma-ray signal in accordance with the steady emission of the low state of M87 detected by *Fermi* and H.E.S.S. Hence, we normalize the CR population to the gamma-ray

emission, which shows the same spectral slope as the CR injection spectrum probed by LOFAR, thereby supporting a common origin. The observable gamma-ray emission implies a CR-to-thermal pressure ratio of $X_{CR} = 0.31$, allowing for a conservative Coulomb cooling timescale of order the radio halo age that modifies the low-energy part of the CRp distribution.

We show that CRs, which stream at the Alfvén velocity with respect to the plasma rest frame, heat the surrounding thermal plasma at a rate that balances that of radiative cooling *on average* at each radius (Pfrommer 2013). However, the resulting global thermal equilibrium is locally unstable to isobaric temperature perturbations and allows for the formation of the observed cooling multi-phase medium through thermal instability (see Fig. 4.3). Provided CR heating balances cooling during the emerging "cooling flow", the collapse of the majority of the gas is halted around 1 keV—in accordance with X-ray data. We show that both the existence of a temperature floor and the similar radial scaling of the heating and cooling rates are generic predictions of the CR heating model.

4.4. Summary and Outlook

The previous two sections demonstrated that a single physical process (namely CR streaming) may hold the key for understanding the physics underlying "galaxy feedback", in particular for explaining the progressively lower star formation efficiencies toward smaller scales of dwarf galaxies and larger scales of ellipticals and galaxy clusters. Our very successful exploratory studies call for thorough follow-up numerical investigations that couple the presented CR propagation process to MHD in order to understand the non-linear evolution of these components and to quantify their impact on galaxy formation in a fully cosmological setting.

While the energetics of AGN feedback is sufficient to balance radiative cooling, it is unable to transform CC into non-CC clusters on the buoyancy timescale due to the weak coupling between the mechanical energy to the cluster gas (Pfrommer et al. 2012). Matching this observational fact has proven to be difficult in cosmological simulations of AGN feedback that include realistic metal-line cooling (Dubois et al. 2011). This leaves the important question "which physical processes are essential for explaining the observed bimodality of galaxy clusters?" for future work.

5. Indirect dark matter searches in galaxy clusters

Abstract

We identify galaxy clusters as a very competitive target to indirectly detect dark matter (DM) owing to the expected large substructure enhancement. To calculate the DM annihilation signal, we consider (1) leptophilic DM models with Sommerfeld-enhanced cross sections, (2) different representative benchmark models of supersymmetric DM, and (3) CR induced pion decay, which is expected to contribute the largest astrophysical background. Among all clusters/groups of a flux-limited X-ray sample, we single out the Fornax cluster as the "golden" DM target due to a particularly low CR-induced background. Combining the substructure enhancement with the latest limits on the non-detection of gamma-rays from clusters by the Fermi Collaboration enable us to severely challenge the class of leptophilic cold DM models. Alternatively, if this Sommerfeld enhancement is realized in Nature, this would imply a large value of the limiting substructure mass, pointing to additional physics in the dark sector and demonstrating the importance of understanding the gamma-ray emission of clusters.

5.1. Introduction

Elucidating the nature of dark matter is arguably one of the greatest problems in modern physics. Even though there is now overwhelming evidence for the existence of DM, we still do not know its nature. Generic arguments involving the cosmic relic abundance point to elementary particles in the 100 GeV – few TeV mass range as likely candidates. Thus, such a DM particle could either be directly detected at the *Large Hadron Collider* (after the upgrade of the center-of-mass energy) or indirectly through its annihilation/decay products, e.g. gamma-ray photons or positrons. Even if the *Large Hadron Collider* detects particles predicted by the Supersymmetric Standard Model, astrophysical information is still crucial, e.g., to rule out Kaluza-Klein particles that would hint at extra dimensions. There have been a number of papers that directly estimate the annihilation flux from weakly self-interacting massive particles in high-resolution, DM-only simulations of the central regions of the Milky Way and from DM substructures in its halo. Consistently, they find that the annihilation flux may be detectable in the Milky Way, regardless of uncertainties about the densest regions, for the annihilation cross-sections predicted by currently popular elementary particle models for the DM.

Since the annihilation signal scales with the square of the DM density, the most easily detectable signal will be produced by regions with the highest DM density, i.e., towards the Milky Way center (Springel et al. 2008). However, this is exactly the place where most of the baryons and CRs reside that produce an astrophysical confusion of the expected DM signal. Hence, it is advisable to also turn our attention to DM dominated objects with a lower CR-induced background: nearby dwarf satellites and clusters. Hence, in this chapter we are concerned with answering the following questions:

- How does the DM annihilation signal differ for dwarfs and clusters?

- What are the gamma-ray signatures of popular particle physics model of DM?

- Can we already constrain or even rule out certain DM models through gamma-ray non-detections?

5.2. Astrophysical emission models

If a telescope does not resolve the emission from an astrophysical object (as it is the case for *Fermi*-LAT observations of the majority of clusters and dwarfs) then the uncertainty about the central shape of the smoothed DM profile,
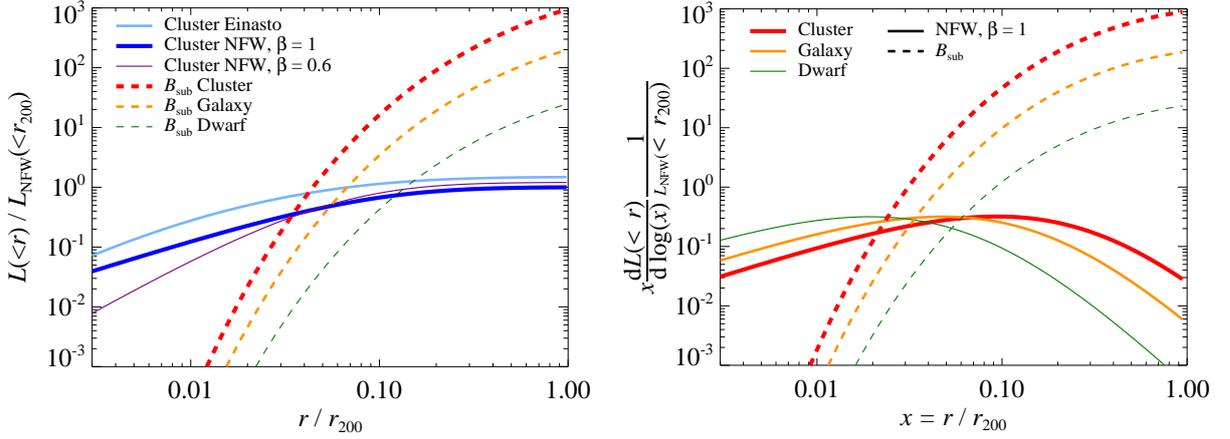
Figure 5.1.: Radial dependence of the DM annihilation luminosity of a smooth halo and its substructures. Left: the solid lines show the cumulative luminosity of a smooth cluster halo with mass $10^{15}\,\mathrm{M}_\odot$ for three different density profiles: an Einasto profile (light blue), a cuspy Navarro-Frenk-White (NFW, 1997) density profile with an inner density slope $\beta = 1.0$ (thick dark blue), and a cored NFW profile with $\beta = 0.6$ (thin purple). The dashed lines show the cumulative luminosity from substructures for three different halo mass scales: a galaxy cluster with $10^{15}\,\mathrm{M}_\odot$ (thick red), a galaxy with $10^{12}\,\mathrm{M}_\odot$ (orange), and a dwarf galaxy with $10^8\,\mathrm{M}_\odot$ (thin green). Here, we assume the standard value for the limiting substructure mass of $M_{\mathrm{lim}} = 10^{-6}\,\mathrm{M}_\odot$. This implies a large substructure boost factor in clusters (~ 1000), and the relative small boost in dwarf galaxies (~ 20). The plot on the right-hand side demonstrates where most of the DM annihilation luminosity originates. We show the differential contribution to the DM annihilation luminosity per logarithmic interval in radius, which scales as $x^3\rho^2$, where ρ is the DM mass density and $x = r/r_{200}$ is the normalized radius. For the smooth profiles, the majority of the flux is delivered by a region around one third of the DM scale radius as indicated by the maximum value of the curves. In contrast, the emission from substructures is dominated by the virial radius r_{200} (from Pinzke et al. 2011).
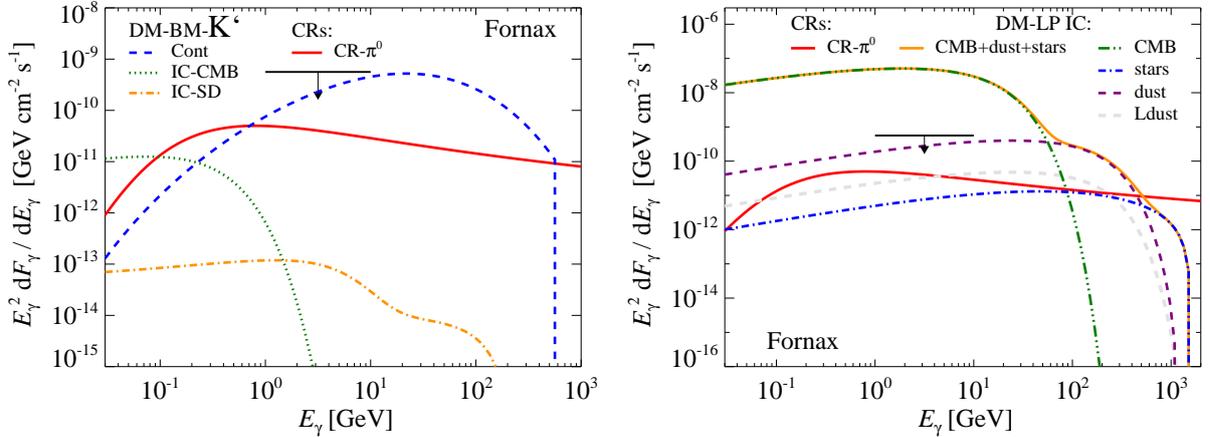
Figure 5.2.: Dark matter annihilation spectrum for the supersymmetric benchmark model K' (left), where the annihilation dominantly occurs in the *s*-channel through exchange of the pseudoscalar Higgs boson and for the leptophilic model, which has a Sommerfeld-enhanced cross section (right). We adopt parameters for the Fornax cluster, which imply a substructure boost of 890. The continuum emission dominates in the supersymmetric model over the various inverse Compton (IC) emission components, which account for seed photon fields of the cosmic microwave background (CMB) and seed photons directly emitted by stars or reprocessed by dust (left). In the leptophilic model, the IC upscattering of CMB photons dominates the emission for $E_\gamma \lesssim 100$ GeV and vastly overproduces the extended upper limit ($< 1°$) from *Fermi*-LAT after 18 months (black arrow, Ackermann et al. 2010). This either limits our saturated Sommerfeld boost of 530 to much smaller values or the substructure boost employed here (or both). For comparison, the CR induced pion decay (red) is below the gamma-ray upper limits (from Pinzke et al. 2011).
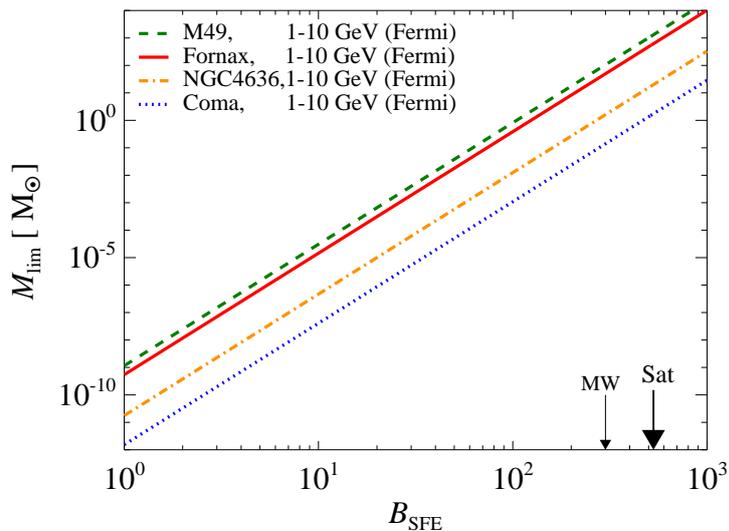
Figure 5.3.: Constraining boost factors using flux upper limits. The requirement of not overproducing the *Fermi*-LAT differential flux upper limits in the energy interval $1 - 10$ GeV constrains the boost from substructures and Sommerfeld enhancement (SFE) in four clusters: M49 (green dashed), Fornax (red solid), NGC4636 (orange dash-dotted), and Coma (blue dotted). We indicate both the saturated SFE of 530 (right black arrow) as well as the local boost in the Milky Way of 300 that is required to explain the electron and positron excess observed at Earth with leptophilic DM (left black arrow, Finkbeiner et al. 2011). If the DM interpretation is correct, we can constrain the smallest size of halos to be larger than $10^4\,M_\odot$. Contrarily, if the smallest size of DM halos is $10^{-6}\,M_\odot$, we can constrain the SFE to $\lesssim 5$ in M49 and Fornax. This corresponds to a maximum SFE in the MW of $\lesssim 3$, which would be too small to support the DM annihilation hypothesis for the PAMELA/*Fermi* excess (from Pinzke et al. 2011).

which may be modified through dissipative baryonic processes, has only a very minor impact on the expected annihilation flux. Instead, the DM density in the region around the scale radius dominates the total DM annihilation flux (see Fig. 5.1). It turns out that the annihilation flux of the smooth DM halo of the best dwarf and cluster candidates is comparable (Pinzke et al. 2009).

However, the true signal is expected to be dramatically enhanced by the presence of substructures within halos. High-resolution simulations of DM halos find that the DM luminosity due to substructures increases by about an order of magnitude for a subhalo mass range of 10^4 (Springel et al. 2008). Hence, adopting a minimum substructure mass that is given by the DM free-streaming scale of an Earth mass ($\sim 10^{-6}\,M_\odot$), the annihilation flux in dwarfs is enhanced by a factor of ~ 20. Importantly, cluster halos maximize the substructure boost for which we find a factor of $\gtrsim 1000$ (see Fig. 5.1), rendering them by far the most promising targets to indirectly detect DM (Pinzke et al. 2011, Gao et al. 2012). Since substructures get tidally depleted toward the dense halo centers, the regions around the virial radius dominate the annihilation flux of substructures. This decreases the substructure boost factor in dwarfs further since the external regions of substructures are stripped through tidal interactions with the host halo. The dominance of the external regions for the annihilation luminosity implies DM surface brightness profiles that are almost flat. This makes it very challenging to detect this flux with imaging atmospheric Cherenkov telescopes since their sensitivity drops approximately linearly with radius and they typically have $5 - 10$ linear resolution elements across a cluster.

5.3. Constraining particle physics models

Recently, it has been shown that electrons and positrons from DM annihilations provide an excellent fit to the *Fermi*, PAMELA, and HESS data (Bergström et al. 2009). This, however, requires an enhancement of the annihilation cross section over its standard value to match the observations. This can be realized in leptophilic cold DM models with a Sommerfeld-enhanced (SFE) cross section (Arkani-Hamed et al. 2009). Hence, we contrast different gamma-

ray emission components in galaxy clusters and explore their spatial and spectral properties. We consider (1) leptophilic DM models, (2) different representative benchmark models of supersymmetric DM, and (3) CR induced pion decay (Pinzke et al. 2011). To model DM annihilation, we consider continuum emission as a result of the hadronization of annihilating neutralinos, internal bremsstrahlung, and inverse Compton emission from the cosmic microwave background as well as from a realistic spatial and spectral distribution of dust and stellar light (for a spectral comparison of the different components in the Fornax cluster, see Fig. 5.2).

Among all clusters/groups of a flux-limited X-ray sample, we predict Virgo, Fornax and M49 to be the brightest DM sources and find a particularly low CR-induced background for Fornax (presumably due to a very efficient past epoch of non-gravitational feedback that pushed a large amount of gas beyond the virial radius). Assuming cold DM with a substructure mass distribution down to an Earth mass and using extended *Fermi* upper limits, we rule out the leptophilic models in their present form in 28 clusters, and limit the boost from SFE in M49 and Fornax to be $\lesssim 5$ (see Fig. 5.3). This corresponds to a limit on SFE in the Milky Way of $\lesssim 3$, which is too small to account for the increasing positron fraction with energy as seen by PAMELA and challenges the DM interpretation (Pinzke et al. 2011). Alternatively, if SFE is realized in Nature, this would imply a limiting substructure mass of $M_{\mathrm{lim}} > 10^4 \, \mathrm{M}_\odot$—a problem for structure formation in most particle physics models.

Using individual cluster observations, it will be challenging for *Fermi* to constrain our selection of DM benchmark models without SFE. Note that we use comparably natural models with "democratic branching ratios" of kinematically allowed final states, i.e., we do not impose an ab initio artificial symmetry in the dark sector that selects a decay channel with a particularly high gamma-ray yield as it is often done for constraining DM parameter space.

5.4. Summary and Outlook

We would like to emphasize that it is necessary to simultaneously simulate the CR and DM physics in order to predict their gamma-ray and radio synchrotron emission. This should enable us to identify optimized observational strategies for extracting the buried DM annihilation signal spectrally and spatially. Depending on the uncertainties of the CR physics, this will allow us to quantitatively identify which regions of the supersymmetric parameter space spanned by the DM mass and its annihilation cross-section are accessible despite astrophysical source confusion.

6. The cosmological impact of TeV blazars

Abstract

The extragalactic gamma-ray sky at TeV energies is dominated by blazars, a subclass of accreting super-massive black holes with powerful relativistic outflows directed at us. Only constituting a small fraction of the total power output of black holes, blazars were thought to have a minor impact on the universe at best. As we argue here, the opposite is true and the gamma-ray emission from TeV blazars can be thermalized via beam-plasma instabilities on cosmological scales with order unity efficiency, resulting in a potentially dramatic heating of the low-density intergalactic medium. Here, we review this novel heating mechanism and explore the consequences for the formation of structure in the universe. In particular, we show how it produces an inverted temperature-density relation of the intergalactic medium that is in agreement with observations of the Lyman-α forest. This suggests that *blazar heating* can potentially explain the paucity of dwarf galaxies in galactic halos and voids, and the bimodality of galaxy clusters. This also transforms our understanding of the evolution of blazars, their contribution to the extra-galactic gamma-ray background, and how their individual spectra can be used in constraining intergalactic magnetic fields.

6.1. Introduction

The extragalactic gamma-ray sky is dominated by "blazars". These are a subclass of super-massive black holes, situated at the center of every galaxy, which drive powerful relativistic jets and electromagnetic radiation out to cosmological distances. An important subset of blazars exhibit hard power-law spectra that extend to TeV photon energies (high-energy-peaked BL Lacs). The Universe is opaque to the emitted TeV gamma rays because they annihilate and pair produce on the extragalactic background light which is emitted by galaxies and quasars through the history of the universe. The mean free path for this reaction is $\lambda_{\gamma\gamma} \sim (700 \dots 35) \, (E/\text{TeV})^{-1}$ Mpc for redshifts $z = 0 \dots 1$, respectively, and is approximately constant at $\lambda_{\gamma\gamma} \sim 35 \, (E/\text{TeV})^{-1}$ Mpc for higher redshifts. The resulting ultra-relativistic pairs of electrons and positrons are commonly assumed to lose energy primarily through inverse Compton scattering with photons of the cosmic microwave background, cascading the original TeV emission a factor of $\sim 10^3$ down to GeV energies.

However, there are two serious problems with this picture: the expected cascaded GeV emission is not seen in the individual spectra of those blazars (Neronov & Vovk 2010) and the emission of all unresolved blazars would overproduce the observed extragalactic gamma-ray background (EGRB) at GeV energies *if* these objects share a similar cosmological evolution as the underlying black hole or parent galaxy population (Venters 2010). As a putative solution to the first problem, comparably large magnetic fields have been hypothesized which would deflect the pairs out of our line-of-sight to these blazars (Neronov & Vovk 2010), diluting the point-source flux into a lower surface brightness "pair halo". However, magnetic deflection of pairs (and hence their inverse Compton emission) out of our line-of-sight is on average balanced by deflecting other pairs into our line-of-sight, so that the resulting isotropic EGRB remains invariant. This represents a substantial problem to unifying the hard gamma-ray blazar population with that of other AGN, is at odds with the underlying physical picture of accreting black hole systems, and suggests an unlikely conspiracy between accretion physics and the formation of structure.

6.2. Beam-plasma instabilities

Recently, we have shown that there is an even more efficient mechanism that competes with this cascading process. Plasma instabilities driven by the highly anisotropic nature of the ultra-relativistic pair distribution provide a plausible way to dissipate the kinetic energy of the TeV pairs locally, heating the intergalactic medium (Broderick et al. 2012). We can understand the two-stream instability intuitively by considering a longitudinal wave-like perturbation of the charge of the background plasma along the beam direction (i.e., a Langmuir wave). The initially homogeneous beam electrons feel repulsive (attractive) forces by the potential minima (maxima) of the electrostatic
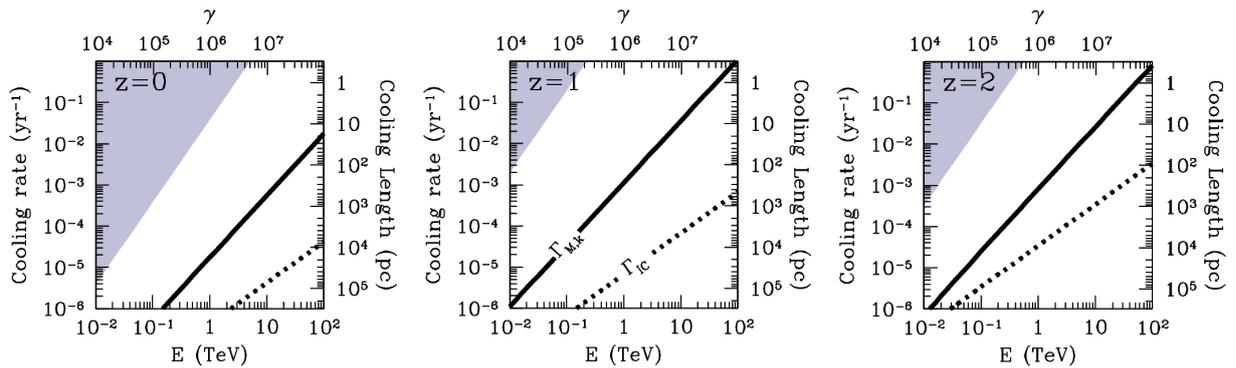
Figure 6.1.: Initial pair beam cooling rates due to the kinetic oblique instability (thick solid) and inverse Compton scattering (dotted) as a function of gamma-ray energy (E) at a number of redshifts (z). In all cases, we consider a mean-density region, and the isotropic-equivalent luminosity of the source at energy E, EL_E, is 10^{45} erg s^{-1}, similar to the brightest TeV blazars seen from Earth. We list the initial pair Lorentz factor, γ, and cooling lengthscale along the top and right axes, respectively (from Broderick et al. 2012).

wave in the background plasma. As a result, electrons (positrons) attain their lowest velocity in the potential minima (maxima), which causes them to bunch up. Hence, the bunching within the beam is simply an excitation of a beam Langmuir wave that couples in phase with the background perturbation. This enhances the background potential and implies stronger forces on the beam pairs. This positive feedback loop causes exponential wave-growth, i.e. the onset of an instability. In practice, oscillatory modes that propagate in an oblique direction to the beam grow substantially faster than the two-stream instability just discussed. The reason is that electric fields can more easily deflect ultra-relativistic particles than change their parallel velocities (see Broderick et al. 2012, for details).

Unstable electromagnetic waves grow fastest when the velocity dispersions are smallest across their wave fronts. As these velocity dispersions get larger and larger, i.e., for increasing temperature, the growth rate of the unstable oblique mode moves into the finite temperature or kinetic regime, where the exponential growth rate is reduced due to the effects of phase mixing and decoherence. In Fig. 6.1, we show the pair beam cooling rates due to the kinetic oblique instability in the linear regime, $\Gamma_{M,k}$ (Bret et al. 2010a) for a beam density that obeys the steady-state Boltzmann equation, i.e., we account for production and various loss processes of the pairs. Most importantly, we find that $\Gamma_{M,k}$ dominates over the inverse Compton cooling rate Γ_{IC} by more than an order of magnitude for the parameters of luminous TeV blazars.

Analytical quasi-linear calculations of the cold regime (Schlickeiser et al. 2012) and numerical work of the oblique instability in the kinetic regime (Bret et al. 2010b) with smaller density contrasts than considered here suggest that the dominance of the oblique instability carries over in the regime of non-linear saturation, although there is currently a debate about the role of induced scattering by thermal ions on this non-linear saturation (Miniati & Elyiv 2013, Schlickeiser et al. 2013, Chang et al. in prep.). In the following, we assume that a large fraction of the free kinetic energy of the pairs is transferred to the electromagnetic modes in the background plasma, which should eventually be dissipated, heating the IGM.

6.3. Implications for the blazar luminosity function and the gamma-ray sky

To assess implications for the gamma-ray sky and the thermal evolution of the IGM, we construct a blazar luminosity function (BLF). In Broderick et al. (2012), we collect the luminosity of all 23 TeV blazars with good spectral measurements and account for selection effects (sky coverage, duty cycle, galactic occultation, TeV flux limit). The resulting BLF is shown in Fig. 6.2. Most notably, the TeV blazar luminosity density is a scaled version of that of quasars. This implies that quasars and TeV blazars appear to be regulated by the same mechanism and are contemporaneous elements of a single AGN population, i.e., the TeV-blazar activity does not lag quasar activity. Hence we adopt the plausible assumption that both distributions trace each other for all redshifts and work out the
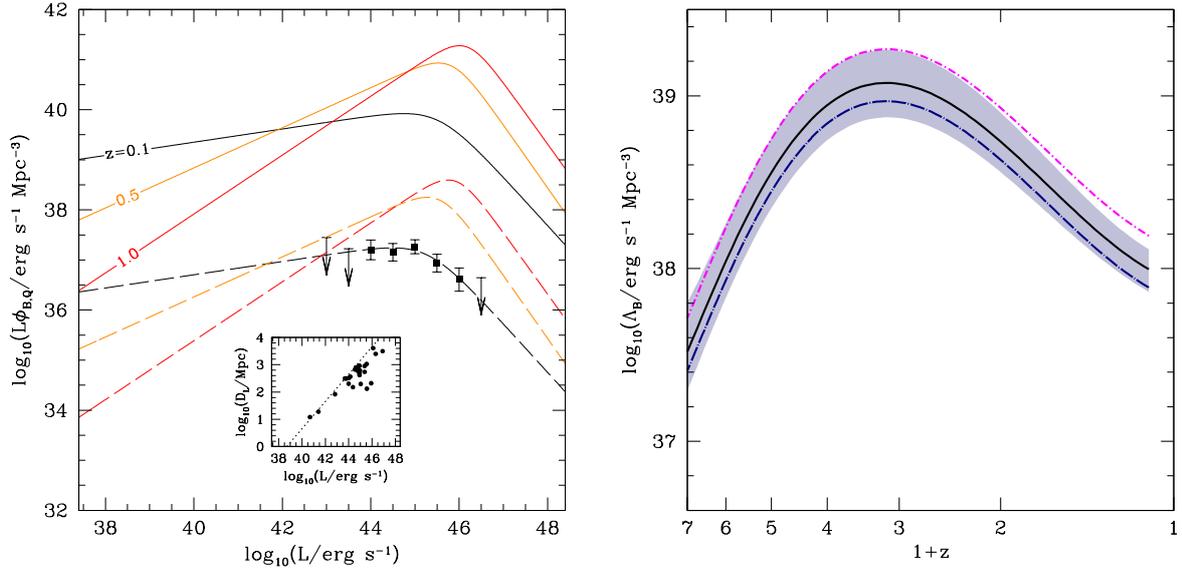
Figure 6.2.: Left. Comparison between the luminosity-weighted quasar and TeV-blazar luminosity functions ($L\phi_Q(z, L)$ and $L\phi_B(z, L)$, respectively). The solid lines show the absolute $L\phi_Q$ (in comoving Mpc), while the dashed lines show $L\phi_Q$ rescaled in magnitude by 2.1×10^{-3} and shifted to lower luminosities by a factor of 0.55. Different redshifts are color coded as indicated in the figure. The points and upper-limits show ϕ_B of all high- and intermediate-energy-peaked blazars with good spectral measurements. Presented in the inset is the TeV source luminosity distance as a function of source luminosity for all of the blazars with redshift estimates (including limits). The dotted line shows the distance-dependence of the flux limit we employ in the completeness correction (from Broderick et al. 2012). Right. Comoving blazar luminosity density $\Lambda_B(z) = \int_{L_{\min}}^{\infty} dL \, \phi_B(z, L)$ as a function of redshift. The shaded region represents the 1-σ uncertainty that results from a combination of the uncertainty in the number of bright blazars that contribute to the local heating and in the uncertainties in the quasar luminosity density (Hopkins et al. 2007) to which we normalize (from Chang et al. 2012).
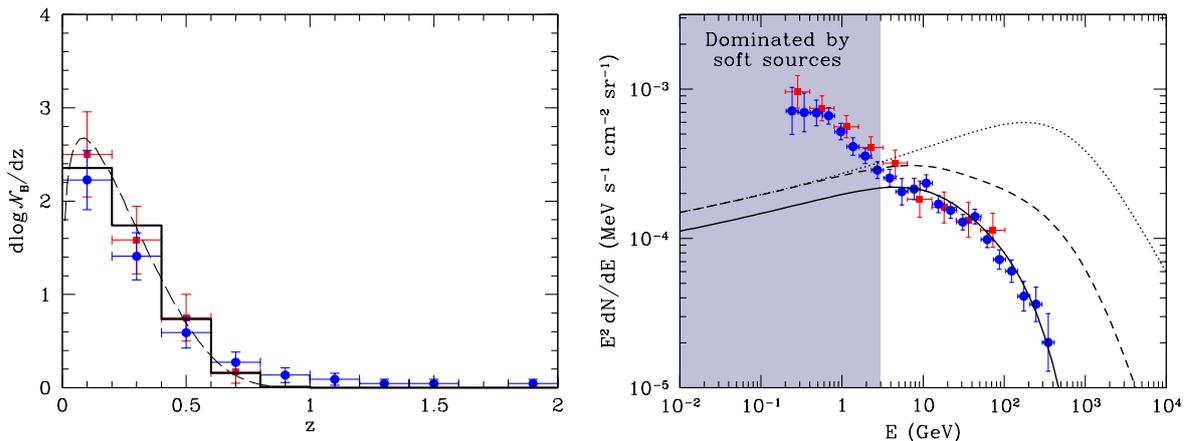
Figure 6.3.: Left. Nearby redshift distribution of the hard gamma-ray blazars above the *Fermi* flux limit, both in continuous form (dashed) and binned with $\Delta z = 0.2$ (continuous). For comparison the redshift distribution of the *Fermi* hard gamma-ray blazars in the 1LAC (red squares) and 2LAC (blue circles) are also shown. For these, the vertical error bars denote Poisson errors. Right. *Fermi* EGRB anticipated by the hard gamma-ray blazars. The dotted, dashed, and solid lines correspond to the unabsorbed spectrum, spectrum corrected for absorption on the extragalactic background light, and spectrum additionally corrected for resolved point sources (assuming all hard gamma-ray blazars with $z \lesssim 0.29$ are resolved). These are compared with the measured *Fermi* EGRB reported in Abdo et al. (2010, red squares) and Ackermann et al. (2012b, blue circles). Note that below ~ 3 GeV the EGRB is dominated by soft sources (from Broderick et al. 2013a).

implications of this assertion.

To quantify the impact on the gamma-ray sky, we need to expand the BLF to include the intrinsic energy spectra, dN/dE, of blazars and adopt a typical broken power-law spectrum

$$\frac{dN}{dE} = f\hat{F}_E = f\left[\left(\frac{E}{E_b}\right)^{\Gamma_l} + \left(\frac{E}{E_b}\right)^{\Gamma_h}\right]^{-1}, \tag{6.1}$$

where $E_b \simeq 1$ TeV is the break energy, $\Gamma_h \simeq 3$ is the high-energy spectral index, and the intrinsic low-energy slope Γ_l is softened with increasing propagation length due to the higher probability of high-energy photons to annihilate on the extragalactic background light. This yields a steeper (larger) observed Γ_F, which we draw from the distribution of local blazars as observed by the *Fermi* gamma-ray telescope (that are not affected by spectral softening due to pair production effects). We arrive at the BLF, $d^4\mathcal{N}/(d\log L_{\mathrm{TeV}}\, dz\, dE\, d\Gamma_l)$, i.e., the distribution of blazars with TeV luminosity L_{TeV}, redshift z, gamma-ray energy E, and Γ_l.

Different projections of this BLF onto its independent variables allow comparison to *Fermi* data. Integrating this distribution over L_{TeV}, E and Γ_l and adopting integration limits that account for the *Fermi* flux limit $S_{\min}$ yields the redshift distribution of *Fermi* blazars (left panel of Fig. 6.3). Interestingly, an evolving (increasing) blazar population is consistent with the observed declining number evolution of blazars due to the *Fermi* flux limit and the low intrinsic luminosity of the hard blazars. Masking these resolved blazars and integrating the blazar distribution over L_{TeV}, z, and Γ_l yields the contribution of blazars to the *isotropic* EGRB (right panel of Fig. 6.3). This demonstrates that an evolving population of hard blazars matches the latest data of the EGRB by the *Fermi* Collaboration at energies $\gtrsim 3$ GeV extremely well. Moreover, the modeled $\log\mathcal{N}$-$\log S$ distribution and the *anisotropic* EGRB (Ackermann et al. 2012a, Broderick et al. 2013b), which mainly probes nearby objects below the detectability limit, provide an excellent match to the *Fermi* data (Broderick et al. 2013a). Hence, this naturally solves the two mysteries introduced in Sect. 6.1 in a *unified model of blazars and their underlying black hole population without the need to invoke large magnetic fields*. Critical to this success is the absence of inverse Compton cascades that would otherwise redistribute energy between the unabsorbed and the absorbed spectrum into the energy range around 10 GeV, thus vastly overproducing the tight limits provided by *Fermi*.
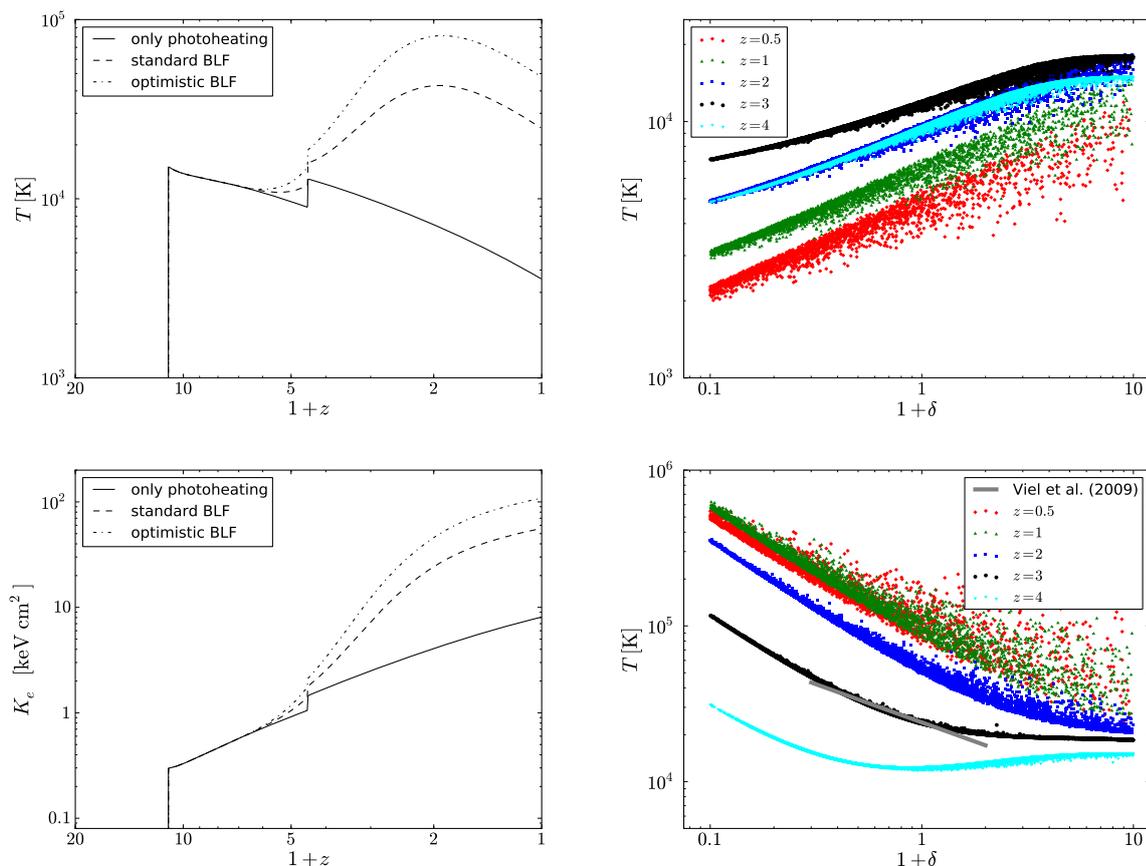
Figure 6.4.: Thermal history (top left) and entropy history (bottom left) of a patch of mean density ($\delta = 0$) of the IGM. The solid curves are for pure photoheating with sudden reionization histories for H and He II at $z_{\mathrm{reion}} = 10$ and $z_{\mathrm{He\,II}} = 3.5$. The dashed (dash-dotted) lines show the evolution for the standard (optimistic) blazar heating model that employs the blazar luminosity density, i.e., using the redshift evolution of the quasar luminosity density and are normalized to the local heating rate, which is subject to an uncertain incompleteness correction factor (from Pfrommer et al. 2012). Temperature-density relation without blazar heating (top right) and for the optimistic blazar heating model (bottom right) at a number of redshifts (from Chang et al. 2012). The grey line is the best-fit model derived from Lyman-α data (Viel et al. 2004).

6.4. Rewriting the thermal history of the intergalactic medium and the Lyman-α forest

We find that for our BLF, every region in the universe is heated by at least one TeV blazar back to $z \sim 5$, providing a novel heating mechanism of the gas at mean density that is ten times larger at the present time than what has been previously considered (Chang et al. 2012). This can be interpreted as a gradually rising (and density dependent) entropy enhancement after $z = 3$ (left panels of Fig. 6.4). Unlike photoheating, the blazar heating rate per unit volume does not depend on density since (1) the distributions of TeV blazars and the extragalactic background light are uniform on the cosmological scales of the mean free path of pair production, $\lambda_{\gamma\gamma}$, and (2) it is nearly independent of the IGM density. Hence this particular heating process deposits more energy per baryon in low-density regions and naturally produces an inverted temperature-density relation in voids that reaches asymptotically $T \propto 1/\rho$ (right panels of Fig. 6.4). This unique property in combination with the recent and continuous nature of blazar heating is needed to solve many problems present in previous calculations of Lyman-α forest spectra.

Detailed cosmological simulations that include blazar heating show superb agreement with all statistics used
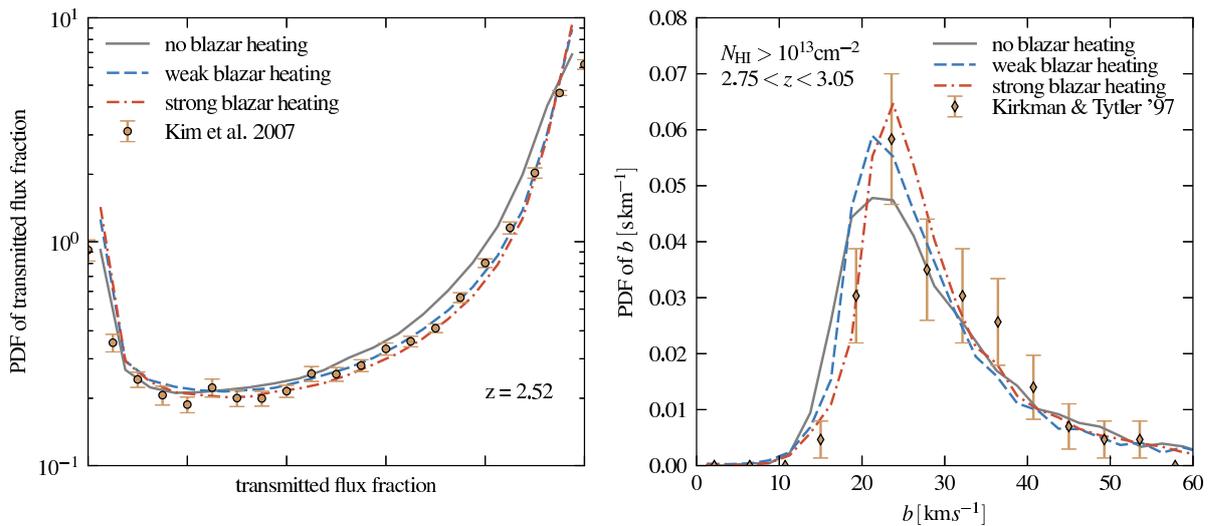
Figure 6.5.: Comparing the Lyman-α forest in hydrodynamical cosmological simulations with and without blazar heating. Left. Probability distribution functions of the transmitted flux fraction for simulations with and without blazar heating for two different normalisations of the blazar heating rate are compared to observational constraints from Kim et al. (2007). Right. The normalised distribution function of Lyman-α line widths, b, for simulations with and without blazar heating at redshift $z = 3$ are compared to observational constraints by Kirkman & Tytler (1997). Both panels show simulation results for a UV background that was *matched* to the observed mean transmission (from Puchwein et al. 2012).

to characterize Lyman-α forest spectra (Puchwein et al. 2012). In particular, our simulations with blazar heating simultaneously reproduce the observed effective optical depth and temperature as a function of redshift, the observed probability distribution functions of the transmitted flux (Fig. 6.5), and the observed flux power spectra, over the full redshift range $2 < z < 3$. Additionally, by deblending the absorption features of Lyman-α spectra into a sum of thermally broadened individual lines, we find superb agreement with the observed lower cutoff of the line-width distribution (Fig. 6.5) and abundances of neutral hydrogen column densities per unit redshift. This concordance between Lyman-α data and simulation results, which are based on the most recent cosmological parameters, also suggests that the inclusion of blazar heating alleviates previous tensions on constraints of the normalization of the density power spectrum, σ_8, derived from Lyman-α measurements and other cosmological data.

6.5. Implications for the formation of dwarf galaxies and galaxy clusters

We have seen that blazar heating dramatically changes the thermal history of the diffuse IGM, which necessarily implies a number of important implications for late-time structure formation (Pfrommer et al. 2012). Unlike photoionization models, which typically invoke the heating at reionization, blazar heating provides a well defined, time-dependent entropy enhancement that rises dramatically after $z \sim 2$, suppressing the formation of late forming dwarf galaxies. On small scales, thermal pressure opposes gravitational collapse. This introduces a characteristic length and mass scale below which galaxies do not form. A hotter intergalactic medium implies a higher thermal pressure and a higher Jeans mass M_J at redshift z,

$$M_J \propto \frac{c_s^3(z)}{\sqrt{G^3 \rho(z)}} \propto \left(\frac{T^3(z)}{G^3 \rho(z)} \right)^{1/2} \quad \rightarrow \quad \frac{M_{J,\text{blazar}}}{M_{J,\text{photo}}} \approx \left(\frac{T_{\text{blazar}}}{T_{\text{photo}}} \right)^{3/2} \gtrsim 30, \tag{6.2}$$

where c_s, ρ, and T_{IGM} are the sound speed, density, and temperature of the IGM, respectively, and G is Newton's gravitational constant. That is, blazar heating increases M_J by 30 over pure photoheating models.
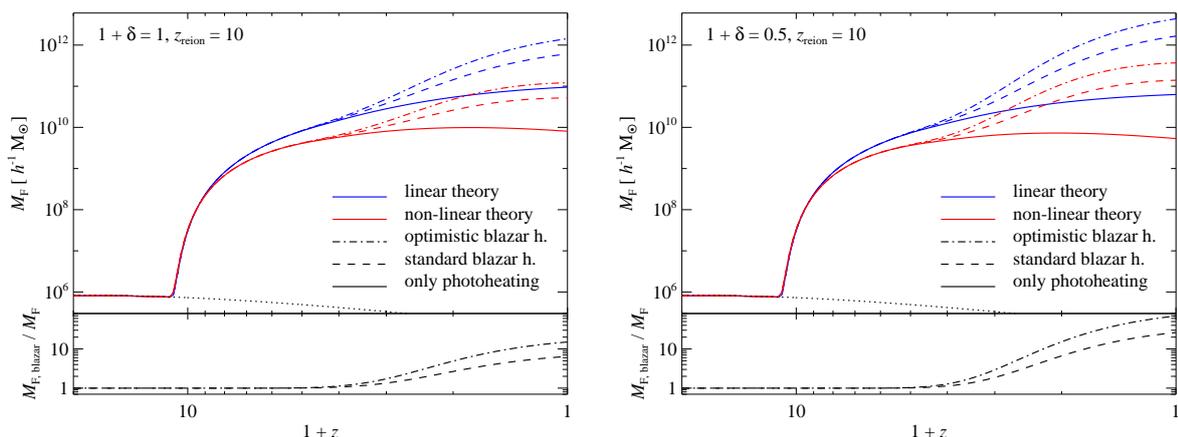
Figure 6.6.: Blazar heating suppresses the formation of late-forming dwarf galaxies. Redshift evolution of the filtering mass, M_F, for the cosmic mean density, $\delta = 0$ (left) and for a void with mean overdensity, $\delta = -0.5$, (right). We contrast M_F in the standard cosmology that employs only photoheating (solid) to the case of blazar heating in our standard model (dashed) and optimistic model (dash-dotted). In the bottom panels, we show the ratio of M_F in our respective blazar heating models to those without blazars. To estimate the effect of nonlinear structure formation on the filtering mass, we compare the linear theory M_F (blue) to the nonlinear theory M_F (red) where we used a correction function derived from hydrodynamic simulations (from Pfrommer et al. 2012).

However, there are complications due to non-linear collapse and a delayed pressure response in an expanding universe. This causes a slight reduction of the suppression factor (Fig. 6.6). Hence, our redshift-dependent entropy enhancement due to blazar heating increases the characteristic halo mass below which dwarf galaxies cannot form by a factor of approximately 10 (50) at mean density (in voids) over that found in the standard model, preventing the formation of late-forming dwarf galaxies. This may help resolve the "missing satellites problem" in the Milky Way of the low observed abundances of dwarf satellites compared to cold dark matter simulations and may bring the observed early star formation histories into agreement with galaxy formation models. At the same time, it is a very plausible explanation of the "void phenomenon" (Peebles & Nusser 2010) by suppressing the formation of galaxies within existing dwarf halos, thus reconciling the number of dwarfs in low-density regions in simulations and the paucity of those in observations.

Finally, this suggests a scenario for the origin of the cool core/non-cool core bimodality in galaxy clusters and groups, which are separated into different classes depending on their core temperatures. Early forming galaxy groups are unaffected because they can efficiently radiate the additional entropy, developing a cool core. However, late-forming groups do not have sufficient time to cool before the elevated entropy enhancement is gravitationally reprocessed through successive mergers—counteracting cooling and potentially raising the core entropy further to potentially form a non-cool core cluster.

6.6. Summary and Outlook

In a series of papers, we have proposed a novel plasma-astrophysical mechanism that promises transformative and potentially radical changes of our understanding of gamma-ray astrophysics and the physics of the intergalactic medium. This can also alter our picture of the formation of dwarf galaxies and galaxy cluster thermodynamics. Detailed comparisons of predictions of blazar heating with Lyman-α forest data and *Fermi* observation of blazar statistics as well as the isotropic and anisotropy gamma-ray backgrounds have been very successful and encouraging.

Nevertheless, we are clearly only beginning to explore the process and implications of plasma-instability driven blazar heating. Many aspects are only poorly understood and are now starting to be investigated, including the physics of the instability in the regime of non-linear saturation. Detailed cosmological simulations of blazar heating are critical in understanding its impact on non-linear structure formation. We hope that this work motivates fruitful

observational and theoretical efforts toward consolidating the presented picture or to modify parts of it.

Part III.

Conclusions and outlook

Conclusions and outlook

While my research area "Interfacing high-energy astrophysics and cosmological structure formation" is still fairly young, the enormous progress obtained within the last years has demonstrated that this field is growing rapidly and promises a successful future. Apart from the theoretical motivations to study the interplay of high-energy astrophysics and structure formation, which have been laid out in this Habilitation thesis, there are strong observational reasons for intensifying research efforts in this direction. The impressive observational progress in this area opens up new windows to the low-frequency radio sky, deepen our knowledge of the gamma-ray universe, and will drastically improve the statistical constraints on galaxy and cluster formation and evolution. To name a few prominent examples, new radio telescopes like LOFAR, Jansky VLA, or the future SKA are bound to revolutionize our understanding of the magnetized high-energy universe. This is complemented at gamma-ray wavelengths with the *Fermi* gamma-ray space telescope and at even higher energies with the successful imaging air Cherenkov telescopes H.E.S.S., MAGIC, VERITAS, and the future CTA that should further open up the high-energy universe. The all-sky surveys in X-rays with eROSITA and at microwaves with *Planck* and SPT/ACT on smaller scales are complementary avenues that are expected to transform our statistical understanding of galaxy clusters. Astro-H will give us a first glance at the intracluster turbulence. Large galaxy surveys that are already taking data or are to commence in this decade (such as Pan-STARRS, Big-BOSS, EUCLID, etc.) will provide an impressive statistical data set with unprecedented details on galaxy formation and evolution. Combining this plethora of data calls for a substantial advance in the theoretical models to get the best possible science return.

This Habilitation thesis focuses on connecting the formation and evolution of galaxies and clusters to high-energy astrophysical phenomena, with particular emphasis on CR physics, magnetic fields, and plasma processes. Its primary goal is to redefine the state-of-the-art of the modeling of those physical processes in our (first generation) cosmological hydrodynamical simulations of galaxy and cluster formation and to seek for a deeper understanding of the fundamental physics. The inherently complicated microphysics of those high-energy astrophysical and plasma physics processes make the sub-resolution modeling and the associated parameter choices far from obvious. However, in this Habilitation thesis first steps have been undertaken that clearly need to be refined and advanced in future work. To this end, I aim at transforming the accuracy and efficiency of present numerical algorithms of the presented CR and plasma physics to the next level. This points to replacing the numerical technique used for solving the hydrodynamical equations from the Lagrangian smoothed particle hydrodynamics (SPH) method to using an unstructured mesh, which was realized in the AREPO code (Springel 2010). This holds the promise to cure some of the known shortcomings of the SPH method while at the same time enabling a superior adaptive resolution capability. To complement these theoretical efforts, I have already joined various observational collaborations. For example, I hold an associate member status of the LOFAR Magnetism Key Science Project and am an external collaboration member of the gamma-ray collaborations MAGIC, VERITAS, and Fermi. The long-term goal of my research is to establish the combination of cosmological hydrodynamic simulations and observations of non-thermal emission as a novel astrophysical tool, complementary to in-situ observations within the solar system and plasma laboratories on Earth.

Bibliography

Abdo, A. A., et al. 2010, ApJ, 720, 435

Ackermann, M., et al. 2010, ApJ, 717, L71

—. 2012a, Phys. Rev. D, 85, 083007

—. 2012b, 4th Fermi Symposium

—. 2013, arXiv:1308.5654

Aleksić, J., et al. 2010, ApJ, 723, L207

—. 2012a, A&A, 541, A99

—. 2012b, A&A, 539, L2

Arkani-Hamed, N., Finkbeiner, D. P., Slatyer, T. R., & Weiner, N. 2009, Phys. Rev. D, 79, 015014

Arlen, T., et al. 2012, ApJ, 757, 123

Balbus, S. A. 2000, ApJ, 534, 420

Battaglia, N., Bond, J. R., Pfrommer, C., & Sievers, J. L. 2012, ApJ, 758, 74

Battaglia, N., Pfrommer, C., Sievers, J. L., Bond, J. R., & Enßlin, T. A. 2009, MNRAS, 393, 1073

Beck, R. 2001, Space Science Reviews, 99, 243

Bergström, L., Edsjö, J., & Zaharijas, G. 2009, Physical Review Letters, 103, 031103

Blandford, R., & Eichler, D. 1987, Phys. Rep., 154, 1

Böhringer, H., Briel, U. G., Schwarz, R. A., Voges, W., Hartner, G., & Trümper, J. 1994, Nature, 368, 828

Bonafede, A., Feretti, L., Murgia, M., Govoni, F., Giovannini, G., Dallacasa, D., Dolag, K., & Taylor, G. B. 2010, A&A, 513, A30

Bond, J. R., Kofman, L., & Pogosyan, D. 1996, Nature, 380, 603

Booth, C. M., Agertz, O., Kravtsov, A. V., & Gnedin, N. Y. 2013, arXiv:1308.4974

Bret, A., Gremillet, L., & Bénisti, D. 2010a, Phys. Rev. E, 81, 036402

Bret, A., Gremillet, L., & Dieckmann, M. E. 2010b, Physics of Plasmas, 17, 120501

Broderick, A. E., Chang, P., & Pfrommer, C. 2012, ApJ, 752, 22

Broderick, A. E., Pfrommer, C., Puchwein, E., & Chang, P. 2013a, arXiv:1308.0340

—. 2013b, arXiv:1308.0015

Brüggen, M., & Kaiser, C. R. 2002, Nature, 418, 301

Brunetti, G., & Lazarian, A. 2011, MNRAS, 410, 127

Burns, J. O. 1998, Science, 280, 400

Cavagnolo, K. W., Donahue, M., Voit, G. M., & Sun, M. 2009, ApJS, 182, 12

Chandran, B. D. G., & Rasera, Y. 2007, ApJ, 671, 1413

Chang, P., Broderick, A. E., & Pfrommer, C. 2012, ApJ, 752, 23

Chung, A., van Gorkom, J. H., Kenney, J. D. P., Crowl, H., & Vollmer, B. 2009, AJ, 138, 1741

Churazov, E., Brüggen, M., Kaiser, C. R., Böhringer, H., & Forman, W. 2001, ApJ, 554, 261

Clarke, T. E., & Ensslin, T. A. 2006, AJ, 131, 2900

Croton, D. J., et al. 2006, MNRAS, 365, 11

Dorfi, E. A., & Breitschwerdt, D. 2012, A&A, 540, A77

Dubois, Y., Devriendt, J., Teyssier, R., & Slyz, A. 2011, MNRAS, 417, 1853

Dursi, L. J. 2007, ApJ, 670, 221

Dursi, L. J., & Pfrommer, C. 2008, ApJ, 677, 993

Enßlin, T., Pfrommer, C., Miniati, F., & Subramanian, K. 2011, A&A, 527, A99

Enßlin, T. A., Biermann, P. L., Klein, U., & Kohle, S. 1998a, A&A, 332, 395

Enßlin, T. A., & Brüggen, M. 2002, MNRAS, 331, 1011

Enßlin, T. A., & Gopal-Krishna. 2001, A&A, 366, 26

Enßlin, T. A., Pfrommer, C., Springel, V., & Jubelgas, M. 2007, A&A, 473, 41

Enßlin, T. A., Simon, P., Biermann, P. L., Klein, U., Kohle, S., Kronberg, P. P., & Mack, K. 2001, ApJ, 549, L39

Enßlin, T. A., Wang, Y., Nath, B. B., & Biermann, P. L. 1998b, A&A, 333, L47

Ettori, S., & Fabian, A. C. 2000, MNRAS, 317, L57

Finkbeiner, D. P., Goodenough, L., Slatyer, T. R., Vogelsberger, M., & Weiner, N. 2011, JCAP, 5, 2

Gao, L., Frenk, C. S., Jenkins, A., Springel, V., & White, S. D. M. 2012, MNRAS, 419, 1721

Gaspari, M., Brighenti, F., & Temi, P. 2012, MNRAS, 424, 190

Guo, F., & Oh, S. P. 2008, MNRAS, 384, 251

Guo, Q., White, S., Li, C., & Boylan-Kolchin, M. 2010, MNRAS, 404, 1111

Helder, E. A., et al. 2009, Science, 325, 719

Hopkins, P. F., Richards, G. T., & Hernquist, L. 2007, ApJ, 654, 731

Hudson, D. S., Mittal, R., Reiprich, T. H., Nulsen, P. E. J., Andernach, H., & Sarazin, C. L. 2010, A&A, 513, A37

Jubelgas, M., Springel, V., Enßlin, T., & Pfrommer, C. 2008, A&A, 481, 33

Kim, T.-S., Bolton, J. S., Viel, M., Haehnelt, M. G., & Carswell, R. F. 2007, MNRAS, 382, 1657

Kim, W.-T., & Narayan, R. 2003, ApJ, 596, L139

Kirkman, D., & Tytler, D. 1997, ApJ, 484, 672

Kravtsov, A. 2010, Advances in Astronomy, 2010

Kulsrud, R., & Pearce, W. P. 1969, ApJ, 156, 445

Kulsrud, R. M. 2005, Plasma physics for astrophysics

Kulsrud, R. M., Cen, R., Ostriker, J. P., & Ryu, D. 1997, ApJ, 480, 481

Lau, E. T., Kravtsov, A. V., & Nagai, D. 2009, ApJ, 705, 1129

Loewenstein, M., Zweibel, E. G., & Begelman, M. C. 1991, ApJ, 377, 392

Lyutikov, M. 2006, MNRAS, 373, 73

Markevitch, M., Gonzalez, A. H., David, L., Vikhlinin, A., Murray, S., Forman, W., Jones, C., & Tucker, W. 2002, ApJ, 567, L27

McNamara, B. R., & Nulsen, P. E. J. 2007, ARA&A, 45, 117

—. 2012, New Journal of Physics, 14, 055023

Miniati, F., & Elyiv, A. 2013, ApJ, 770, 54

Miniati, F., Ryu, D., Kang, H., & Jones, T. W. 2001, ApJ, 559, 59

Miniati, F., Ryu, D., Kang, H., Jones, T. W., Cen, R., & Ostriker, J. P. 2000, ApJ, 542, 608

Moster, B. P., Somerville, R. S., Maulbetsch, C., van den Bosch, F. C., Macciò, A. V., Naab, T., & Oser, L. 2010, ApJ, 710, 903

Narayan, R., & Medvedev, M. V. 2001, ApJ, 562, L129

Navarro, J. F., Frenk, C. S., & White, S. D. M. 1997, ApJ, 490, 493

Neronov, A., & Vovk, I. 2010, Science, 328, 73

Parrish, I. J., & Stone, J. M. 2007, ApJ, 664, 135

Parrish, I. J., Stone, J. M., & Lemaster, N. 2008, ApJ, 688, 905

Peebles, P. J. E., & Nusser, A. 2010, Nature, 465, 565

Peterson, J. R., & Fabian, A. C. 2006, Phys. Rep., 427, 1

Pfrommer, C. 2008, MNRAS, 385, 1242

—. 2013, ApJ, in print, arXiv:1303.5443

Pfrommer, C., Chang, P., & Broderick, A. E. 2012, ApJ, 752, 24

Pfrommer, C., & Dursi, L. J. 2010, Nature Physics, 6, 520

Pfrommer, C., Enßlin, T. A., & Springel, V. 2008, MNRAS, 385, 1211

Pfrommer, C., Enßlin, T. A., Springel, V., Jubelgas, M., & Dolag, K. 2007, MNRAS, 378, 385

Pfrommer, C., & Jones, T. W. 2011, ApJ, 730, 22

Pfrommer, C., Springel, V., Enßlin, T. A., & Jubelgas, M. 2006, MNRAS, 367, 113

Pinzke, A., Oh, S. P., & Pfrommer, C. 2013, MNRAS

Pinzke, A., & Pfrommer, C. 2010, MNRAS, 409, 449

Pinzke, A., Pfrommer, C., & Bergström, L. 2009, Physical Review Letters, 103, 181302

—. 2011, Phys. Rev. D, 84, 123509

Puchwein, E., Pfrommer, C., Springel, V., Broderick, A. E., & Chang, P. 2012, MNRAS, 423, 149

Puchwein, E., & Springel, V. 2013, MNRAS, 428, 2966

Ruszkowski, M., & Begelman, M. C. 2002, ApJ, 581, 223

Ruszkowski, M., Enßlin, T. A., Brüggen, M., Heinz, S., & Pfrommer, C. 2007, MNRAS, 378, 662

Ruszkowski, M., Lee, D., Brüggen, M., Parrish, I., & Oh, S. P. 2011, ApJ, 740, 81

Ryu, D., Kang, H., & Biermann, P. L. 1998, A&A, 335, 19

Ryu, D., Kang, H., Cho, J., & Das, S. 2008, Science, 320, 909

Ryu, D., Kang, H., Hallman, E., & Jones, T. W. 2003, ApJ, 593, 599

Salem, M., & Bryan, G. L. 2013, arXiv:1307.6215

Schlickeiser, R. 2002, Cosmic Ray Astrophysics

Schlickeiser, R., Ibscher, D., & Supsar, M. 2012, ApJ, 758, 102

Schlickeiser, R., Krakau, S., & Supsar, M. 2013, ApJ, in print, arXiv:1308.4594

Sharma, P., Chandran, B. D. G., Quataert, E., & Parrish, I. J. 2009, ApJ, 699, 348

Springel, V. 2005, MNRAS, 364, 1105

—. 2010, MNRAS, 401, 791

Springel, V., et al. 2008, Nature, 456, 73

Uchiyama, Y., Aharonian, F. A., Tanaka, T., Takahashi, T., & Maeda, Y. 2007, Nature, 449, 576

Uhlig, M., Pfrommer, C., Sharma, M., Nath, B. B., Enßlin, T. A., & Springel, V. 2012, MNRAS, 423, 2374

van den Aarssen, L. G., Bringmann, T., & Pfrommer, C. 2012, Physical Review Letters, 109, 231301

Vazza, F., Dolag, K., Ryu, D., Brunetti, G., Gheller, C., Kang, H., & Pfrommer, C. 2011, MNRAS, 418, 960

Veilleux, S., Cecil, G., & Bland-Hawthorn, J. 2005, ARA&A, 43, 769

Venters, T. M. 2010, ApJ, 710, 1530

Viel, M., Haehnelt, M. G., & Springel, V. 2004, MNRAS, 354, 684

Vikhlinin, A., Markevitch, M., & Murray, S. S. 2001, ApJ, 551, 160

Vikhlinin, A., et al. 2009, ApJ, 692, 1060

Voit, G. M. 2005, Reviews of Modern Physics, 77, 207

Völk, H. J., Aharonian, F. A., & Breitschwerdt, D. 1996, Space Sci. Rev., 75, 279

Vollmer, B., Soida, M., Beck, R., Urbanik, M., Chyży, K. T., Otmianowska-Mazur, K., Kenney, J. D. P., & van Gorkom, J. H. 2007, A&A, 464, L37

Wadepuhl, M., & Springel, V. 2011, MNRAS, 410, 1975

Part IV.

Supplement

A. Publications of this Habilitation

Topically ordered list of publications that cumulatively constitute this Habilitation thesis (numbering corresponds to thesis chapters).

1. Cosmic rays in galaxy clusters

1.1. Cosmological simulations and theory

1. **C. Pfrommer**, T. A. Enßlin, V. Springel, M. Jubelgas, K. Dolag, *Simulating cosmic rays in clusters of galaxies – I. effects on the Sunyaev-Zel'dovich effect and the X-ray emission*, 2007, *MNRAS*, 378, 385.

2. **C. Pfrommer**, T. A. Enßlin, V. Springel, *Simulating cosmic rays in clusters of galaxies – II. A unified scheme for radio halos and relics with predictions of the gamma-ray emission*, 2008, *MNRAS*, 385, 1211.

3. **C. Pfrommer**, *Simulating cosmic rays in clusters of galaxies – III. Non-thermal scaling relations and comparison to observations*, 2008, *MNRAS*, 385, 1242.

4. A. Pinzke & **C. Pfrommer**, *Simulating the gamma-ray emission from galaxy clusters: a universal cosmic ray spectrum and spatial distribution*, 2010, *MNRAS*, 409, 449.

5. T. A. Enßlin, **C. Pfrommer**, F. Miniati, K. Subramanian, *Cosmic ray transport in galaxy clusters: implications for radio halos, gamma-ray signatures, and cool core heating*, 2011, *A&A*, 527, 99.

1.2. Observational collaborations (only lead theory author papers)

6. The MAGIC Collaboration: J. Aleksic et al., incl. **C. Pfrommer (corresponding author)**, *MAGIC gamma-ray observation of the Perseus galaxy cluster: implications for cosmic rays, dark matter and NGC1275*, 2010, *ApJ*, 710, 634.

7. The MAGIC Collaboration: J. Aleksic et al., incl. **C. Pfrommer (corresponding author)**, *Constraining cosmic rays and magnetic fields in the Perseus galaxy cluster with TeV observations by the MAGIC telescopes*, 2012, *A&A*, 541, A99.

8. The VERITAS Collaboration: T. Arlen et al., incl. **C. Pfrommer (corresponding author)**, *Constraints on cosmic rays, magnetic fields, and dark matter from gamma-ray observations of the Coma cluster of galaxies with VERITAS and Fermi*, 2012, *ApJ*, 757, 123.

9. The Fermi/LAT Collaboration: M. Ackermann et al., incl. **C. Pfrommer (corresponding author)**, *Search for cosmic-ray induced gamma-ray emission in galaxy clusters*, 2013, submitted, arXiv:1308.75654.

2. Magnetic fields in galaxy clusters

10. J. L. Dursi & **C. Pfrommer**, *Draping of cluster magnetic fields over bullets and bubbles—morphology and dynamic effects*, 2008, *ApJ*, 677, 993.

11. **C. Pfrommer** & L. J. Dursi, *Detecting the orientation of magnetic fields in galaxy clusters*, 2010, *Nature Phys.*, 6, 520, (including supplementary material).

3. Cosmological structure formation shocks

12. **C. Pfrommer** & T. W. Jones, *Radio galaxy NGC 1265 unveils the accretion shock onto the Perseus galaxy cluster*, 2011, *ApJ*, 730, 22.

13. N. Battaglia, **C. Pfrommer**, J. L. Sievers, J. R. Bond, T. A. Enßlin, *Exploring the magnetized cosmic web through low frequency radio emission*, 2009, *MNRAS*, 393, 1073.

14. A. Pinzke, S. P. Oh, **C. Pfrommer**, *Giant radio relics in galaxy clusters: re-acceleration of fossil relativistic electrons?*, 2013, *MNRAS*, in print, arXiv:1301.75644.

4. The impact of cosmic rays on galaxy and cluster formation

15. M. Uhlig, **C. Pfrommer**, M. Sharma, B. Nath, T. A. Enßlin, V. Springel, *Galactic winds driven by cosmic-ray streaming*, 2012, *MNRAS*, 423, 2374.

16. **C. Pfrommer**, *Toward a comprehensive model for feedback by active galactic nuclei: new insights from M87 observations by LOFAR, Fermi and H.E.S.S.*, 2013, *ApJ*, in print, arXiv:1303.75443.

5. Indirect dark matter searches in galaxy clusters

17. A. Pinzke, **C. Pfrommer**, L. Bergström, *Gamma-rays from dark matter annihilations strongly constrain the substructure in halos*, 2009, *Phys. Rev. Lett.*, 103, 181302.

18. A. Pinzke, **C. Pfrommer**, L. Bergström, *Prospects of detecting gamma-ray emission from galaxy clusters: cosmic rays and dark matter annihilations*, 2011, *Phys. Rev. D* 84, 123509.

6. The cosmological impact of TeV blazars

19. A. E. Broderick, P. Chang, **C. Pfrommer**, *The cosmological impact of luminous TeV blazars I: implications of plasma instabilities for the intergalactic magnetic field and extragalactic gamma-ray background*, 2012, *ApJ*, 752, 22.

20. P. Chang, A. E. Broderick, **C. Pfrommer**, *The cosmological impact of luminous TeV blazars II: rewriting the thermal history of the intergalactic medium*, 2012, *ApJ*, 752, 23.

21. **C. Pfrommer**, P. Chang, A. E. Broderick, *The cosmological impact of luminous TeV blazars III: implications for galaxy clusters and the formation of dwarf galaxies*, 2012, *ApJ*, 752, 24.

22. E. Puchwein, **C. Pfrommer**, V. Springel, A. E. Broderick, P. Chang, *The Lyman-α forest in a blazar-heated Universe*, 2012, *MNRAS*, 423, 149.

23. A. E. Broderick, **C. Pfrommer**, E. Puchwein, P. Chang, *Implications of plasma beam instabilities for the statistics of the Fermi hard gamma-ray blazars and the origin of the extragalactic gamma-ray background*, 2013, submitted, arXiv:1308.0340.

24. A. E. Broderick, **C. Pfrommer**, E. Puchwein, P. Chang, *Lower limits upon the anisotropy of the extragalactic gamma-ray background implied by the 2FGL and 1FHL catalogs*, 2013, submitted, arXiv:1308.0015.

Extra-curriculum: Cosmology with galaxy clusters

25. N. Battaglia, J. R. Bond, **C. Pfrommer**, J. L. Sievers, D. Sijacki, *Simulations of the Sunyaev-Zel'dovich power spectrum with active galactic nucleus feedback*, 2010, *ApJ*, 725, 91.

26. N. Battaglia, J. R. Bond, **C. Pfrommer**, J. L. Sievers, *On the cluster physics of Sunyaev-Zel'dovich and X-ray surveys I: the influence of feedback, non-thermal pressure and cluster shapes on $Y - M$ scaling relations*, 2012, *ApJ*, 758, 74.

27. N. Battaglia, J. R. Bond, **C. Pfrommer**, J. L. Sievers, *On the cluster physics of Sunyaev-Zel'dovich and X-ray surveys II: deconstructing the thermal SZ power spectrum*, 2012, *ApJ*, 758, 75.

28. N. Battaglia, J. R. Bond, **C. Pfrommer (corresponding author)**, J. L. Sievers, *On the cluster physics of Sunyaev-Zel'dovich and X-ray surveys III: measurement biases and cosmological evolution of gas and stellar mass fractions*, 2013, *ApJ*, in print, arXiv:1209.4082.

29. A. Hajian, N. Battaglia, D. N. Spergel, J. R. Bond, **C. Pfrommer**, J. L. Sievers, *Measuring the thermal Sunyaev-Zel'dovich effect through the cross correlation of Planck and WMAP maps with ROSAT galaxy cluster catalogs*, 2013, *JCAP*, in print, arXiv:1309.3282.

B. Publications (complete list)

Publications are listed in reverse chronological order. I indicate lead authorship position (or lead theory authorship position within observational collaborations) of papers with alphabetical ordering by "corresponding author".

Refereed Publications

1. A. Hajian, N. Battaglia, D. N. Spergel, J. R. Bond, **C. Pfrommer**, J. L. Sievers, *Measuring the thermal Sunyaev-Zel'dovich effect through the cross correlation of Planck and WMAP maps with ROSAT galaxy cluster catalogs*, 2013, *JCAP*, in print, arXiv:1309.3282.

2. **C. Pfrommer**, *Toward a comprehensive model for feedback by active galactic nuclei: new insights from M87 observations by LOFAR, Fermi and H.E.S.S.*, 2013, *ApJ*, in print, arXiv:1303.5443.

3. N. Battaglia, J. R. Bond, **C. Pfrommer (corresponding author)**, J. L. Sievers, *On the cluster physics of Sunyaev-Zel'dovich and X-ray surveys III: measurement biases and cosmological evolution of gas and stellar mass fractions*, 2013, *ApJ*, in print, arXiv:1209.4082.

4. A. Pinzke, S. P. Oh, **C. Pfrommer**, *Giant radio relics in galaxy clusters: re-acceleration of fossil relativistic electrons?*, 2013, *MNRAS*, in print, arXiv:1301.5644.

5. L. G. van den Aarssen, T. Bringmann, **C. Pfrommer**, *Dark matter with long-range interactions as a solution to all small-scale problems of ΛCDM cosmology?* 2012, *Phys. Rev. Lett.* 109, 231301.

6. N. Battaglia, J. R. Bond, **C. Pfrommer**, J. L. Sievers, *On the cluster physics of Sunyaev-Zel'dovich and X-ray surveys I: the influence of feedback, non-thermal pressure and cluster shapes on $Y - M$ scaling relations*, 2012, *ApJ*, 758, 74.

7. N. Battaglia, J. R. Bond, **C. Pfrommer**, J. L. Sievers, *On the cluster physics of Sunyaev-Zel'dovich and X-ray surveys II: deconstructing the thermal SZ power spectrum*, 2012, *ApJ*, 758, 75.

8. The VERITAS Collaboration: T. Arlen et al., incl. **C. Pfrommer (corresponding author)**, *Constraints on cosmic rays, magnetic fields, and dark matter from gamma-ray observations of the Coma cluster of galaxies with VERITAS and Fermi*, 2012, *ApJ*, 757, 123.

9. M. Uhlig, **C. Pfrommer**, M. Sharma, B. Nath, T. A. Enßlin, V. Springel, *Galactic winds driven by cosmic-ray streaming*, 2012, *MNRAS*, 423, 2374.

10. E. Puchwein, **C. Pfrommer**, V. Springel, A. E. Broderick, P. Chang, *The Lyman-α forest in a blazar-heated Universe*, 2012, *MNRAS*, 423, 149.

11. **C. Pfrommer**, P. Chang, A. E. Broderick, *The cosmological impact of luminous TeV blazars III: implications for galaxy clusters and the formation of dwarf galaxies*, 2012, *ApJ*, 752, 24.

12. P. Chang, A. E. Broderick, **C. Pfrommer**, *The cosmological impact of luminous TeV blazars II: rewriting the thermal history of the intergalactic medium*, 2012, *ApJ*, 752, 23.

13. A. E. Broderick, P. Chang, **C. Pfrommer**, *The cosmological impact of luminous TeV blazars I: implications of plasma instabilities for the intergalactic magnetic field and extragalactic gamma-ray background*, 2012, *ApJ*, 752, 22.

14. The MAGIC Collaboration: J. Aleksic et al., incl. **C. Pfrommer (corresponding author)**, *Constraining cosmic rays and magnetic fields in the Perseus galaxy cluster with TeV observations by the MAGIC telescopes*, 2012, *A&A*, 541, A99.

15. The MAGIC Collaboration: J. Aleksic et al., incl. **C. Pfrommer**, *Detection of very high energy gamma-ray emission from NGC 1275 by the MAGIC telescopes*, 2012, *A&A*, 539, L2.

16. A. Pinzke, **C. Pfrommer**, L. Bergström, *Prospects of detecting gamma-ray emission from galaxy clusters: cosmic rays and dark matter annihilations*, 2011, *Phys. Rev. D* 84, 123509.

17. F. Vazza, K. Dolag, D. Ryu, G. Brunetti, C. Gheller, H. Kang, **C. Pfrommer**, *A comparison of cosmological codes: properties of thermal gas and shock waves in large scale structures*, 2011, *MNRAS*, 418, 960.

18. **C. Pfrommer** & T. W. Jones, *Radio galaxy NGC 1265 unveils the accretion shock onto the Perseus galaxy cluster*, 2011, *ApJ*, 730, 22.

19. T. A. Enßlin, **C. Pfrommer**, F. Miniati, K. Subramanian, *Cosmic ray transport in galaxy clusters: implications for radio halos, gamma-ray signatures, and cool core heating*, 2011, *A&A*, 527, 99.

20. A. J. Cuesta, T. E. Jeltema, F. Zandanel, S. Profumo, F. Prada, G. Yepes, A. Klypin, Y. Hoffman, J. Primack, M. A. Sanchez-Conde, **C. Pfrommer**, *Dark matter decay and annihilation in the Local Universe: CLUES from Fermi*, 2011, *ApJL*, 726, L6.

21. **C. Pfrommer** & L. J. Dursi, *Detecting the orientation of magnetic fields in galaxy clusters*, 2010, *Nature Phys.*, 6, 520.

22. The MAGIC Collaboration: J. Aleksic et al., incl. **C. Pfrommer**, *Detection of very high energy gamma-ray emission from the Perseus cluster head-tail galaxy IC 310 by the MAGIC telescopes*, 2010, *ApJL*, 723, L207.

23. The Fermi/LAT Collaboration: M. Ackermann et al., incl. **C. Pfrommer**, *GeV gamma-ray flux upper limits from clusters of galaxies*, 2010, *ApJL*, 717, L71.

24. N. Battaglia, J. R. Bond, **C. Pfrommer**, J. L. Sievers, D. Sijacki, *Simulations of the Sunyaev-Zel'dovich power spectrum with active galactic nucleus feedback*, 2010, *ApJ*, 725, 91.

25. A. Pinzke & **C. Pfrommer**, *Simulating the gamma-ray emission from galaxy clusters: a universal cosmic ray spectrum and spatial distribution*, 2010, *MNRAS*, 409, 449.

26. The MAGIC Collaboration: J. Aleksic et al., incl. **C. Pfrommer (corresponding author)**, *MAGIC gamma-ray observation of the Perseus galaxy cluster: implications for cosmic rays, dark matter and NGC1275*, 2010, *ApJ*, 710, 634.

27. A. Pinzke, **C. Pfrommer**, L. Bergström, *Gamma-rays from dark matter annihilations strongly constrain the substructure in halos*, 2009, *Phys. Rev. Lett.*, 103, 181302.

28. N. Battaglia, **C. Pfrommer**, J. L. Sievers, J. R. Bond, T. A. Enßlin, *Exploring the magnetized cosmic web through low frequency radio emission*, 2009, *MNRAS*, 393, 1073.

29. D. Sijacki, **C. Pfrommer**, T. A. Enßlin, V. Springel, *Simulations of cosmic ray feedback by AGN in galaxy clusters*, 2008, *MNRAS*, 387, 1403.

30. **C. Pfrommer**, *Simulating cosmic rays in clusters of galaxies – III. Non-thermal scaling relations and comparison to observations*, 2008, *MNRAS*, 385, 1242.

31. **C. Pfrommer**, T. A. Enßlin, V. Springel, *Simulating cosmic rays in clusters of galaxies – II. A unified scheme for radio halos and relics with predictions of the gamma-ray emission*, 2008, *MNRAS*, 385, 1211.

32. J. L. Dursi & **C. Pfrommer**, *Draping of cluster magnetic fields over bullets and bubbles—morphology and dynamic effects*, 2008, *ApJ*, 677, 993.

33. M. Jubelgas, V. Springel, T. A. Enßlin, **C. Pfrommer**, *Cosmic ray feedback in hydrodynamical simulations of galaxy formation*, 2008, *A&A*, 481, 33.

34. M. Ruszkowski, T. A. Enßlin, M. Brüggen, S. Heinz, **C. Pfrommer**, *Impact of magnetic fields on AGN-blown bubbles*, 2007, *MNRAS*, 378, 662.

35. **C. Pfrommer**, T. A. Enßlin, V. Springel, M. Jubelgas, K. Dolag, *Simulating cosmic rays in clusters of galaxies – I. effects on the Sunyaev-Zel'dovich effect and the X-ray emission*, 2007, *MNRAS*, 378, 385.

36. T. A. Enßlin, **C. Pfrommer**, V. Springel, M. Jubelgas, *Cosmic ray physics in calculations of cosmological structure formation*, 2007, *A&A*, 473, 41.

37. **C. Pfrommer**, V. Springel, T. A. Enßlin, M. Jubelgas, *Detecting shock waves in cosmological smoothed particle hydrodynamics simulations*, 2006, *MNRAS*, 367, 113.

38. B. M. Schäfer, **C. Pfrommer**, M. Bartelmann, V. Springel, L. Hernquist, *Detecting Sunyaev-Zel'dovich clusters with Planck – I. Construction of all-sky thermal and kinetic SZ-maps*, 2006, *MNRAS*, 370, 1309.

39. B. M. Schäfer, **C. Pfrommer**, R. Hell, M. Bartelmann, *Detecting Sunyaev-Zel'dovich clusters with Planck – II. Foreground components and optimised filtering schemes*, 2006, *MNRAS*, 370, 1713.

40. I. Golombek, M. Bartelmann, T. A. Enßlin, M. Jubelgas, **C. Pfrommer**, V. Springel, *Radio emission of galaxy clusters*, 2006, *AN*, 327, 569.

41. **C. Pfrommer**, T. A. Enßlin, C. Sarazin, *Unveiling the composition of radio plasma bubbles in galaxy clusters with the Sunyaev-Zel'dovich effect*, 2005, *A&A*, 430, 799.

42. B. M. Schäfer, **C. Pfrommer**, S. Zaroubi, *Redshift estimation of clusters by wavelet decomposition of their Sunyaev-Zel'dovich morphology*, 2005, *MNRAS*, 362, 1418.

43. T. Hamana, M. Bartelmann, N. Yoshida, **C. Pfrommer**, *Statistical distribution of gravitational-lensing excursion angles: Winding ways to us from the deep universe*, 2005, *MNRAS*, 356, 829.

44. **C. Pfrommer** & T. A. Enßlin, *Estimating galaxy cluster magnetic fields by the classical and hadronic minimum energy criterion*, 2004, *MNRAS*, 352, 76.

45. **C. Pfrommer** & T. A. Enßlin, *The quest for cosmic ray protons in clusters of galaxies*, 2004, *JKAS*, 37, 455.

46. **C. Pfrommer** & T. A. Enßlin, *Constraining the population of cosmic ray protons in cooling flow clusters with gamma-ray and radio observations: Are radio mini-halos of hadronic origin?*, 2004, *A&A*, 413, 17.

47. **C. Pfrommer** & T. A. Enßlin, *Probing the cosmic ray population of the giant elliptical galaxy M 87 with observed TeV gamma-rays*, 2003, *A&A*, 407, L73.

Submitted Publications

48. The Fermi/LAT Collaboration: M. Ackermann et al., incl. **C. Pfrommer (corresponding author)**, *Search for cosmic-ray induced gamma-ray emission in galaxy clusters*, 2013, submitted, arXiv:1308.5654.

49. A. E. Broderick, **C. Pfrommer**, E. Puchwein, P. Chang, *Implications of plasma beam instabilities for the statistics of the Fermi hard gamma-ray blazars and the origin of the extragalactic gamma-ray background*, 2013, submitted, arXiv:1308.0340.

50. A. E. Broderick, **C. Pfrommer**, E. Puchwein, P. Chang, *Lower limits upon the anisotropy of the extragalactic gamma-ray background implied by the 2FGL and 1FHL catalogs*, 2013, submitted, arXiv:1308.0015.

51. F. Zandanel, **C. Pfrommer**, F. Prada, *On the physics of radio halos: scaling relations and luminosity function*, 2012, submitted, arXiv:1207.6410.

Contributed Publications

1. **C. Pfrommer**, *Introduction to extragalactic sources of very high-energy photons*. In *Rencontres de Moriond: Very High Energy Phenomena in the Universe*, 2013, conference held at La Thuile, Italy, arXiv:1308.6582.

2. **C. Pfrommer**, A. E. Broderick, P. Chang, E. Puchwein, V. Springel, *The physics and cosmology of TeV blazars in a nutshell*. In *Rencontres de Moriond: Very High Energy Phenomena in the Universe*, 2013, conference held at La Thuile, Italy, arXiv:1308.6284.

3. **C. Pfrommer**, T. A. Enßlin, F. Miniati, K. Subramanian, *Cosmic ray transport in galaxy clusters: implications for radio halos and gamma-rays*, Proceedings of a conference in Nice, 15-18 November 2010; published in *MmSAI*, 82, 598 (2011).

4. T. E. Clarke, T. A. Enßlin, A. Finoguenov, H. Intema, **C. Pfrommer**, R. van Weeren, H. Röttgering, R. Oonk, *The Curious Case of Abell 2256*, Proceedings of a conference in Nice, 15-18 November 2010; published in *MmSAI*, 82, 547 (2011).

5. S. Lombardi et al. (for the MAGIC Collaboration), **C. Pfrommer**, A. Pinzke, *Observation of the Perseus cluster of galaxies with the MAGIC telescopes*, 2011 Fermi Symposium proceedings, arXiv:1111.0143.

6. D. Hildebrand et al. (for the MAGIC Collaboration), **C. Pfrommer**, A. Pinzke, *MAGIC detection of VHE Gamma-ray emission from NGC 1275 and IC 310*, 2011, Proc. of the 32nd Int'l Cosmic Ray Conference, Beijing, China, arXiv:1110.5358.

7. S. Lombardi et al. (for the MAGIC Collaboration), **C. Pfrommer**, A. Pinzke, *Observation of the Perseus galaxy cluster with the MAGIC telescopes*, 2011, Proc. of the 32nd Int'l Cosmic Ray Conference, Beijing, China, arXiv:1109.6216.

8. S. T. Myers, **C. Pfrommer**, et al., *Galaxy Cluster Astrophysics and Cosmology: Questions and Opportunities for the Coming Decade*, Astro2010: The Astronomy and Astrophysics Decadal Survey, Science White Papers, no. 218, arXiv:0903.0401.

9. S. R. Golwala et al. (including **C. Pfrommer**), *Calibrating Galaxy Clusters as a Tool for Cosmology via Studies of the Intracluster Medium*, Astro2010: The Astronomy and Astrophysics Decadal Survey, Science White Papers, no. 96.

10. L. Rudnick et al. (including **C. Pfrommer**), *Clusters and Large-Scale Structure: the Synchrotron Keys*, Astro2010: The Astronomy and Astrophysics Decadal Survey, Science White Papers, no. 253, arXiv:0903.0824.

11. **C. Pfrommer**, V. Springel, M. Jubelgas, T. A. Enßlin, *Cosmic ray feedback in hydrodynamical simulations of galaxy and galaxy cluster formation*. In *Comic Frontiers*, 2006, conference held at Durham University, UK, astro-ph/0611084.

12. **C. Pfrommer**, V. Springel, T. A. Enßlin, M. Jubelgas, *Cosmological structure formation shocks and cosmic rays in hydrodynamical simulations*. In *Heating vs. Cooling in Galaxies and Clusters of Galaxies*, 2006, conference held at Garching, Germany, astro-ph/0611085.

13. T. A. Enßlin & **C. Pfrommer**, *Particle acceleration processes in the cosmic large-scale structure*. In *Highlights of Astronomy, Volume 14*, 2006, proceedings of the XXVIth IAU General Assembly, Prague, Czech Republic.

14. **C. Pfrommer**, V. Springel, T. A. Enßlin, M. Jubelgas, *Detecting shock waves in smoothed particle hydrodynamics simulations*. In *Rencontres de Moriond: Contents and Structures of the Universe*, 2006, conference held at La Thuile, Italy.

15. T. A. Enßlin, M. Jubelgas, **C. Pfrommer**, V. Springel, *Cosmic ray physics in calculations of cosmological structure formation*, 2006. In *Rencontres de Moriond: Contents and Structures of the Universe*, 2006, conference held at La Thuile, Italy.

16. T. A. Enßlin, C. Vogt, **C. Pfrommer**, *Magnetic fields in clusters of galaxies*. In *The Magnetized Plasma in Galaxy Evolution*, 2004, conference held in Krakow, Poland, astro-ph/0501338.

17. T. A. Enßlin, C. Vogt, **C. Pfrommer**, *Magnetic fields and cosmic rays in cooling flows*. In *The Riddle of Cooling Flows in Galaxies and Clusters of Galaxies*, 2003, conference held in Charlottesville, VA, USA, astro-ph/0310028.

C. Teaching record

The lecture "The Physics of Galaxy Clusters" is in fulfillment of the formal teaching requirement for the Habilitation, with Prof. Springel acting as my mentor.

Teaching Courses

1. *Cosmology* (13 × 3 hours, master & PhD level)   winter term 2013
   lectures at Universität Heidelberg

2. *Experimental Physics 2* (13 × 2 hours, bachelor level)   summer term 2013
   tutoring exercise classes at Universität Heidelberg

3. *The Physics of Galaxy Clusters* (13 × 2 hours, master & PhD level)   summer term 2012
   lectures at Universität Heidelberg

4. *High-Energy Astrophysics—Selected Topics* (8 × 2 hours, master & PhD level)   spring term 2008
   lectures jointly taught with Dr. Yan at University of Toronto

5. *Synchrotron Theory,* (2 × 2 hours, master & PhD level)   winter term 2006
   lectures within Prof. Dr. Wu's course *Radiative Processes in Astrophysics* at University of Toronto

6. *Introductory Seminar for Mathematics* (10 × 2 hours, bachelor level)   winter term 2000
   seminar at Universität Jena

Teaching at Summer Schools

7. *Non-Thermal Processes* (2 × 1 hour, master & PhD level)   Aug 2008
   lectures at the summer school *Cosmology with the CMB and Large-Scale Structure* at IUCAA, Pune, India

8. *Simulating Galaxy Clusters* (2 × 1 hour, master & PhD level)   Jul 2007
   lecture at the *Santa Fe 2007 Cosmology Summer Workshop*, Santa Fe, USA

D. Thesis supervision

1. *Anders Pinzke*   2006 – 2010
   PhD thesis on *Gamma-ray emission from galaxy clusters—dark matter and cosmic rays,*
   co-supervision with Prof. Dr. Bergström,
   Department of Physics, Stockholm University, Sweden.

2. *Nicholas Battaglia*   2006 – 2011
   PhD thesis on *The impact of non-thermal processes in the intracluster medium on cosmological cluster ob-
   servables,* co-supervision with Prof. Dr. Bond,
   Canadian Institute for Theoretical Astrophysics, University of Toronto, Canada.

3. *Fabio Zandanel*   2009 – 2012
   PhD thesis on *High-energy phenomena in clusters of galaxies,*
   co-supervision with Dr. Prada,
   Instituto de Astrofísica de Andalucía, Universidad de Granada, Spain.

4. *Maximilian Uhlig*   2011 – 2012
   Diploma thesis on *Galactic winds driven by cosmic-ray streaming,*
   co-supervision with Dr. Enßlin,
   Max-Planck Institute for Astrophysics, Ludwig-Maximilians-Universität München, Germany.